SOME APPLICATIONS OF COMPLETE GENERAL SOLUTIONS OF STOKES EQUATIONS

Thesis submitted to the

University of Hyderabad

for the Degree of

DOCTOR OF PHILOSOPHY

by

DEBARJOYTI CHOUDHURI

DEPARTMENT OF MATHEMATICS AND STATISTICS,

SCHOOL OF MCIS,

UNIVERSITY OF HYDERABAD,

HYDERABAD - 500 046, INDIA.

November 2011

Contents

Chapter 1

An account of the basic results

The motion of solid bodies in a viscous fluid was first studied by Stokes [103] in 1850. He discussed the motion of a sphere moving in a straight line with uniform velocity and the motion of cylindrical pendulums performing small oscillations in a straight line. The remarkable formula given by Stokes [103] for the resistance experienced by a slowly moving sphere has proved to be vital in the research related to the field of Fluid Dynamics. The appearance of the sixth edition of Lamb's [50] 'Hydrodynamics' may be taken as a reference point of our discussion which is related to low Reynolds number flows (Stokes flows). For the most part of pre-1932, research in the area of low Reynolds number flows was carried out in solving boundary value problems based on Stokes and Oseen [74] equations for simple and tractable geometries (like cylinder and sphere). The celebrated solution of Lamb [50] in spherical polar coordinates

gave the much needed push to the investigations of viscous, incompressible flows past particles which have many applications in science and engineering. A testimony of all the concepts discovered during that period can be found in the two volume set of 'Modern Developments in Fluid Dynamics' [26]. Other notable contributions which helped in the growth of the subject of viscous, incompressible flows were by Lorentz [57, 58], Oseen [74], Happel and Brenner [32], Proudman and Pearson [87], G.I.Taylor [107], Batchelor [3], Lighthill [55], Lagerstrom [49] to name a few. The theory of low Reynolds number flows has always generated a lot of attention amongst mathematicians, physicists and engineers due to its manifold applications to subjects like lubrication [50, 101], chemical engineering [32], manufacture of colour film and magnetic recording tape [101, 94], flagellar propulsion of micro organisms [55] etc. The literature pertaining to low Reynolds number flows is vast and keeps growing continuously. Hence covering all the aspects of the theory of low Reynolds number flows is a tough task. However, we shall briefly review some of the topics of Stokes flows in the forthcoming sections of this chapter.

In Section 1.1, we give a brief account of the steady and unsteady Stokes equations. We discuss some solutions of Stokes equations proposed by Basset [5], Lorentz [57, 58], Lamb [50], Ranger [91, 92]. We also give an account of Faxén's laws [21] for drag and torque acting on a sphere in an unbounded, arbitrary Stokes flow. We then discuss the solution of steady Stokes equations proposed by Palaniappan et al. [79] and its advantages over other solutions. The solution of the unsteady Stokes equations by

Venkatlaxmi et al. [113, 114] is also presented. We define a '*complete general solution*' of Stokes equations. We also discuss some applications of '*complete general solutions*' of the steady and unsteady Stokes equations. In particular, we describe the problems discussed and the main results obtained in this thesis using these solutions.

1.1 Stokes equations

The Navier-Stokes equations governing the motion of a viscous incompressible fluid are given as follows.

$$\rho\frac{\partial\vec{\mathbf{q}}}{\partial t}+\rho\vec{\mathbf{q}}.\nabla\vec{\mathbf{q}} = -\nabla p+\mu\nabla^2\vec{\mathbf{q}}+\rho\vec{\mathbf{f}}, \tag{1.1.1}$$

$$\nabla.\vec{\mathbf{q}} = 0, \tag{1.1.2}$$

where $\vec{\mathbf{q}}$ is the velocity, p the pressure, ρ the density, μ the coefficient of dynamic viscosity of the fluid and $\vec{\mathbf{f}}$ the body force per unit mass. Due to the presence of the inertial term $\rho\vec{\mathbf{q}}.\nabla\vec{\mathbf{q}}$, equation (1.1.1) is nonlinear which makes solving the boundary value problems involving these equations difficult. It is known that every fluid flow past an object has a characteristic length L which characterizes the size of the object and speed U which characterizes the mean speed of the object relative to the fluid based on which one can define the '*Reynolds number*' which is equal to $\frac{LU\rho}{\mu}$. It is essentially the ratio of the inertial to the viscous forces. If the viscous forces are dominant compared to the inertial forces, we can linearize the Navier-Stokes equations by dropping the inertial terms which are nonlinear. The resulting linear equations

are called Stokes equations which are the governing equations of motion for the flow of a viscous, incompressible fluid at low Reynolds numbers. Throughout the thesis we will deal only with flows at low Reynolds numbers. The Stokes equations for the steady flow of a viscous, incompressible fluid are as follows.

$$\mu\nabla^2\vec{\mathbf{q}} = \nabla p, \tag{1.1.3}$$

$$\nabla.\vec{\mathbf{q}} = 0. \tag{1.1.4}$$

The fundamental solution of (1.1.3)-(1.1.4), which represents a point force, was given by Oseen [74] and was named as '*Stokeslet*' by Hancock [30]. The '*curl*' of a Stokeslet is called a '*rotlet*' or a '*couplet*' or a rotational Stokeslet. Other higher order singularities can be obtained by taking the directional derivatives of these singular solutions.
A brief note on harmonic and biharmonic functions: A function $f(x, y, z)$ is said to be harmonic in a domain Ω if

$$\nabla^2 f = 0 \ \ in \ \ \Omega, \tag{1.1.5}$$

where $\nabla^2 = \frac{\partial^2}{\partial x^2} + \frac{\partial^2}{\partial y^2} + \frac{\partial^2}{\partial z^2}$. As the name suggests, a function $g(x, y, z)$ is said to be biharmonic in Ω if

$$\nabla^4 g = 0 \ \ in \ \ \Omega. \tag{1.1.6}$$

A well known result due to Almansi [1] is that, any biharmonic function, say ϕ, can be represented as $\phi = \phi_1 + r^2\phi_2$, where ϕ_1 and ϕ_2 are harmonic functions. If $\phi_1 = 0$

and $\phi_2 \neq 0$, then we say that ϕ is purely biharmonic.

An immediate consequence of (1.1.3)-(1.1.4) is that the velocity $\vec{\mathbf{q}}$ is biharmonic and the pressure p and the vorticity $\nabla \times \vec{\mathbf{q}}$ are harmonic.

1.1.1 Some solutions of Stokes equations

Many techniques were developed and several solutions were proposed to solve boundary value problems in Stokes flows. The method of singularities was used independently by Lorentz [57, 58], Oseen [74] and Burgers [10] to solve some problems of Stokes flows. Oseen [74] proposed the method of images adopting the Green's function technique. The self-propulsion of micro organisms was studied by Sir G.I.Taylor [107] and Sir James Grey [102]. The biological and fluid mechanical aspects were studied later by Hancock [30], Hancock and Grey [31], Cox [16], Batchelor [3], Blake and Chwang [6], Chwang and Wu [13] using the method of singularities. The celebrated book by Sir M.J.Lighthill [55] gives a comparative account of aquatic animal locomotion at low Reynolds numbers. Some solutions of Stokes equations which are comparatively simpler to use have also been proposed which make use of scalar functions that satisfy partial differential equations whose solutions are known.

Axisymmetric flows: When the flow quantities are the same at all points in any plane passing through a fixed line, we call such a flow as an axisymmetric flow. In any axisymmetric flow, the velocity can be expressed in terms of a scalar function ψ

called the '*Stokes stream function*' as

$$\vec{\mathbf{q}} = \nabla \times (\psi \hat{\mathbf{e}}_\phi),$$

where $\hat{\mathbf{e}}_\phi$ is the unit vector corresponding to the azimuthal angle ϕ.

Further, if $\vec{\mathbf{q}}$ satisfies Stokes equations (1.1.3)-(1.1.4), then ψ satisfies $D^4\psi = 0$, where $D^2 = \frac{\partial^2}{\partial r^2} + \frac{\sin\theta}{r^2}\frac{\partial}{\partial\theta}\left(\frac{1}{\sin\theta}\frac{\partial}{\partial\theta}\right)$. In a similar way, in the case of general, not necessarily axisymmetric, Stokes flows there have been several solutions proposed in terms of scalar functions which satisfy simple partial differential equations like Laplace or biharmonic equations which can be solved easily. To solve the equations (1.1.3)-(1.1.4) we need to determine four unknowns, namely, the three components of the velocity vector $\vec{\mathbf{q}}$ and the pressure p. Using Almansi's [1] result, we observe that the vector equation (1.1.3) consists of three equations in a scalar form and so together with equation (1.1.4), the four equations of motion involve seven harmonics because $\vec{\mathbf{q}}$ is biharmonic and p is harmonic.

Naghdi and Hsu's solution: A solution of Stokes equations was given by Naghdi and Hsu [71] as

$$\vec{\mathbf{q}} = \frac{1}{4\pi}\nabla \int\int\int_\Omega \frac{\nabla.\vec{\mathbf{F}}}{\rho} d\xi d\eta d\varsigma + \vec{\mathbf{F}}, \tag{1.1.7}$$

$$p = -\mu \nabla.\vec{\mathbf{F}}, \tag{1.1.8}$$

where

$$\nabla^2\vec{\mathbf{F}} = \vec{\mathbf{0}}, \tag{1.1.9}$$

$$\rho = [(x-\xi)^2+(y-\eta)^2+(z-\varsigma)^2]^{1/2}, \tag{1.1.10}$$

and $\Omega \subset \mathbb{R}^3$ is the region occupied by the fluid.

We define a solution $(\vec{\mathbf{q}}, p)$ of Stokes equations (1.1.3)-(1.1.4) to be a '*complete general solution*', if every other solution of Stokes equations can be obtained from $(\vec{\mathbf{q}}, p)$. The solution proposed by Naghdi and Hsu [71] was shown to be complete by Xu and Wang [116] in the sense that for any given solution $(\vec{\mathbf{q}}, p)$, we can find $\vec{\mathbf{F}}$ such that $\vec{\mathbf{q}}$ and p can be expressed in terms of $\vec{\mathbf{F}}$ as in (1.1.7) and (1.1.8). But due to its integral form, it is not considered suitable for boundary value problems in Stokes flows.

Basset's solution: Basset's [5] representation of a solution of Stokes equations (1.1.3)-(1.1.4) is given as follows.

$$\vec{\mathbf{q}} = \nabla\times\nabla\times\vec{\mathbf{F}} + \nabla\phi, \tag{1.1.11}$$

$$p = P_0 + \mu\nabla.\nabla^2\vec{\mathbf{F}}, \tag{1.1.12}$$

where P_0 is a constant and the four unknowns ϕ and $\vec{\mathbf{F}}$ satisfy

$$\nabla^2\phi = 0, \tag{1.1.13}$$

$$\nabla^4\vec{\mathbf{F}} = 0. \tag{1.1.14}$$

All the solutions of Stokes equations (1.1.3)-(1.1.4) cannot be expressed in this form, i.e., for a given $(\vec{\mathbf{q}}, p)$ we cannot always find suitable $\vec{\mathbf{F}}$ and ϕ such that $(\vec{\mathbf{q}}, p)$ are

given by (1.1.11) and (1.1.12). For example, it is known that this represenation is not adequate to represent a rotlet located at the origin with its axis in the positive direction of y-axis.

Lorentz's solution: Lorentz [57, 58] proposed a representation of velocity and pressure of Stokes equations as follows.

$$\vec{\mathbf{q}} = \nabla \times \nabla \times \vec{\mathbf{A}} + \nabla \times \vec{\mathbf{B}}, \tag{1.1.15}$$

$$p = P_0 + \mu \nabla . \nabla^2 \vec{\mathbf{A}}, \tag{1.1.16}$$

where P_0 is a constant and

$$\nabla^4 \vec{\mathbf{A}} = 0, \quad \nabla^2 \vec{\mathbf{B}} = 0. \tag{1.1.17}$$

Although this solution is a complete general solution, there are too many harmonics to be determined than required for this solution. In fact, it involves nine harmonics whereas the solution (1.1.7)-(1.1.8) due to Naghdi and Hsu [71] requires only three scalar harmonic functions.

Lamb's solution: Horace Lamb [50] gave a general solution of the Stokes equations (1.1.3)-(1.1.4) in his book 'Hydrodynamics' in 1932. The motivation behind formulating this solution was the fact that the velocity is biharmonic and the pressure and the vorticity are both harmonic. The solution is given as follows.

$$\begin{aligned} \vec{\mathbf{q}} &= \sum_{-\infty}^{\infty} \left[\nabla \times (\vec{\mathbf{r}} \chi_n) + \nabla \phi_n + \frac{(n+3)}{2\mu(n+1)(2n+3)} r^2 \nabla p_n - \frac{n p_n \vec{\mathbf{r}}}{\mu(n+1)(2n+3)} \right], \\ p &= \sum_{-\infty}^{\infty} p_n, \end{aligned} \tag{1.1.18}$$

where p_n, ϕ_n and χ_n are solid harmonics of order n. It has been used to study many problems of Stokes flow past spherical boundaries.

Usha [110] used Lamb's [50] solution to find axisymmetric and asymmetric (non-axisymmetric) flows generated due to singularities like Stokeslet and rotlet located both exterior and interior to a sphere.

The drag force $\vec{\mathbf{D}}$ and torque $\vec{\mathbf{T}}$ on a sphere were given by Happel and Brenner [32] using Lamb's solution as

$$\vec{\mathbf{D}} = -4\pi\nabla(r^3 p_{-2}), \tag{1.1.19}$$

$$\vec{\mathbf{T}} = -8\pi\mu\nabla(r^3\chi_{-2}). \tag{1.1.20}$$

Ranger's solution: One drawback of Lamb's [50] solution is that it is given as a double infinite series. It is not always possible that the infinite series can be approximated by a function in a closed form barring in a few simple cases like uniform flow where only a finite number of terms survive. Ranger [91] suggested a closed form solution of velocity and pressure for flows whose velocity is linear in $\cos\phi$ and $\sin\phi$. It is given as follows.

$$\vec{\mathbf{q}} = \nabla\times\nabla\times\left(\frac{\psi}{r\sin\theta}\vec{\mathbf{r}}\cos\phi\right) + \nabla\left(\frac{\chi}{r\sin\theta}\vec{\mathbf{r}}\sin\phi\right), \tag{1.1.21}$$

$$p = P_0 + \frac{\mu}{r\sin\theta}\frac{\partial}{\partial r}(D^2\psi)\cos\phi, \tag{1.1.22}$$

where $D^4\psi = 0$, $D^2\chi = 0$ and P_0 is a constant. This solution was used by Shail [99] to study the axisymmetric Stokes flow due to a Stokeslet within a sphere. It was also

used by Shail and Onslow [100] to analyze some Stokes flows past spherical boundaries and also by Hackborn and O'Neill [27] for studying the structure of asymmetric or non-axisymmetric Stokes flows. Even though Ranger's [91] solution (1.1.21)-(1.1.22) is adequate to represent the velocity and pressure for the motion of a viscous, incompressible fluid due to a Stokeslet or a rotlet, it fails to represent the same due to higher order singularities.

Palaniappan et al.'s [79] solution: Due to the limitations of Ranger's [91] solution, the hunt for a complete, general representation of the velocity and pressure continued for a while. Later Palaniappan et al. [79] proposed a representation of velocity and pressure $(\vec{\mathbf{q}}, p)$ in terms of scalar functions A and B given as follows.

$$\vec{\mathbf{q}} = \nabla \times \nabla \times (\vec{\mathbf{r}}A) + \nabla \times (\vec{\mathbf{r}}B), \tag{1.1.23}$$

$$p = P_0 + \mu \frac{\partial}{\partial r}(r\nabla^2 A), \tag{1.1.24}$$

where P_0 is a constant and $\nabla^4 A = 0$ and $\nabla^2 B = 0$. Hence this solution is expressed in terms of three independent harmonic functions.

This solution proposed by Palaniappan et al. [79] is a complete general solution which was proved to be so later by Padmavathi et al. [77]. Hence all other solutions of Stokes equations can be derived from it. For instance, Ranger's solution can be obtained by the following choice of A and B.

$$A = \frac{\psi}{r\sin\theta}\cos\phi, B = \frac{\chi}{r\sin\theta}\sin\phi. \tag{1.1.25}$$

Lamb's [50] solution also can be obtained by taking A and B as follows.

$$A = \sum_{-\infty}^{\infty} \left[\frac{\phi_n}{n+1} + \frac{r^2 p_n}{2\mu(n+1)(2n+3)} \right], \tag{1.1.26}$$

$$B = \sum_{-\infty}^{\infty} \chi_n. \tag{1.1.27}$$

Using the solution of Palaniappan et al. [79], the solutions of the problems of non-axisymmetric Stokes flow past a sphere with rigid and shear-free boundary conditions were obtained by Palaniappan et al. [78, 79] in a closed form in the form of sphere theorems. Another advantage of this representation is the ease with which the boundary conditions can be written using the scalar functions A and B in a simple form. If $B \equiv 0$, $A(r,\theta,\phi) \equiv A(r,\theta)$, $\frac{\partial A}{\partial \theta} = \frac{\psi}{r\sin\theta}$, where ψ is the Stokes stream function, then we can retrieve the formulae for velocity and pressure in the axisymmetric case. The velocity components are given for axisymmetric flows as follows.

$$q_r = -\frac{1}{r^2 \sin\theta} \frac{\partial \psi}{\partial \theta}, \tag{1.1.28}$$

$$q_\theta = \frac{1}{r\sin\theta} \frac{\partial \psi}{\partial r}, \tag{1.1.29}$$

$$q_\phi = 0, \tag{1.1.30}$$

where q_r, q_θ and q_ϕ are the radial, tangential and azimuthal velocity components in spherical polar coordinates (r,θ,ϕ).

Unsteady Stokes equations: The equations of motion governing the motion of an

unsteady Stokes flow of a viscous, incompressible fluid are given by

$$\rho\frac{\partial\vec{\mathbf{q}}}{\partial t} = -\nabla p + \mu\nabla^2\vec{\mathbf{q}}, \tag{1.1.31}$$

$$\nabla.\vec{\mathbf{q}} = 0. \tag{1.1.32}$$

When the velocity and pressure distribution are of oscillatory nature which are given by $\vec{\mathbf{q}} = \hat{\vec{\mathbf{q}}}e^{-i\omega t}$ and $p = P + \hat{p}e^{-i\omega t}$ respectively, P being a constant, then the equations of motion (1.1.31)-(1.1.32) can be rewritten as

$$\mu(\nabla^2 - \lambda^2)\hat{\vec{\mathbf{q}}} = \nabla\hat{p}, \tag{1.1.33}$$

$$\nabla.\hat{\vec{\mathbf{q}}} = 0, \tag{1.1.34}$$

where $\lambda^2 = -\frac{i\omega}{\nu}$, ω is the frequency of oscillation, $\sqrt{-1} = i$ and $\nu = \frac{\mu}{\rho}$ is the kinematic viscosity. We drop the hats for convenience in our subsequent discussion.

The '*complete general solution*' of unsteady Stokes equations (1.1.31)-(1.1.32) and (1.1.33)-(1.1.34) can be defined in a similar manner as in the case of steady Stokes equations. A complete general solution of equations (1.1.33)-(1.1.34) was proposed by Venkatlaxmi et al. [113, 114] which is as follows.

$$\vec{\mathbf{q}} = \nabla\times\nabla\times(\vec{\mathbf{r}}A) + \nabla\times(\vec{\mathbf{r}}B), \tag{1.1.35}$$

$$p = P_0 + \mu\frac{\partial}{\partial r}(r(\nabla^2 - \lambda^2)B), \tag{1.1.36}$$

where P_0 is a constant and

$$\nabla^2(\nabla^2 - \lambda^2)A = 0, \tag{1.1.37}$$

$$(\nabla^2 - \lambda^2)B = 0. \tag{1.1.38}$$

The general solution of (1.1.37)-(1.1.38) is

$$A = \sum_{n=1}^{\infty} \left(\alpha_n r^n + \alpha'_n f_n(\lambda r) + \frac{\beta_n}{r^{n+1}} + \beta'_n g_n(\lambda r) \right) S_n(\theta, \phi), \tag{1.1.39}$$

$$B = \sum_{n=1}^{\infty} \left(\epsilon_n f_n(\lambda r) + \epsilon'_n g_n(\lambda r) \right) T_n(\theta, \phi), \tag{1.1.40}$$

where

$$S_n(\theta, \phi) = \sum_{m=0}^{n} P_n^m(\zeta)(A_{nm} \cos m\phi + B_{nm} \sin m\phi),$$

$$T_n(\theta, \phi) = \sum_{m=0}^{n} P_n^m(\zeta)(C_{nm} \cos m\phi + D_{nm} \sin m\phi),$$

where α_n, α'_n, β_n, β'_n, A_{nm}, B_{nm}, C_{nm}, D_{nm} are constants and $Re(\lambda^2) \leq 0$. The functions $f_n(R) = \sqrt{\frac{\pi}{2R}} I_{n+\frac{1}{2}}(R)$ and $g_n(R) = \sqrt{\frac{\pi}{2R}} K_{n+\frac{1}{2}}(R)$ are the modified Bessel functions of fractional order, where $f_n(R)$ is finite at $R = 0$ and $g_n(R)$ is finite at infinity.

1.2 Boundary conditions

Physical problems that are modelled by partial differential equations are always provided with initial or boundary conditions or both. In the problems discussed in the thesis, we chose the boundary to be smooth. In the boundary value problems, usually the information about the values of the unknown function or (the values of) the derivatives of the unknown function are prescribed on the boundary. The following

boundary conditions have been used in the subsequent chapters.

No-slip boundary condition: Consider a particle Ω whose surface is denoted by the boundary $\partial\Omega$. Then the no-slip boundary condition is mathematically given by

$$\vec{\mathbf{q}}|_{\partial\Omega} = 0. \tag{1.2.1}$$

This means that both the normal and the tangential components of the velocity vanish on the boundary $\partial\Omega$.

Shear-free boundary conditions: The shear-free boundary conditions are given as follows.

$$\begin{aligned} \vec{\mathbf{q}}.\hat{\mathbf{n}}|_{\partial\Omega} &= 0, \\ \vec{\mathbf{T}}^{\hat{\mathbf{n}}}.\hat{\mathbf{t}}_1|_{\partial\Omega} &= 0, \\ \vec{\mathbf{T}}^{\hat{\mathbf{n}}}.\hat{\mathbf{t}}_2|_{\partial\Omega} &= 0, \end{aligned} \tag{1.2.2}$$

where $[\hat{\mathbf{n}}, \hat{\mathbf{t}}_1, \hat{\mathbf{t}}_2]$ is the set of a local orthonormal basis, $\hat{\mathbf{n}}$ is the unit normal to the surface, $\hat{\mathbf{t}}_1$, $\hat{\mathbf{t}}_2$ are two unit orthonormal vectors in the tangent plane to the surface. $\vec{\mathbf{T}}^{\hat{\mathbf{n}}} = \mathbf{T}.\hat{\mathbf{n}}$, $\mathbf{T}$ being the stress tensor of rank 2. In particular, if the boundary $\partial\Omega$ has the form $r = f(\theta, \phi)$, then in the spherical polar coordinates (r, θ, ϕ), we write $\hat{\mathbf{n}} = n_1\hat{\mathbf{e}}_r + n_2\hat{\mathbf{e}}_\theta + n_3\hat{\mathbf{e}}_\phi$,

and $\vec{\mathbf{T}}^{\hat{\mathbf{n}}} = \mathbf{T}.\hat{\mathbf{n}} = \begin{pmatrix} T_{rr}\hat{\mathbf{e}}_r\hat{\mathbf{e}}_r & T_{r\theta}\hat{\mathbf{e}}_r\hat{\mathbf{e}}_\theta & T_{r\phi}\hat{\mathbf{e}}_r\hat{\mathbf{e}}_\phi \\ T_{\theta r}\hat{\mathbf{e}}_\theta\hat{\mathbf{e}}_r & T_{\theta\theta}\hat{\mathbf{e}}_\theta\hat{\mathbf{e}}_\theta & T_{\theta\phi}\hat{\mathbf{e}}_\theta\hat{\mathbf{e}}_\phi \\ T_{\phi r}\hat{\mathbf{e}}_\phi\hat{\mathbf{e}}_r & T_{\phi\theta}\hat{\mathbf{e}}_\phi\hat{\mathbf{e}}_\theta & T_{\phi\theta}\hat{\mathbf{e}}_\phi\hat{\mathbf{e}}_\phi \end{pmatrix} \begin{pmatrix} n_1\hat{\mathbf{e}}_r \\ n_2\hat{\mathbf{e}}_\theta \\ n_3\hat{\mathbf{e}}_\phi \end{pmatrix}.$

Moreover,

$$\begin{aligned}
\hat{\mathbf{t}}_1 &= \frac{1}{k_2}(f_\theta \hat{\mathbf{e}_r} + f\hat{e_\theta}), \\
\hat{\mathbf{t}}_2 &= \frac{1}{k_1 k_2 k_3}\left(\left(\frac{f f_\phi}{r\sin\theta}\right)\hat{\mathbf{e}_r} - \left(\frac{f_\theta f_\phi}{r\sin\theta}\right)\hat{\mathbf{e}_\theta} + \left(\frac{f_\theta^2}{r} + f\right)\hat{\mathbf{e}_\phi}\right), \\
\mathbf{T}.\hat{\mathbf{n}} &= \frac{1}{k_1}\left[\left(T_{rr} - \frac{T_{r\theta}f_\theta}{r} - \frac{T_{r\phi}f_\phi}{r\sin\theta}\right)\hat{\mathbf{e}_r} + \left(T_{\theta r} - \frac{T_{\theta\theta}f_\theta}{r} - \frac{T_{\theta\phi}f_\phi}{r\sin\theta}\right)\hat{\mathbf{e}_\theta}\right. \\
&\quad \left. + \left(T_{\phi r} - \frac{T_{\phi\theta}f_\theta}{r} - \frac{T_{\phi\phi}f_\phi}{r\sin\theta}\right)\hat{\mathbf{e}_\phi}\right],
\end{aligned}$$

where $k_1 = \sqrt{1 + \left(\frac{f_\theta}{r}\right)^2 + \left(\frac{f_\phi}{r\sin\theta}\right)^2}$, $k_2 = \sqrt{(f_\theta^2 + f^2)}$,
$k_3 = \sqrt{\left(\frac{f f_\phi}{r k_1 k_2 \sin\theta}\right)^2 + \left(\frac{f_\theta f_\phi}{r k_1 k_2 \sin\theta}\right)^2 + \left(\frac{f_\theta^2}{r k_1 k_2} + \frac{f}{k_1 k_2}\right)^2}$.
In addition, suppose $q_n = \vec{\mathbf{q}}.\hat{\mathbf{n}}$, $q_{t_1} = \vec{\mathbf{q}}.\hat{\mathbf{t}}_1$, $q_{t_2} = \vec{\mathbf{q}}.\hat{\mathbf{t}}_2$, $T_{t_1} = \vec{\mathbf{T}}^{\hat{\mathbf{n}}}.\hat{\mathbf{t}}_1$ and $T_{t_2} = \vec{\mathbf{T}}^{\hat{\mathbf{n}}}.\hat{\mathbf{t}}_2$ then

$$\begin{aligned}
q_n &= \frac{1}{k_1}\left(q_r - q_\theta\frac{f_\theta}{r} - q_\phi\frac{f_\phi}{r\sin\theta}\right), \\
q_{t_1} &= \frac{1}{k_2}(q_r f_\theta + q_\theta f), \\
q_{t_2} &= \frac{1}{k_3}\left[q_r\left(\frac{f f_\phi}{r\sin\theta k_1 k_2}\right) - q_\theta\left(\frac{f_\theta f_\phi}{r\sin\theta k_1 k_2}\right) + q_\phi\left(\frac{f_\theta^2}{r k_1 k_2} + \frac{f}{k_1 k_2}\right)\right]. \\
T_{t_1} &= \frac{1}{k_2}\left[\left(T_{rr} - \frac{T_{r\theta}f_\theta}{r} - \frac{T_{r\phi}f_\phi}{r\sin\theta}\right)f_\theta + \left(T_{\theta r} - \frac{T_{\theta\theta}f_\theta}{r} - \frac{T_{\theta\phi}f_\phi}{r\sin\theta}\right)f\right] \\
T_{t_2} &= \frac{1}{k_3}\left[\left(T_{rr} - \frac{T_{r\theta}f_\theta}{r} - \frac{T_{r\phi}f_\phi}{r\sin\theta}\right)\left(\frac{f f_\phi}{r\sin\theta}\right) - \left(T_{\theta r} - \frac{T_{\theta\theta}f_\theta}{r} - \frac{T_{\theta\phi}f_\phi}{r\sin\theta}\right)\left(\frac{f_\theta f_\phi}{r\sin\theta}\right)\right. \\
&\quad \left. + \left(T_{\phi r} - \frac{T_{\phi\theta}f_\theta}{r} - \frac{T_{\phi\phi}f_\phi}{r\sin\theta}\right)\left(\frac{f_\theta^2}{r} + r\right)\right]. \qquad (1.2.3)
\end{aligned}$$

Here $\hat{\mathbf{e}}_r$, $\hat{\mathbf{e}}_\theta$, $\hat{\mathbf{e}}_\phi$ are the unit vectors in the radial, tangential and azimuthal directions in spherical polar coordinates (r, θ, ϕ) and are given in terms of $\hat{\mathbf{i}}$, $\hat{\mathbf{j}}$, $\hat{\mathbf{k}}$ as follows.

$$\begin{aligned}
\hat{\mathbf{e}}_r &= \sin\theta\cos\phi\hat{\mathbf{i}} + \sin\theta\sin\phi\hat{\mathbf{j}} + \cos\theta\hat{\mathbf{k}}, \\
\hat{\mathbf{e}}_\theta &= \cos\theta\cos\phi\hat{\mathbf{i}} + \cos\theta\sin\phi\hat{\mathbf{j}} - \sin\theta\hat{\mathbf{k}}, \\
\hat{\mathbf{e}}_\phi &= -\sin\phi\hat{\mathbf{i}} + \cos\phi\hat{\mathbf{j}},
\end{aligned}$$

where $0 \leq \theta < \pi$, $0 \leq \phi < 2\pi$. The components of stress in spherical polar coordinates (r, θ, ϕ) are given as follows.

$$\begin{aligned}
T_{rr} &= -p + 2\mu\frac{\partial q_r}{\partial r}, \\
T_{r\theta} &= \mu\left(\frac{\partial q_\theta}{\partial r} - \frac{q_\theta}{r} + \frac{1}{r}\frac{\partial q_r}{\partial \theta}\right), \\
T_{r\phi} &= \mu\left(\frac{1}{r\sin\theta}\frac{\partial q_r}{\partial \phi} + \frac{\partial q_\phi}{\partial r} - \frac{q_\phi}{r}\right), \\
T_{\theta\theta} &= -p + 2\mu\left(\frac{1}{r}\frac{\partial q_\theta}{\partial \theta} + \frac{q_r}{r}\right), \\
T_{\phi\phi} &= -p + 2\mu\left(\frac{1}{r\sin\theta}\frac{\partial q_\phi}{\partial \phi} + \frac{q_r}{r} + \frac{q_\theta\cot\theta}{r}\right), \\
T_{\theta\phi} &= \mu\left(\frac{1}{r}\frac{\partial q_\phi}{\partial \theta} - \frac{\cot\theta q_\phi}{r} + \frac{1}{r\sin\theta}\frac{\partial q_\theta}{\partial \phi}\right). \qquad (1.2.4)
\end{aligned}$$

If the surface is a sphere of radius a, then the shear-free boundary conditions reduce to the following conditions

$$\begin{aligned}
q_r(a, \theta, \phi) &= 0, \\
T_{r\theta}(a, \theta, \phi) &= 0, \\
T_{r\phi}(a, \theta, \phi) &= 0.
\end{aligned}$$

Slip-stick boundary conditions: It was revealed by experiments [37] that some slipping may take place at the surface of contact, in the case of many fluids, when in contact with the surface of a solid. When the velocity of the fluid relative to the solid is small, it is assumed that the tangential force exerted by the solid upon the fluid acts in the same direction as that of the relative velocity and is proportional to it. Mathematically the general slip-stick boundary conditions are given as follows.

$$\begin{aligned} \vec{\mathbf{q}}.\hat{\mathbf{n}}|_{\partial\Omega} &= 0, \\ \vec{\mathbf{q}}.\hat{\mathbf{t}}_1|_{\partial\Omega} &= \frac{\overline{\lambda}}{\mu}\vec{\mathbf{T}}^{\hat{\mathbf{n}}}.\hat{\mathbf{t}}_1|_{\partial\Omega}, \\ \vec{\mathbf{q}}.\hat{\mathbf{t}}_2|_{\partial\Omega} &= \frac{\overline{\lambda}}{\mu}\vec{\mathbf{T}}^{\hat{\mathbf{n}}}.\hat{\mathbf{t}}_2|_{\partial\Omega}, \end{aligned} \tag{1.2.5}$$

where $\overline{\lambda}$ is the slip parameter and $\partial\Omega$ is the boundary of the solid body.

Basset [5] considered the motion of a sphere of radius a, moving along a straight line with a uniform velocity in a viscous fluid, assuming that there is some slipping at the surface of the sphere. He considered the following boundary conditions.

$$\begin{aligned} q_r(a,\theta,\phi) &= 0, \\ q_\theta(a,\theta,\phi) &= \frac{\overline{\lambda}}{\mu}T_{r\theta}(a,\theta,\phi), \\ q_\phi(a,\theta,\phi) &= \frac{\overline{\lambda}}{\mu}T_{r\phi}(a,\theta,\phi). \end{aligned} \tag{1.2.6}$$

For a viscous, incompressible flow inside a cavity the boundary conditions are modified [109] suitably. In fact, the modified slip-stick boundary conditions for a viscous,

incompressible flow generated due to the presence of singularities inside a sphere of radius a are given as follows.

$$\begin{aligned} q_r(a,\theta,\phi) &= 0, \\ q_\theta(a,\theta,\phi) &= -\frac{\overline{\lambda}}{\mu} T_{r\theta}(a,\theta,\phi), \\ q_\phi(a,\theta,\phi) &= -\frac{\overline{\lambda}}{\mu} T_{r\phi}(a,\theta,\phi). \end{aligned} \tag{1.2.7}$$

It is interesting to note that when $\overline{\lambda} = 0$, we obtain the no-slip boundary conditions. When $\overline{\lambda} \to \infty$, the shear-free or perfect slip boundary conditions are obtained.

1.2.1 Drag and Torque

The general expressions for the drag and the torque experienced by an arbitrarily shaped particle Ω are given respectively by

$$\vec{\mathbf{D}} = \int_{\partial\Omega} \vec{\mathbf{T}}^{\hat{\mathbf{n}}} dS, \tag{1.2.8}$$

$$\vec{\mathbf{T}} = \int_{\partial\Omega} (\vec{\mathbf{r}} \times \vec{\mathbf{D}}) dS, \tag{1.2.9}$$

where dS is the surface element of the particle Ω. In particular, for a sphere of radius a, the formulae (1.2.8)-(1.2.9) are as follows.

$$\vec{\mathbf{D}} = \int_0^{2\pi} \int_0^{\pi} [T_{rr}\hat{\mathbf{e}}_r + T_{r\theta}\hat{\mathbf{e}}_\theta + T_{r\phi}\hat{\mathbf{e}}_\phi]_{r=a} a^2 \sin\theta \; d\theta d\phi, \tag{1.2.10}$$

$$\vec{\mathbf{T}} = \int_0^{2\pi} \int_0^{\pi} [rT_{r\theta}\hat{\mathbf{e}}_\phi - rT_{r\phi}\hat{\mathbf{e}}_\theta]_{r=a} a^2 \sin\theta \; d\theta d\phi. \tag{1.2.11}$$

In 1924, Faxén [21] showed that, in an unbounded, arbitrary steady Stokes flow, the drag $\vec{\mathbf{D}}$ and torque $\vec{\mathbf{T}}$ acting on a rigid sphere of radius a are given by

$$\vec{\mathbf{D}} = 6\pi\mu a[\vec{\mathbf{q}}_0]_0 + \pi\mu a^3[\nabla^2\vec{\mathbf{q}}_0]_0, \tag{1.2.12}$$

$$\vec{\mathbf{T}} = 4\pi\mu a^3[\nabla \times \vec{\mathbf{q}}_0]_0, \tag{1.2.13}$$

where $\vec{\mathbf{q}}_0$ is the velocity of the basic unperturbed flow and $[\ ]_0$ denotes the value at the centre of the sphere.

Hence, the information of the basic, unperturbed flow is sufficient to compute the drag and the torque on a rigid sphere of radius a. The formulae (1.2.12) and (1.2.13) are often referred to as Faxén's laws. Payne and Pell [82] gave a simple formula for the computation of the force experienced by a rigid body in an axisymmetric, steady Stokes flow in terms of the stream function ψ which is as follows.

$$F_z = 8\pi\mu \lim_{r\to\infty} \frac{r\psi}{\varpi^2}, \tag{1.2.14}$$

where F_z denotes the force exerted by the fluid on the body in the positive z direction, $\varpi = r\sin\theta$.

If the fluid is not at rest at infinity, then the drag is given by

$$F_z = 8\pi\mu \lim_{r\to\infty} \frac{r(\psi - \psi_\infty)}{\varpi^2}, \tag{1.2.15}$$

where ψ_∞ denotes the stream function corresponding to the fluid velocity at infinity. However there is no such formula available in the literature for general non-axisymmetric Stokes flows past bodies of arbitrary shape.

1.3 Non-dimensionalization of Stokes equations

Throughout the thesis, we have used the non-dimensionalized Stokes equations (in both the steady and the unsteady Stokes flows). The unsteady Stokes equations for an oscillatory distribution of velocity and pressure (1.1.33)-(1.1.34) are non-dimensionalized by using the following transformations.

$$\vec{\mathbf{q}}' = \frac{\vec{\mathbf{q}}}{U}, \quad p' = \frac{Lp}{\mu U}, \quad P' = \frac{LP}{\mu U}, \quad \lambda^{2\prime} = L^2\lambda^2, \quad \vec{\mathbf{r}}' = \frac{\vec{\mathbf{r}}}{L},$$

where U and L are the characteristic velocity and length respectively. We drop the primes in the non-dimensional form of (1.1.33)-(1.1.34) to obtain the following equations.

$$(\nabla^2 - \lambda^2)\vec{\mathbf{q}} = \nabla p, \tag{1.3.1}$$

$$\nabla.\vec{\mathbf{q}} = 0. \tag{1.3.2}$$

The steady Stokes equations (1.1.3)-(1.1.4) are non-dimensionalized by using the following transformations.

$$\vec{\mathbf{q}}' = \frac{\vec{\mathbf{q}}}{U}, \quad p' = \frac{L}{\mu U}p, \quad x' = \frac{x}{L}, \quad y' = \frac{y}{L}, \quad z' = \frac{z}{L}.$$

Similar to the unsteady case, we drop the primes to get the following form of the non-dimensional Stokes equations.

$$\nabla^2\vec{\mathbf{q}} = \nabla p, \tag{1.3.3}$$

$$\nabla.\vec{\mathbf{q}} = 0. \tag{1.3.4}$$

Throughout the thesis, we consider the unsteady and steady Stokes equations to be as given in (1.3.1)-(1.3.2) and (1.3.3)-(1.3.4) respectively.

1.4 An overview of the thesis

After an introduction to the basic results discussed so far, we now give an overview of the thesis where we discuss some problems pertaining to steady and unsteady Stokes flows both in and around spherical and non-spherical particles. The thesis consists of six chapters which can be broadly divided into three parts. In the first part (Chapters 2 and 3), we address the problems of Stokes flow of a viscous, incompressible fluid in and around spherical boundaries separating two immiscible fluids of different viscosities. In the second part (Chapters 4 and 5), we discuss the problems of Stokes flow of a viscous, incompressible fluid in and around spherical and non-spherical boundaries using slip-stick boundary conditions. In the third part (Chapter 6), we give a brief summary of the results in this thesis. We have used the solutions of Palaniappan et al. [79] and Venkatlaxmi et al. [113, 114] for steady and unsteady Stokes equations respectively because they are complete general solutions and are simple to use.

In particular, the problem discussed in **Chapter 2** pertains to the steady, incompressible Stokes flow past a sphere coated with a viscous fluid which is immersed in an immiscible viscous fluid of a different viscosity. The problem addressed in this chapter is important owing to its applications in science and engineering. The liquid

films around the rigid spheres in the microencapsulation process are instrumental in protecting the core material from mechanical and chemical damage. Previously Kawano et al. [43, 44, 45] studied the problem of liquid spherical shells moving in an immiscible liquid at intermediate values of Reynolds numbers. Dimitrakopoulos and Higdon [18] numerically studied the problem of displacement of liquid drops from solid boundaries in low Reynolds number shear flows. The motivation of the problem discussed in this chapter is from the work of O'Neill and Ranger [72] who had considered a slow uniform flow past a coated sphere in an immiscible viscous fluid. Johnson [42] discussed a similar problem of steady, axisymmetric Stokes flow past a sphere with a thin coating of an immiscible fluid around it, in a uniform flow. In this chapter we considered a more general problem by considering an arbitrary Stokes flow past a fluid coated sphere in an immiscible fluid of a different viscosity where it was assumed that the spherical shape of the coating is retained under the assumption that the surface tension forces are large enough to balance the viscous forces. This is an important problem owing to the fact that it serves as a good model for certain problems in science and engineering as illustrated subsequently in Chapter 2. We have employed the solution of Palaniappan et al. [79], as it is a complete general solution which is simple to use in such boundary value problems, to obtain the modified flow field in the presence of a coated sphere. The expressions for the drag $\vec{\mathbf{D}}_c$ and torque $\vec{\mathbf{T}}_c$ experienced by the coated sphere were derived similar to Faxén's laws [21]. An immediate result is that, if the flow velocity is harmonic or purely biharmonic then

the magnitude of the drag on the coated sphere is lesser compared to the magnitude of the drag on a rigid sphere of radius equal to that of the coated sphere. A result obtained by Johnson [42], who considered a uniform flow, was that the drag reduces on the sphere with a fluid-film, when the ratio of the viscosity of the outer fluid to the viscosity of the fluid-film is greater than 4. We obtained a more general result in the case of arbitrary flows that the drag on the coated sphere reduces compared to the drag on an uncoated rigid sphere of unit radius when the ratio of the viscosity of the outer fluid to the viscosity of the coating is greater than 4 and also when the unperturbed velocity is harmonic or purely biharmonic, uniform flow being a particular kind of flow where the velocity is harmonic. However this result is not true in general, i.e., when the unperturbed velocity is a sum of both harmonic and purely biharmonic functions.

In **Chapter 3**, we discuss the problem of an oscillatory flow of a fluid of a certain viscosity past a liquid sphere of a different viscosity. The problems of deformation and dynamics of liquid droplets find their use in rheological studies where biological cells in various flow environments are considered. Some of the literature available pertaining to this problem is due to Hadamard [28, 29] and Rybczynski [95] who considered the translational motion of a spherical liquid drop in another immiscible fluid in a steady Stokes flow. Taylor and Acrivos [108] considered a liquid drop in a quiescent flow and calculated the drag on it besides studying the deformation of the drop. We draw motivation from the work of Hetsroni and Haber [38] who used

Lamb's [50] solution to determine the flow field in and around a liquid drop. They had adopted the formula of Landau and Lifshitz [51] to determine the equation of the deformed surface of the liquid drop in a steady Stokes flow. We assume here the flow to be generated due to a singularity of oscillating strength. The liquid sphere is assumed to be of spherical shape of radius a as the zeroth order approximation. The boundary conditions are the vanishing of normal velocities, continuity of tangential velocities and tangential stresses. Using Venkatalaxmi's [113, 114] representation of velocity and pressure for the unsteady Stokes equations, which is a complete general solution, we solve for the flow field inside and outside the fluid sphere using the boundary conditions. The expressions for the drag and torque have been derived akin to Faxén's laws [21]. As limiting cases, we obtain the drag and torque on a rigid sphere which agree with the formulae due to Kim and Karrila [47]. We further obtain as limiting cases, the drag and torque on a shear-free sphere in an oscillating flow. We then shift our attention to study the deformation of the droplet. We assume that the sphere undergoes a slight deformation from its spherical shape, i.e., we assume that the surface of the deformed liquid sphere is given by $r = F(\theta, \phi, t)$ where $F(\theta, \phi, t) = a(1 + f(\theta, \phi)e^{-i\omega t})$ and $\max |f(\theta, \phi)| << 1$ such that the radius of the 'equivalent' spherical liquid drop is given by $|F(\theta, \phi, t)|$, ω being the frequency of oscillations. The condition that the difference between the normal stresses is balanced by the surface tension forces has been used to compute the equation of the deformed sphere upto the first order approximation, on the lines of Hetsroni and Haber [38].

The method of determining the equation of the surface of the deformed sphere has been demonstrated by examples for singularity driven flows both outside and inside the fluid spheres. Another important result that has been verified in this chapter is the fact that the spherical shape of the liquid sphere is retained for flow velocities which have terms only upto $n = 1$ in the series representation of the solution, thereby agreeing with the result of Chisnell [11] who considered a uniform flow. We found that the capillary number of the flow as well as the ratio of viscosities play an important role in the deformation of the fluid sphere.

In **Chapter 4**, we discuss the problem of a viscous, incompressible fluid flow due to a singularity located inside a spherical container centred at the origin using slip-stick boundary conditions. Experiments by Helmholtz and Piotrowsky [37] confirmed that fluid at the boundary of a solid particle may undergo some amount of slip. Such boundary conditions also find their use in fields of engineering such as in rarefied gas dynamics. There have been numerous studies on flows exterior to the bounding surface with slip [20, 75, 98] in view of their applications in micro device technology (Barber and Liu [4, 56], and references therein) and the interest in these boundary conditions has been growing continuously. It is observed that the no-slip and the shear-free boundary conditions can be retrieved from the slip-stick boundary conditions as limiting cases [75]. The problem discussed here has been motivated by the work of Maul and Kim [63] who considered a Stokes flow generated due to the presence of a Stokeslet located inside a rigid sphere. One interesting phenomenon

observed by Maul and Kim [63] is the 'Stokeslet reversal'. Using Palaniappan et al.'s [79] representation of velocity and pressure of Stokes equations, we found the modified flow field inside a sphere generated by a Stokeslet by employing slip-stick boundary conditions. The solution has been found in a closed form in terms of two scalar functions A and B and is presented in the form of a sphere theorem. The drag experienced by the sphere due to the fluid inside has been obtained from which we can conclude that the drag is independent of the slip parameter. We illustrated these results by studying two examples.

In particular, the axisymmetric Stokes flow inside a spherical container due to a Stokeslet was analysed by considering two cases.

(a) *Flow due to a Stokeslet located at the origin.* The axisymmetric flow due to a Stokeslet located at the origin has been analysed separately owing to many interesting results. We found the modified flow field inside the sphere using the slip-stick boundary conditions. The solution has been found in a closed form in terms of the Stokes stream function. An important observation made while finding the stagnation points in this case is that the radius of stagnation circle for the no-slip case matches with the one obtained by Shail [99]. It is also seen that as $\overline{\lambda} \to \infty$, i.e., for a shear-free boundary, the radius of the stagnation circle approaches 0.5, hence proving that the slip parameter plays a role in the location of the stagnation points. We then computed the points of zero vorticity or the separation points and found that for $\overline{\lambda} > 0.5$ the separation points are absent in the flow domain. We observed that when the slip

parameter lies between 0 and 0.5 the stagnation points and the points of zero vorticity co-exist in the fluid domain. From the plots of the streamlines we conjecture that the co-existence of stagnation points and points of zero vorticity in the interior of the flow is a necessary condition for the eddy patterns to occur in the case of a Stokeslet induced flow in a spherical container. Another important observation made is that the vorticity on the boundary always vanishes when the slip parameter is equal to 0.5.

(b) *Flow due to a Stokeslet located away from the origin.* We gave a closed form representation of the stream function corresponding to an axisymmetric flow due to a Stokeslet located away from the origin. We found in the case of axisymmetric flow due to an off-centred Stokeslet that the stagnation points and the points of zero vorticity always co-exist and hence the eddy patterns in the flow domain always exist. We found analytically in this case that there are only two stagnation points in the flow domain. Further we do not find any new sets of points of zero vorticity for $\overline{\lambda} > 0.5$ and hence we conjecture that due the co-existence of the same sets of stagnation points and points of zero vorticity, the flow patterns remain the same thereafter.

We further discuss about '*Stokeslet reversal*', i.e., the position of the Stokeslet inside the sphere is found at which the strength of the image Stokeslet vanishes. In other words, we find the location where there is a sign change in the strength of the image Stokeslet indicating that the strength vanishes for some location of the Stokeslet inside the sphere.

In the case of slip-stick boundary conditions, it was found that this phenomenon does not occur for a non-axisymmetric flow due to a Stokeslet located away from the origin along the axis of symmetry. However for an axisymmetric flow with slip-stick boundary conditions it is found that the Stokeslet, if located at $c = \frac{1}{\sqrt{3(1+2\overline{\lambda})}}$, where $\overline{\lambda}$ is the slip parameter, makes the strength of the image Stokeslet vanish. As a limiting case, if $\overline{\lambda} \to 0$ the location of the Stokeslet inside the sphere is found to agree with that obtained by Maul and Kim [63] in the rigid case. It has been observed that, for an axisymmetric flow due to a Stokeslet located at the origin, there is no Stokeslet reversal.

In **Chapter 5**, we study the problem of a steady, Stokes flow past a particle of arbitrary shape satisfying slip-stick boundary conditions. Earlier, Payne and Pell [82] gave a formula for calculating the drag experienced by a rigid body in an axisymmetric flow of a viscous, incompressible fluid in terms of the Stokes stream function. But, for long, there was no such formula available for particles of arbitrary shape in the non-axisymmetric Stokes flows. Bourot [8], Hellou and Coutanceau [36] studied the problems of two-dimensional Stokes flows by using a technique of applying the no-slip condition using the method of least squares. Later, Lecoq et al. [53] extended this method to study the problems of the axisymmetric Stokes flows. G.B.Jeffery [41] studied the problem of viscous flow past an ellipsoidal particle. However, there was a need to develop methods to solve the more general problems of an arbitrary Stokes flow past an arbitrarily shaped body and there were several attempts to find solu-

tions to such problems [7], [46], [73], [112]. Recently, Radha et al. [88] found an approximate analytical solution for the problem of a steady, Stokes flow past an arbitrarily shaped rigid body with no-slip boundary conditions. They gave an analytic but approximate solution using the method of least squares. Their solution being analytic is valid in the entire domain rather than at certain pre-determined points as is often the case in some numerical methods. They demonstrated their method by considering an axisymmetric Stokes flow past two intersecting rigid spheres. We adopted the technique proposed by Radha et al. [88] to suggest a method for solving the problem of a steady, Stokes flow past a body of arbitrary shape with slip-stick boundary conditions by using the method of least squares. This method also gives an analytic but approximate solution. In particular, we demonstrate this method for a non-axisymmetric Stokes flow of a viscous incompressible fluid past an ellipsoid, where the flow is generated by a Stokeslet. We have scaled down the domain of the slip parameter $\overline{\lambda}$ from $[0, \infty)$ to $[0, 1)$ by using a suitable transformation. We observe that the magnitude of the drag and torque decreases with increasing value of the slip-parameter.

In **Chapter 6**, we give a summary of the important results obtained in the previous chapters.

Chapter 2

An arbitrary Stokes flow past a coated sphere in a fluid of a different viscosity

2.1 Introduction

The flow due to a spherical body moving in a viscous, incompressible fluid at low Reynolds numbers has been a problem of utmost importance both from the practical and theoretical point of view. Stokes [103] was the first to study the effects of viscosity on the motion of pendulums. Basset [5] studied the translational motion of a solid

sphere by considering a slip condition at the surface of the sphere. Hadamard [28, 29] and Rybczynski [95] examined the translational motion of a spherical fluid drop in another immiscible fluid. Hetsroni and Haber [38] discussed the problem of a single spherical droplet submerged in an unbounded viscous fluid of a different viscosity. Kawano et al. [43] have also studied thin liquid spherical shells moving at intermediate Reynolds numbers in immiscible liquids both numerically and experimentally. Dimitrakopoulos and Higdon [18] discussed the displacement of fluid droplets from solid boundaries in low Reynolds number shear flows using numerical computations. Numerous other works considering the motion of rigid and fluid spheres in both bounded and unbounded domains have been studied. The problem of Stokes flow past a fluid coated sphere in a fluid of a different viscosity is an important one owing to the manifold applications in science and engineering and has been studied by many researchers. O'Neill and Ranger [72] discussed the slow motion of a sphere moving through an interface of two immiscible fluids. By taking into account the displaced fluid by regarding it as a coating, where the no-slip boundary condition was modified permitting a certain degree of slip, O'Neill and Ranger [72] considered the slow uniform flow past a coated sphere in an immiscible viscous fluid and discussed its motion. Later Johnson [42], in his paper, examined the steady, axisymmetric Stokes flow past a solid sphere with a thin layer of immiscible fluid covering its surface, i.e., a fluid-film, in a uniform flow. In his work, he considered the fluid-fluid interface to be approximately spherical. The solution was obtained using a simple perturbation

technique where the perturbation expansion of the flow field is assumed in terms of the film thinness parameter to construct the solution. Gupalo et al. [25] also studied the Stokes flow past a sphere coated by a liquid film using the method of matched asymptotic expansions. Kawano and Hasimoto [43, 44] investigated the motion of multiphase compound drops by examining a liquid-solid compound drop, i.e., a rigid sphere completely coated with a thin liquid film. They made a numerical study on the motion of a sphere coated with a thin liquid film at low and intermediate Reynolds numbers. The problem of Stokes flow past a rigid sphere with a thin fluid layer of another viscous, incompressible fluid of a different viscosity has been studied analytically and numerically owing to the fact that it serves as a reasonably good model for many problems in science and industry. For instance, Anderson and Solomentsev [2] considered a general quadratic flow past a sphere and studied the hydrodynamic effects of a thin layer of material on the surface of the sphere where the fluid in the thin layer has a lower effective viscosity than the bulk solution. This is considered as a model for the surface of colloidal particles suspended in a liquid containing polymer molecules which do not hold on to the surface of the particles resulting in a '*depletion layer*' whose thickness is small compared to the radius of the spherical particles. Spherical solid shells coated with a thin layer of a fluid which are produced by solidifying liquid shells have applications in high performance solid fuels, artificial organs with filtration, high functional medicines, foods and compound structural materials which were discussed by Lee et al. [54] and Kawano et al. [43]. Kawano et al. [44] dis-

cussed the sequential production of spherical rigid shells by solidifying liquid shells. Kondo and Koishi [48] discussed the production of multilayer rigid shells or balls with diameter of micrometer size called microcapsules by controlling the interfacial polymerization in the physicochemical method. In this chapter, we suggest a method for solving the problem of an arbitrary Stokes flow of a viscous, incompressible fluid past a sphere coated with a thin film of fluid of a different viscosity. If the motion is sufficiently slow or the particle is sufficiently small and the fluid-film coating is very thin, then we can assume that the coating remains spherical, if the surface tension σ between the coating fluid and the ambient fluid is very high. Hence we assume that the fluid-film is very thin and that the surface tension forces are large enough to retain the spherical shape of the coating. We examine the relation between the ratio of the film-fluid viscosity to the surrounding fluid viscosity and the drag on the coated sphere in an arbitrary Stokes flow, when the unperturbed velocity is either harmonic or purely biharmonic. An important result obtained by Johnson [42], who considered a uniform flow, was that the drag reduction occurs when the sphere has a fluid-film where the ratio of the viscosity of the outer fluid to the viscosity of the fluid-film is greater than 4. We compare our result pertaining to the drag on the coated sphere in a general arbitrary Stokes flow with that of Johnson [42]. We also discuss the optimal thickness of coating required for the reduction of drag as a function of the above ratio of viscosities.

2.2 Mathematical formulation

We consider the steady arbitrary Stokes flow of a viscous, incompressible fluid of viscosity μ^e past a sphere of radius a coated with a thin layer of another immiscible fluid of a different viscosity μ^i whose thickness is $(b-a)$ where $b = a(1+\epsilon)$, $\epsilon > 0$. We shall use throughout our discussion, the superscript 'i' for the inner flow quantities in the region of the thin fluid film (coating) $a < r < b$, and 'e' for the outer flow quantities in the region $r > b$ respectively.

We also assume that the surface tension forces are large enough compared to the viscous forces which deform the fluid-film so as to retain the spherical shape of the coating. The discontinuity of normal stress across the interface of the two fluids is manifested as the pressure difference $p^i - p^e = \frac{2\sigma}{b}$, where σ is the surface tension and $b = a(1+\epsilon)$.

By non-dimensionalizing the variables as in Section 1.3 in Chapter 1, where $L = a$, we obtain the governing equations of motion in a non-dimensional form are as follows.

$$\nabla^2 \vec{\mathbf{q}}^{\alpha} = \nabla p^{\alpha}, \tag{2.2.1}$$

$$\nabla \cdot \vec{\mathbf{q}}^{\alpha} = 0, \tag{2.2.2}$$

where $\alpha = i$ for the region $1 < r < 1+\epsilon$ and $\alpha = e$ for the region $r > 1+\epsilon$ (outside the fluid film coating). The Stokes equations (2.2.1)-(2.2.2) admit the following representations for the velocity and pressure [79] in both the regions as follows.

$$\vec{\mathbf{q}}^{\alpha} = \nabla \times \nabla \times (\vec{\mathbf{r}} A^{\alpha}) + \nabla \times (\vec{\mathbf{r}} B^{\alpha}), \tag{2.2.3}$$

$$p^{\alpha} = \frac{\partial}{\partial r}(r \nabla^2 A^{\alpha}), \tag{2.2.4}$$

where

$$\nabla^4 A^{\alpha} = 0, \tag{2.2.5}$$

$$\nabla^2 B^{\alpha} = 0. \tag{2.2.6}$$

Suppose, in the absence of any rigid boundaries, the velocity $\vec{\mathbf{q}}_0$ and the pressure p_0 corresponding to the unperturbed flow is given by the representation (2.2.3)-(2.2.6) where $(\vec{\mathbf{q}}^{\alpha}, p^{\alpha}) = (\vec{\mathbf{q}}_0, p_0)$ in terms of the scalar functions $(A^{\alpha}, B^{\alpha}) = (A_0, B_0)$. Then the scalar functions A_0 and B_0 can be expanded in terms of spherical harmonics as follows

$$A_0 = \sum_{n=1}^{\infty} (\alpha_n r^n + \alpha'_n r^{n+2}) S_n(\theta, \phi), \tag{2.2.7}$$

$$B_0 = \sum_{n=1}^{\infty} \chi_n r^n T_n(\theta, \phi), \tag{2.2.8}$$

where

$$S_n(\theta, \phi) = \sum_{m=0}^{n} P_n^m(\zeta)(A_{nm} \cos m\phi + B_{nm} \sin m\phi), \qquad \zeta = \cos\theta$$

$$T_n(\theta, \phi) = \sum_{m=0}^{n} P_n^m(\zeta)(C_{nm} \cos m\phi + D_{nm} \sin m\phi),$$

$0 \le \theta \le \pi,\ 0 \le \phi \le 2\pi$ and $\alpha_n, \alpha'_n, \chi_n, A_{nm}, B_{nm}, C_{nm}, D_{nm}$ are known constants.

In the presence of a sphere of radius 1 with a coating of a thin film of fluid of thickness ϵ, we assume the modified flow to be as follows.

$$A^e = \sum_{n=1}^{\infty}(\alpha_n r^n + \alpha'_n r^{n+2} + \beta_n r^{-n-1} + \beta'_n r^{-n+1})S_n(\theta,\phi), \tag{2.2.9}$$

$$B^e = \sum_{n=1}^{\infty}(\chi_n r^n + \sigma_n r^{-n-1})T_n(\theta,\phi), \tag{2.2.10}$$

$$A^i = \sum_{n=1}^{\infty}(A_n r^n + B_n r^{n+2} + C_n r^{-n-1} + D_n r^{-n+1})S_n(\theta,\phi), \tag{2.2.11}$$

$$B^i = \sum_{n=1}^{\infty}(E_n r^n + F_n r^{-n-1})T_n(\theta,\phi), \tag{2.2.12}$$

where the unknown constants $A_n, B_n, C_n, D_n, E_n, F_n, \sigma_n, \beta_n$, and β'_n are to be determined from the following boundary conditions.

1. On the surface $r = 1$,

   the no-slip condition is satisfied

$$q^i_r(1,\theta,\phi) = q^i_\theta(1,\theta,\phi) = q^i_\phi(1,\theta,\phi) = 0. \tag{2.2.13}$$

2. On the surface $r = 1+\epsilon$,

   (a) the normal component of velocity vanishes

$$q^e_r(1+\epsilon,\theta,\phi) = q^i_r(1+\epsilon,\theta,\phi) = 0, \tag{2.2.14}$$

   (b) the tangential components of velocities are continuous

$$q^e_\theta(1+\epsilon,\theta,\phi) = q^i_\theta(1+\epsilon,\theta,\phi), \tag{2.2.15}$$

$$q^e_\phi(1+\epsilon,\theta,\phi) = q^i_\phi(1+\epsilon,\theta,\phi), \tag{2.2.16}$$

(c) the tangential components of stresses are continuous

$$\overline{\mu}T^e_{r\theta}(1+\epsilon,\theta,\phi) = T^i_{r\theta}(1+\epsilon,\theta,\phi), \tag{2.2.17}$$

$$\overline{\mu}T^e_{r\phi}(1+\epsilon,\theta,\phi) = T^i_{r\phi}(1+\epsilon,\theta,\phi), \tag{2.2.18}$$

where $\overline{\mu} = \frac{\mu^e}{\mu^i}$, μ^α is the dimensional viscosity, and $T^\alpha_{r\theta}$ and $T^\alpha_{r\phi}$ are the tangential stresses for $\alpha = e, i$ in the outer and inner regions of the fluid-film coating respectively.

Using the boundary conditions (2.2.13)-(2.2.18), we solve for the nine unknown constants in terms of α_n, α'_n and χ_n as follows :

$$\begin{aligned}
A_n &= -\overline{\mu}[(1+\epsilon)^{2n}(2(1+\epsilon)^{2n+3} + (2n+1) \\
&\quad -(1+\epsilon)^2(2n+3))((2n-1)\alpha_n + (2n+3)(1+\epsilon)^2\alpha'_n)]/M_n, \qquad (2.2.19)\\
B_n &= \overline{\mu}[(1+\epsilon)^{2n}(2(1+\epsilon)^{2n+1} + (2n-1) \\
&\quad -(1+\epsilon)^2(2n+1))((2n-1)\alpha_n + (2n+3)(1+\epsilon)^2\alpha'_n)]/M_n, \qquad (2.2.20)\\
C_n &= \overline{\mu}[((1+\epsilon)^{2n+1}(-2(1+\epsilon) - (1+\epsilon)^{2n+2}(2n-1) \\
&\quad +(1+\epsilon)^{2n}(2n+1))((2n-1)\alpha_n + (2n+3)(1+\epsilon)^2\alpha'_n))]/M_n, \qquad (2.2.21)\\
D_n &= \overline{\mu}[(1+\epsilon)^{2n}(2 + (1+\epsilon)^{2n+3}(2n+1) \\
&\quad -(1+\epsilon)^{2n+1}(2n+3))((2n-1)\alpha_n + (2n+3)(1+\epsilon)^2\alpha'_n)]/M_n, \qquad (2.2.22)
\end{aligned}$$

$$
\begin{aligned}
E_n &= [-(1+\epsilon)^{2n+1}(2n+1)\overline{\mu}\chi_n]/N_n, && (2.2.23)\\
F_n &= [(1+\epsilon)^{2n+1}(2n+1)\overline{\mu}\chi_n]/N_n, && (2.2.24)\\
\sigma_n &= [(1+\epsilon)^{2n+1}(-(1+\epsilon)^{2n+1}(n-1)(\overline{\mu}-1)\\
&\quad +((n+2)+\overline{\mu}(n-1)))\chi_n]/N_n, && (2.2.25)\\
\beta_n &= [(1+\epsilon)^{2n+1}(-2(1+\epsilon)^{2n+4}(4n^2+4n-3)\overline{\mu}\alpha_n'\\
&\quad +2(1+\epsilon)^{4n+3}((2n-1)\alpha_n+(2n-2\overline{\mu}+1)\alpha_n')\\
&\quad -(1+\epsilon)^{2n+4}(2n+1)((2n-1)\alpha_n-(2n+1)(\overline{\mu}-1)(1+\epsilon)^2\alpha_n')\\
&\quad +(1+\epsilon)^{2n}(2n+1)((2n-1)\alpha_n+(2n+1)(1+\epsilon)^2(\overline{\mu}+1)\alpha_n')\\
&\quad -2(1+\epsilon)((2n-1)\alpha_n+(2n+2\overline{\mu}+1)\alpha_n'))]/M_n, && (2.2.26)\\
\beta_n' &= [(1+\epsilon)^{2n-1}(-2(1+\epsilon)^{2n+2}(4n^2+4n-3)\overline{\mu}\alpha_n\\
&\quad +(1+\epsilon)^{2n}(2n+1)((2n+1)(\overline{\mu}-1)\alpha_n\\
&\quad -(2n+3)(1+\epsilon)^2\alpha_n')+2(1+\epsilon)((2n-2\overline{\mu}+1)\alpha_n\\
&\quad +(2n+3)(1+\epsilon)^2\alpha_n')+(1+\epsilon)^{2n+4}(2n+1)((2n+1)(\overline{\mu}+1)\alpha_n\\
&\quad +(2n+3)(1+\epsilon)^2\alpha_n')-2(1+\epsilon)^{4n+3}((2n+2\overline{\mu}+1)\alpha_n\\
&\quad +(2n+3)(1+\epsilon)^2\alpha_n'))]/M_n, && (2.2.27)
\end{aligned}
$$

where

$$
\begin{aligned}
M_n &= 4(1+\epsilon)(\overline{\mu}-1)+2(1+\epsilon)^{2n+2}(4n^2+4n-3)\overline{\mu}\\
&\quad +4(1+\epsilon)^{4n+3}(\overline{\mu}+1)-(1+\epsilon)^{2n}(2n+1)((2n+1)\overline{\mu}-2)\\
&\quad -(1+\epsilon)^{2n+4}(2n+1)((2n+1)\overline{\mu}+2),
\end{aligned}
$$

$$N_n = (n+2)(\overline{\mu}-1) - (1+\epsilon)^{2n+1}((n+2)\overline{\mu}+n-1).$$

2.3 Drag

The drag experienced by the coated sphere in a dimensionless form is

$$\begin{aligned}
\vec{\mathbf{D}}_c &= \int_0^{\pi}\int_0^{2\pi} [T^e_{rr}\hat{\mathbf{e}}_r + T^e_{r\theta}\hat{\mathbf{e}}_\theta + T^e_{r\phi}\hat{\mathbf{e}}_\phi]_{r=(1+\epsilon)}(1+\epsilon)^2\sin\theta d\theta d\phi, \\
&= 8\pi(1+\epsilon)\left[\left(\frac{3(2+\epsilon)(2\epsilon^2+5\epsilon+5)+\overline{\mu}\epsilon(4\epsilon^2+15\epsilon+15)}{2(2+\epsilon)(2\epsilon^2+5\epsilon+5)+\overline{\mu}\epsilon(4\epsilon^2+15\epsilon+15)}\right)\alpha_1\right. \\
&\quad \left. + \left(\frac{5(1+\epsilon)^2(2+\epsilon)(2\epsilon^2+5\epsilon+5)}{2(2+\epsilon)(2\epsilon^2+5\epsilon+5)+\overline{\mu}\epsilon(4\epsilon^2+15\epsilon+15)}\right)\alpha_1'\right] \\
&\quad \times(A_{11}\hat{\mathbf{i}} + B_{11}\hat{\mathbf{j}} + A_{10}\hat{\mathbf{k}}), \\
&= \left(8\pi(1+\epsilon)\left(\frac{3X+Y}{2X+Y}\right)\alpha_1 + 40\pi(1+\epsilon)^3\left(\frac{X}{2X+Y}\right)\alpha_1'\right) \\
&\quad \times(A_{11}\hat{\mathbf{i}} + B_{11}\hat{\mathbf{j}} + A_{10}\hat{\mathbf{k}}), \qquad (2.3.1) \\
&= \left(4\pi(1+\epsilon)\left(\frac{3X+Y}{2X+Y}\right)[\vec{\mathbf{q}}_0]_0 + 2\pi(1+\epsilon)^3\left(\frac{X}{2X+Y}\right)[\nabla^2\vec{\mathbf{q}}_0]_0\right), \qquad (2.3.2)
\end{aligned}$$

where

$$X = (2+\epsilon)(2\epsilon^2+5\epsilon+5), \qquad (2.3.3)$$

$$Y = \overline{\mu}\epsilon(4\epsilon^2+15\epsilon+15), \qquad (2.3.4)$$

T^e_{rr} is the dimensionless normal component of stress of the ambient fluid. Observe that we have used the relations

$$[\vec{\mathbf{q}}_0]_0 = 2\alpha_1(A_{11}\hat{\mathbf{i}} + B_{11}\hat{\mathbf{j}} + A_{10}\hat{\mathbf{k}}), \qquad (2.3.5)$$

$$[\nabla^2\vec{\mathbf{q}}_0]_0 = 20\alpha_1'(A_{11}\hat{\mathbf{i}} + B_{11}\hat{\mathbf{j}} + A_{10}\hat{\mathbf{k}}), \tag{2.3.6}$$

where $[\vec{\mathbf{q}}_0]_0$ and $[\nabla^2\vec{\mathbf{q}}_0]_0$ denote the unperturbed velocity and its Laplacian evaluated at the centre of the sphere $r = 0$ respectively.

We find it convenient to express the drag on the coated sphere as follows to enable us to discuss some special cases.

$$\vec{\mathbf{D}}_c = 6\pi(1+\epsilon)\left[\frac{2(3X+Y)}{3(2X+Y)}\right][\vec{\mathbf{q}}_0]_0 + \pi(1+\epsilon)^3\left[\frac{2X}{2X+Y}\right][\nabla^2\vec{\mathbf{q}}_0]_0, \tag{2.3.7}$$

$$= 6\pi(1+\epsilon)[1-A][\vec{\mathbf{q}}_0]_0 + \pi(1+\epsilon)^3[1-B][\nabla^2\vec{\mathbf{q}}_0]_0, \tag{2.3.8}$$

where $A = \frac{Y}{3(2X+Y)}$, $B = \frac{Y}{2X+Y}$. Since $\epsilon > 0$, we observe that $X > 0$ and $Y > 0$. Hence $0 < Y < 2X + Y$. Thus we find that $0 < A < 1$ and $0 < B < 1$.

Using Almansi's result [1], $\vec{\mathbf{q}}_0$ can be expressed as $\vec{\mathbf{q}}_0 = \vec{\mathbf{q}}_1 + r^2\vec{\mathbf{q}}_2$, where $\nabla^2\vec{\mathbf{q}}_1 = 0$, $\nabla^2\vec{\mathbf{q}}_2 = 0$. Then we observe that $\nabla^2\vec{\mathbf{q}}_0 = 6\vec{\mathbf{q}}_2 + 4r\frac{\partial\vec{\mathbf{q}}_2}{\partial r}$. We now discuss some special cases making use of these results.

1. **Case A**: Suppose $\vec{\mathbf{q}}_0$ is harmonic, i.e., $\vec{\mathbf{q}}_2 = 0$. This implies that

$$\vec{\mathbf{D}}_c = 6\pi(1+\epsilon)(1-A)[\vec{\mathbf{q}}_1]_0. \tag{2.3.9}$$

The drag experienced by a rigid sphere of radius $(1+\epsilon)$ in this case is [21]

$$\vec{\mathbf{D}}_\epsilon = 6\pi(1+\epsilon)[\vec{\mathbf{q}}_1]_0. \tag{2.3.10}$$

Hence we can conclude that $|\vec{\mathbf{D}}_c| < |\vec{\mathbf{D}}_\epsilon|$ since $0 < A < 1$. □

2. **Case B**: Suppose $\vec{\mathbf{q}}_0$ is purely biharmonic, i.e., $\vec{\mathbf{q}_0} = r^2\vec{\mathbf{q}}_2 \neq 0, \vec{\mathbf{q}}_1 = 0$. Then $[\vec{\mathbf{q}}_0]_0 = [r^2\vec{\mathbf{q}}_2]_0 = 0$ and $[\nabla^2\vec{\mathbf{q}}_0]_0 = [\nabla^2(\vec{\mathbf{q}}_1 + r^2\vec{\mathbf{q}}_2)]_0 = [6\vec{\mathbf{q}}_2]_0$. In this case, the drag experienced by a rigid sphere [21] of radius $(1+\epsilon)$ and the drag experienced by the coated sphere are respectively given by

$$\vec{\mathbf{D}}_\epsilon = \pi(1+\epsilon)^3[\nabla^2\vec{\mathbf{q}}_0]_0 = 6\pi(1+\epsilon)^3[\vec{\mathbf{q}}_2], \tag{2.3.11}$$

$$\vec{\mathbf{D}}_c = \pi(1+\epsilon)^3(1-B)[\nabla^2\vec{\mathbf{q}}_0]_0 = 6\pi(1+\epsilon)^3(1-B)[\vec{\mathbf{q}}_2]_0. \tag{2.3.12}$$

Again we can conclude that $|\vec{\mathbf{D}}_c| < |\vec{\mathbf{D}}_\epsilon|$ since $0 < B < 1$. □

So in both the above cases, i.e., when the velocity is harmonic or purely biharmonic, the magnitude of drag on the coated sphere decreases compared to the drag on a rigid sphere of radius $(1+\epsilon)$.

The drag experienced by an uncoated rigid sphere of radius 1 in the steady Stokes flow of a viscous, incompressible fluid in a dimensionless form is [21]

$$\vec{\mathbf{D}}_0 = 6\pi[\vec{\mathbf{q}}_0]_0 + \pi[\nabla^2\vec{\mathbf{q}}_0]_0. \tag{2.3.13}$$

Let $0 < \epsilon << 1$, where ϵ is the thickness of the thin fluid-film coating the sphere of radius 1. Expanding (2.3.2) in terms of ϵ, we get the drag as

$$\begin{aligned}\vec{\mathbf{D}}_c &= 6\pi\left[1+\epsilon\left(1-\frac{\overline{\mu}}{4}\right)+O(\epsilon^2)\right][\vec{\mathbf{q}}_o]_o \\ &\quad +\pi\left[1+3\epsilon\left(1-\frac{\overline{\mu}}{4}\right)+O(\epsilon^2)\right][\nabla^2\vec{\mathbf{q}}_o]_o.\end{aligned} \tag{2.3.14}$$

We also observe that for $\epsilon = 0$, we can deduce the expression for drag on an uncoated rigid sphere of radius 1 given by (2.3.13).

For a harmonic $\vec{\mathbf{q}}_0$, i.e., $\nabla^2\vec{\mathbf{q}}_0 = 0$ and for very small values of ϵ,

$$\vec{\mathbf{D}}_c = 6\pi\left[1+\epsilon\left(1-\frac{\overline{\mu}}{4}\right)\right][\vec{\mathbf{q}}_0]_0. \tag{2.3.15}$$

The formula for drag on a coated sphere given by Johnson [42] can be deduced as a special case of the above formula as he considered a uniform flow, which is a particular case of the unperturbed velocity being harmonic. Johnson [42] concluded that the magnitude of drag on the coated sphere reduces when $\overline{\mu} > 4$. While this result is observed to be true from (2.3.15), when the unperturbed velocity is harmonic, we find that the drag may also increase in a general Stokes flow. We illustrate this by giving the following two examples.

(a) **Harmonic case**: Consider a uniform flow for which the unperturbed velocity $\vec{\mathbf{q}}_0$ is given by the scalar functions A_0, B_0 as follows

$$A_0 = \frac{r}{2}\sin\theta\cos\phi, \tag{2.3.16}$$

$$B_0 = 0. \tag{2.3.17}$$

Let $\overline{\mu} = 8$. Then, from (2.3.13), $|\vec{\mathbf{D}}_0|$ which is the magnitude of drag on a rigid sphere of radius 1 is here equal to 6π.

The drag on the coated sphere is given from (2.3.15) as

$$\vec{\mathbf{D}}_c = 6\pi[1-\epsilon]\hat{\mathbf{i}}. \tag{2.3.18}$$

Hence we observe that $|\vec{\mathbf{D}}_c| < |\vec{\mathbf{D}}_0|$ which agrees with the result of Johnson [42] that the drag reduces when $\overline{\mu} > 4$. □

(b) **Non-harmonic case**: For the same values of $\overline{\mu}$, we now consider a flow for which

$$A_0 = \left(\frac{r}{2} - \frac{3r^3}{20}\right)\sin\theta\cos\phi, \tag{2.3.19}$$

$$B_0 = 0. \tag{2.3.20}$$

Then, from (2.3.13), the magnitude of drag on a rigid sphere of radius 1 is equal to

$$|\vec{\mathbf{D}}_0| = 3\pi. \tag{2.3.21}$$

Also, the drag on the coated sphere is given from (2.3.14) as

$$\vec{\mathbf{D}}_c = 6\pi\,(1-\epsilon)\,\hat{\mathbf{i}} - 3\pi\,(1-3\epsilon)\,\hat{\mathbf{i}}, \tag{2.3.22}$$

$$= 3\pi(1+\epsilon)\hat{\mathbf{i}}. \tag{2.3.23}$$

So we observe that $|\vec{\mathbf{D}}_c| > |\vec{\mathbf{D}}_0|$ even though $\overline{\mu} > 4$. Thus we cannot conclude that the drag reduces in a general case even if $\overline{\mu} > 4$. □

Optimal fluid-film coating required for minimum drag:

We observed that when $\overline{\mu} > 4$, the drag on the coated sphere decreases when the unperturbed flow is harmonic. Motivated by this fact, we now calculate the thickness of the fluid-film coating for which the drag is minimum for different values of $\overline{\mu} > 4$, when the unperturbed velocity is harmonic. For this, we observe that the formula for drag given in (2.3.2) can be rewritten as $\vec{\mathbf{D}}_c = D_H[\vec{\mathbf{q}_o}]_0$ where

$$D_H = 6\pi(1+\epsilon)\left[\frac{6(2+\epsilon)(2\epsilon^2+5\epsilon+5)+2\overline{\mu}\epsilon(4\epsilon^2+15\epsilon+15)}{6(2+\epsilon)(2\epsilon^2+5\epsilon+5)+3\overline{\mu}\epsilon(4\epsilon^2+15\epsilon+15)}\right]. \tag{2.3.24}$$

For each value of μ, we determine the corresponding value of ϵ (coating thickness) for which D_H assumes a minimum value (refer Table 2.3.1). This is done by differentiating (2.3.24) with respect to ϵ and equating it to zero. The resulting value of ϵ (refer Table 2.3.1 and Figure 2.3.1(a)) is observed to give a minimum value of D_H. Repeating this process for different values of $\overline{\mu} > 4$, we find the thickness of coating for which the drag is minimum for each value of $\overline{\mu}$. The corresponding values of $\overline{\mu}$, ϵ and D_H are tabulated in Table 2.3.1. From Table 2.3.1, we observe that if $\overline{\mu}$ is increased, then the thickness of the coating ϵ for which the drag is minimum also increases. From equation (2.3.2), we observe that in a similar manner, for very small values of ϵ, the drag on the coated sphere decreases when the unperturbed flow is purely biharmonic when $\overline{\mu} > 4$. We write $\vec{\mathbf{D}}_c = D_{BH}[\nabla^2 \vec{\mathbf{q}_o}]_0$ where

$$D_{BH} = \pi(1+\epsilon)^3 \left[\frac{2(2+\epsilon)(2\epsilon^2+5\epsilon+5)}{2(2+\epsilon)(2\epsilon^2+5\epsilon+5)+\overline{\mu}\epsilon(4\epsilon^2+15\epsilon+15)}\right]. \qquad (2.3.25)$$

For this case also, we have tabulated the values of ϵ and D_{BH} for increasing values of $\overline{\mu} > 4$. Here also we can conclude that the thickness of the fluid-film coating, for which the drag is minimum, increases with increasing values of $\overline{\mu}$ (refer Figure 2.3.1(b), Table 2.3.2). Thus in both these cases, we find that the viscosity of the coating should be lower than the viscosity of the ambient fluid so that the drag is minimum for a given thickness of coating.

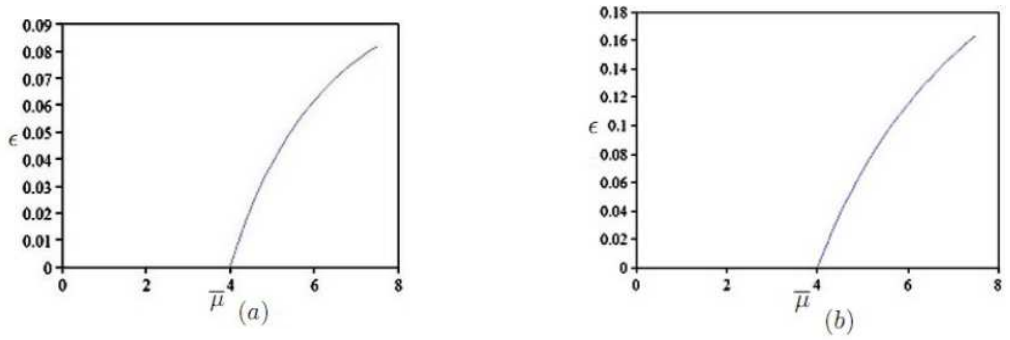

Figure 2.3.1: *Change in ϵ with $\overline{\mu}$ for unperturbed (a) harmonic velocity, (b) biharmonic velocity when the magnitude of the drag is minimum.*

$\overline{\mu}$	ϵ	*Drag on the coated sphere*	$\overline{\mu}$	ϵ	*Drag on the coated sphere*
4.00	0	18.8495	6.00	0.061643	18.5876
4.25	0.0111644	18.8428	6.25	0.069857	18.5027
4.50	0.03063	18.7985	6.75	0.07335	18.4544
5.00	0.038416	18.7658	7.00	0.076498	18.4058
5.25	0.045291	18.7282	7.25	0.079339	18.3573
5.50	0.056806	18.6432	7.50	0.081909	18.309

Table 2.3.1: *Optimal coating thickness ϵ needed for a given $\overline{\mu}$ for the drag to be minimum when the unperturbed velocity is harmonic.*

$\overline{\mu}$	ϵ	*Drag on the coated sphere*	$\overline{\mu}$	ϵ	*Drag on the coated sphere*
4.00	0	3.1416	6.00	0.114981	3.9255
4.25	0.019719	3.13596	6.25	0.12455	3.88502
4.50	0.037439	3.12081	6.50	0.133437	3.84386
4.75	0.053455	3.09835	6.75	0.141714	3.80236
5.00	0.068005	3.07031	7.00	0.14944	3.76078
5.50	0.0104647	3.96487	7.50	0.16345	3.67819

Table 2.3.2: *Optimal coating thickness ϵ needed for a given $\overline{\mu}$ for the drag to be minimum when the unperturbed velocity is biharmonic.*

2.4 Torque

The torque on an uncoated rigid sphere of radius 1 in a dimensionless form is $\vec{\mathbf{T}}_0 = 4\pi[\nabla \times \vec{\mathbf{q}_0}]_0$. The torque on the coated sphere is

$$\vec{\mathbf{T}}_c = 4\pi \left[1 + \frac{(\epsilon^3 + 3\epsilon^2 + 3\epsilon)(1-\overline{\mu})}{(\epsilon^3 + 3\epsilon^2 + 3\epsilon)\overline{\mu} + 1}\right] [\nabla \times \vec{\mathbf{q}_o}]_o, \tag{2.4.1}$$

$$= 4\pi(1+\epsilon)^3 \left[1 - \frac{(\epsilon^3 + 3\epsilon^2 + 3\epsilon)\overline{\mu}}{(\epsilon^3 + 3\epsilon^2 + 3\epsilon)\overline{\mu} + 1}\right] [\nabla \times \vec{\mathbf{q}_o}]_o. \tag{2.4.2}$$

It is clear from (2.4.1) that the magnitude of torque on the coated sphere increases when $\overline{\mu} < 1$ and reduces when $\overline{\mu} > 1$ compared to the torque experienced by an uncoated rigid sphere of unit radius. However the torque on the coated sphere always decreases compared to that on a rigid sphere of radius $(1+\epsilon)$ as observed from (2.4.2).

2.5 Axisymmetric flow

The axisymmetric flow can be discussed by choosing [79]

$$\frac{\partial A^e(r,\theta)}{\partial\theta} = \frac{\psi^e(r,\theta)}{r\sin\theta}, \frac{\partial A^i(r,\theta)}{\partial\theta} = \frac{\psi^i(r,\theta)}{r\sin\theta}, B^e(r,\theta) = B^i(r,\theta) = 0,$$

in (2.2.3)-(2.2.6). Then the radial and cross-radial velocities in both the regions are given as follows

$$q_r^e(r,\theta) = -\frac{1}{r^2\sin\theta}\frac{\partial\psi^e(r,\theta)}{\partial\theta}, \tag{2.5.1}$$

$$q_\theta^e(r,\theta) = \frac{1}{r\sin\theta}\frac{\partial\psi^e(r,\theta)}{\partial r}, \tag{2.5.2}$$

$$q_r^i(r,\theta) = -\frac{1}{r^2\sin\theta}\frac{\partial\psi^i(r,\theta)}{\partial\theta}, \tag{2.5.3}$$

$$q_\theta^i(r,\theta) = \frac{1}{r\sin\theta}\frac{\partial\psi^i(r,\theta)}{\partial r}. \tag{2.5.4}$$

Then the drag experienced by the coated sphere in terms of the stream function of the unperturbed flow in a dimensionless form, turns out to be

$$\begin{aligned}\vec{\mathbf{D}}_c = & -6\pi(1+\epsilon)\left[\frac{2(3X+Y)}{3(2X+Y)}\right][\nabla\times(\hat{\mathbf{e}}_\phi\frac{\psi_0}{r\sin\theta})]_0 \\ & -\pi(1+\epsilon)^3\left[\frac{2X}{2X+Y}\right]\left[\nabla\times\left(\hat{\mathbf{e}}_\phi\frac{D^2\psi_0}{r\sin\theta}\right)\right]_0.\end{aligned} \tag{2.5.5}$$

The torque in this case is zero.

2.6 Examples

2.6.1 Stokeslet : Consider a Stokeslet of strength $(F_1/8\pi)$ located at $(0,0,c)$ $(c>1+\epsilon)$ whose axis is along the positive direction of the x-axis. The corresponding

expressions for A_0 and B_0 due to the presence of the Stokeslet when $1+\epsilon < r < c$ are

$$\begin{aligned} A_0(r,\theta,\phi) &= \frac{F_1}{8\pi}\sum_{n=1}^{\infty}\left[\frac{r^{n+2}}{(n+1)(2n+3)c^{n+2}}\right. \\ &\quad \left. - \frac{(n-2)r^n}{n(n+1)(2n-1)c^n}\right] P_n^1(\zeta)\cos\phi, \qquad (2.6.1) \\ B_0(r,\theta,\phi) &= \frac{F_1}{4\pi}\sum_{n=1}^{\infty}\left[\frac{r^n}{n(n+1)c^{n+1}}\right] P_n^1(\zeta)\sin\phi. \qquad (2.6.2) \end{aligned}$$

From the above expressions, we find that

$$\alpha_1 = \left(\frac{F_1}{8\pi}\right)\frac{1}{2c}, \quad \alpha_1' = \left(\frac{F_1}{8\pi}\right)\frac{1}{10c^3}, \quad \chi_1 = \left(\frac{F_1}{4\pi}\right)\frac{1}{2c^2}.$$

The drag experienced by a coated sphere is given from equation (2.3.2) as

$$\vec{\mathbf{D}}_c = \frac{(1+\epsilon)F_1[(3c^2+(1+\epsilon)^2)X + c^2Y]}{2c^3(2X+Y)}\hat{\mathbf{i}}. \qquad (2.6.3)$$

2.6.2 Potential doublet : Consider a doublet of strength M with its axis along the positive direction of z-axis in an axisymmetric flow located at $(0,0,c)$ $(c > 1+\epsilon)$. The stream function due to the doublet in an unbounded fluid is given by

$$\psi_0 = -\frac{Mr^2\sin^2\theta}{R_1^3}, \quad R_1^2 = r^2 - 2rc\cos\theta + c^2. \qquad (2.6.4)$$

For $r < c$

$$\psi_0 = -M\sum_{n=1}^{\infty}\frac{r^{n+1}}{c^{n+2}}P_n^1(\zeta)\sin\theta. \qquad (2.6.5)$$

Here, $\alpha_n = M/c^{n+2}$, $\alpha_n' = 0$.

From (2.5.5), the drag on the coated sphere is given by

$$\vec{\mathbf{D}}_c = 6\pi(1+\epsilon)\left[\frac{2(3X+Y)}{3(2X+Y)}\right]\left(\frac{2M}{c^3}\hat{\mathbf{k}}\right). \qquad (2.6.6)$$

2.7 Conclusions

We suggested a general method to discuss an arbitrary Stokes flow of a viscous, incompressible fluid past a sphere coated with a thin layer of a fluid of a different viscosity. In particular, we gave the expressions for the drag and the torque on the coated sphere in both axisymmetric and non-axisymmetric Stokes flows. We showed that the drag on the coated sphere decreases compared to the drag on a rigid sphere of the same radius whenever the unperturbed velocity is either harmonic or purely biharmonic. We also showed that the drag on a rigid sphere is greater than the drag on a coated sphere whenever the unperturbed flow either purely harmonic or biharmonic which is a generalization of the result by Johnson [42] who considered the unperturbed flow velocity to be uniform. Moreover, we determined the thickness of the coating for which the drag is minimum for $\overline{\mu} > 4$ for a fixed value of the viscosity of the ambient fluid, when the unperturbed velocity is harmonic or purely biharmonic. We also showed that the magnitude of the torque experienced by the fluid coated sphere always decreases compared to the torque experienced by a rigid sphere of the same radius.

Chapter 3

An arbitrary unsteady Stokes flow in and around a liquid sphere

3.1 Introduction

Taylor and Acrivos [108] studied the deformation and drag of a liquid drop in an unbounded quiescent fluid. Matunobu [61, 62], Hetsroni and Haber [38] employed Lamb's [50] solution of steady Stokes equations to study the flow fields exterior and interior to a liquid droplet immersed in an unbounded viscous fluid with a different viscosity. Similarly, Fuentes et al. [23, 24] studied the images of singularities which lie outside the droplet using Lamb's solution. Later Palaniappan et al. [79] gave the solution in a closed form for a general non-axisymmetric, steady Stokes flow in and around a fluid sphere when the singularities of

the given flow lie outside the sphere using a solution of Stokes equations proposed by them [79] in the form of a Sphere theorem. Using the same solution (Palaniappan et al. [79]), the general non-axisymmetric motion inside a liquid sphere generated by singularities inside was studied by Padmavathi et al. [76] by presenting the solution as a Sphere theorem in a closed form which complements the result of Hetsroni and Haber [38]. All existing Sphere theorems were recovered as special cases of these theorems. In the recent years, the problem of unsteady Stokes flow past a particle has also engaged the attention of scientists and researchers. The motion of particles of different geometries in unsteady, viscous flows have been studied by several researchers like Lawrence and Weinbaum [52], Kim and Karrila [47], Pozrikidis [83], Lovalenti and Brady [59, 60], Sano [34], Coimbra and Rangel [14], Feng and Joseph [22], Yang and Leal [117], Maxey and Riley [64], Mazur and Bedeaux [65], Michaelidis and Feng [68], Stone and Bush [105], Dohara [19] and Venkatlaxmi et al. [113, 114]. Pozrikidis [83] used a singularity method for the computation of unsteady Stokes flows. In particular, he considered the translational oscillations of a spherical drop convected in a uniform streaming flow or moving under the influence of a body force, placed in an ambient fluid of a different viscosity and concluded that the spherical shape of the liquid drop is retained independent of the surface tension of the liquid drop. A similar result was arrived at Sy and Lightfoot [106] who considered the flow due to a spherical inviscid bubble executing translational oscillations in a viscous fluid and also by Chisnell [11] who considered the unsteady motion of a liquid drop moving vertically under gravity. Pozrikidis [85] also discussed the contributions of other researchers on the unsteady motion of a viscous drop in a bibliographical note. Rallison [89, 90] discussed about the

deformation of small viscous drops and bubbles in shear flows and reviewed the theory of shear induced small deformation of viscous drops in a note on time-dependent deformation of almost spherical viscous drops. Stone [104] also discussed the dynamics of drop deformation and breakup in viscous fluids at low Reynolds numbers.

The problem discussed in this chapter pertains to an oscillatory Stokes flow of a viscous incompressible fluid past a liquid sphere of a different viscosity where a general method to determine the shape of the liquid droplet which undergoes a slight deformation has been suggested. We make use of the complete general solution of unsteady Stokes equations proposed by Venkatlaxmi et al. [113, 114] to discuss this problem. The motivation for the current work is drawn from that of Hetsroni and Haber [38] who considered a steady Stokes flow inside and around a liquid 'droplet'. They used the Landau and Lifshitz's [51] condition to discuss the deformation of the liquid drop in a steady Stokes flow. We use a similar approach to study the flow generated by an arbitrary oscillatory Stokes flow past a fluid sphere of a different viscosity and give a method to find the flow quantities inside and outside the liquid sphere. The drag on the liquid sphere is also calculated. The droplet is assumed to be spherical as a first approximation and then the equation of the interface is later obtained by adopting an iterative method as in the work of Hetsroni and Haber [38]. We also deal with the flow inside and outside a liquid sphere generated due to an oscillating singularity located in the interior of the sphere. We also determine the shape of the deformed liquid spheres in both the cases. We observe that the deformation is mainly affected by two parameters, namely, the ratio of the viscosities of the two fluids and also the capillary number which is a ratio of the viscous forces and the surface tension forces.

3.2 Statement of the problem

We consider an arbitrary unsteady Stokes flow of a viscous, incompressible fluid of viscosity μ_0 past a liquid sphere of radius a of a different viscosity μ^i. We assume that the flow inside and outside the liquid sphere is governed by unsteady Stokes equations. We use the suffix 0 to denote the flow quantities corresponding to the unperturbed flow and the superscripts e and i to denote the flow quantities corresponding to perturbed flow in the regions $r > a$ and $r < a$ respectively.

Assume $\vec{\mathbf{q}}^j = \vec{\tilde{\mathbf{q}}}^j e^{-i\omega t}$, $p^j = P^j + \tilde{p}^j e^{-i\omega t}$, where $j = 0, e, i$, P^j is a constant, ω is the frequency of oscillation. Then by equations (1.1.33)-(1.1.34) in Section 1.1 of Chapter 1, the governing equations of motion can be expressed in the form

$$\mu^j(\nabla^2 - \lambda_j^2)\vec{\mathbf{q}}^j = \nabla p^j, \tag{3.2.1}$$

$$\nabla.\vec{\mathbf{q}}^j = 0, \tag{3.2.2}$$

where $\lambda_j^2 = \frac{-i\omega}{\nu^j}$.

Flow past a sphere $r = 1$:

We non-dimensionalize equations (3.2.1)-(3.2.2) by using the non-dimensional variables (with $L = a$) as in Section 1.3 in Chapter 1, to obtain

$$(\nabla^2 - \lambda_j^2)\vec{\mathbf{q}}^j = \nabla p^j, \tag{3.2.3}$$

$$\nabla.\vec{\mathbf{q}}^j = 0. \tag{3.2.4}$$

Using the representation of the solution for unsteady Stokes equations due to Venkatlaxmi

et al. [113, 114], we can express the flow fields as follows.

$$\vec{\mathbf{q}}^j = \nabla \times \nabla \times (\vec{\mathbf{r}} A^j) + \nabla \times (\vec{\mathbf{r}} B^j), \tag{3.2.5}$$

$$p^j = P^j + \frac{\partial}{\partial r}(r(\nabla^2 - \lambda_j^2)A^j), \tag{3.2.6}$$

where P^j is a constant, $j = 0, e, i$. Then the scalar functions corresponding to the unperturbed flow can be written as

$$A_0 = \sum_{n=1}^{\infty}(\alpha_n r^n + \alpha'_n f_n(\lambda_e r))S_n(\theta,\phi), \tag{3.2.7}$$

$$B_0 = \sum_{n=1}^{\infty}(\epsilon_n f_n(\lambda_e r))T_n(\theta,\phi), \tag{3.2.8}$$

and

$$S_n(\theta,\phi) = \sum_{m=0}^{n} P_n^m(\zeta)(A_{nm}\cos m\phi + B_{nm}\sin m\phi),$$

$$T_n(\theta,\phi) = \sum_{m=0}^{n} P_n^m(\zeta)(C_{nm}\cos m\phi + D_{nm}\sin m\phi).$$

Here $\mu_0 = \mu^e$ and $\lambda_0 = \lambda_e$. The constants α_n, α'_n and ϵ_n as well as A_{nm}, B_{nm}, C_{nm} and D_{nm} are known constants for a given unperturbed flow. In the presence of a liquid sphere $r = 1$, the flow in the region $r > 1$ is given as follows.

$$A^e = \sum_{n=1}^{\infty}(\alpha_n r^n + \alpha'_n f_n(\lambda_e r) + \beta_n r^{-n-1} + \beta'_n g_n(\lambda_e r))S_n(\theta,\phi), \tag{3.2.9}$$

$$B^e = \sum_{n=1}^{\infty}(\epsilon_n f_n(\lambda_e r) + \epsilon'_n g_n(\lambda_e r))T_n(\theta,\phi). \tag{3.2.10}$$

Similarly, the flow inside the liquid sphere in the region $r < 1$ is given as follows.

$$A^i = \sum_{n=1}^{\infty}(a_n r^n + b_n f_n(\lambda_i r))S_n(\theta,\phi), \tag{3.2.11}$$

$$B^i = \sum_{n=1}^{\infty}(e_n f_n(\lambda_i r))T_n(\theta,\phi), \tag{3.2.12}$$

where $R = \lambda_j r$, $j = e, i$ in the regions $r > 1$ and $r < 1$ respectively.

The unknown constants to be determined are β_n, β'_n, ϵ'_n, a_n, b_n and e_n. The boundary conditions in a non-dimensional form are as follows.

On the interface of the two fluid regions, i.e. $(r = 1)$,

(1) the vanishing of the normal velocities

$$q_r^e(1,\theta,\phi) = q_r^i(1,\theta,\phi), \tag{3.2.13}$$

$$= 0, \tag{3.2.14}$$

(2) continuity of the tangential velocities and stresses.

$$q_\theta^e(1,\theta,\phi) = q_\theta^i(1,\theta,\phi), \tag{3.2.15}$$

$$q_\phi^e(1,\theta,\phi) = q_\phi^i(1,\theta,\phi), \tag{3.2.16}$$

$$\overline{\mu}T_{r\theta}^e(1,\theta,\phi) = T_{r\theta}^i(1,\theta,\phi), \tag{3.2.17}$$

$$\overline{\mu}T_{r\phi}^e(1,\theta,\phi) = T_{r\phi}^i(1,\theta,\phi), \tag{3.2.18}$$

where $\overline{\mu} = \frac{\mu^e}{\mu^i}$, q_θ^j, q_ϕ^j are the tangential velocities and $T_{r\theta}^j$, $T_{r\phi}^j$ are the tangential components of stress for $j = e, i$. Thus we have six unknowns and six constraints. As a first approximation, we assume the shape of the droplet to be spherical and determine the unknown

constants in terms of the known constants α_n, α'_n and ϵ_n using conditions (3.2.13)-(3.2.18).

$$
\begin{aligned}
\beta_n &= -[\lambda_e\{\alpha_n((\lambda_i f_n(\lambda_i)g_{n+1}(\lambda_e) - 2f_{n+1}(\lambda_i)g_{n+1}(\lambda_e)) \\
&\quad +\overline{\mu}(2f_{n+1}(\lambda_i)g_{n+1}(\lambda_e))) + \alpha'_n((\lambda_i f_n(\lambda_i) \\
&\quad -2f_{n+1}(\lambda_i))(g_n(\lambda_e)f_{n+1}(\lambda_e) + f_n(\lambda_e)g_{n+1}(\lambda_e)) \\
&\quad +\overline{\mu}(2f_{n+1}(\lambda_i)(g_n(\lambda_e)f_{n+1}(\lambda_e) \\
&\quad +f_n(\lambda_e)g_{n+1}(\lambda_e))))\}]/N_n, \\
\beta'_n &= -[\alpha_n((2n+1)(\lambda_i f_n(\lambda_i) - 2f_{n+1}(\lambda_i)) \\
&\quad +2(2n+1)\overline{\mu}f_{n+1}(\lambda_i)) \\
&\quad +\alpha'_n(((2n+1)f_n(\lambda_e)(\lambda_i f_n(\lambda_i) - 2f_{n+1}(\lambda_i)) \\
&\quad +\lambda_e\lambda_i f_n(\lambda_i)f_{n+1}(\lambda_e) - 2\lambda_e f_{n+1}(\lambda_i)f_{n+1}(\lambda_e)) \\
&\quad +\overline{\mu}(2\lambda_e f_{n+1}(\lambda_i)f_{n+1}(\lambda_e) + 2(2n+1)f_n(\lambda_e)f_{n+1}(\lambda_i) \\
&\quad -\lambda_e^2 f_n(\lambda_e)f_{n+1}(\lambda_i)))]/N_n, \\
\epsilon'_n &= -\epsilon_n[\{f_n(\lambda_e)(f_n(\lambda_i)(n-1) - \lambda_i f_{n+1}(\lambda_i))\} \\
&\quad -\overline{\mu}\{\lambda_i f_{n+1}(\lambda_e)f_n(\lambda_i)\}]/M_n, \\
a_n &= [\lambda_e^2\overline{\mu}f_n(\lambda_i)(\alpha_n(2n+1)g_n(\lambda_e) \\
&\quad +\lambda_e\alpha'_n(g_n(\lambda_e)f_{n+1}(\lambda_e) + f_n(\lambda_e)g_{n+1}(\lambda_e)))]/\lambda_i N_n, \\
b_n &= -[\lambda_e^2(\alpha_n(2n+1)g_n(\lambda_e) \\
&\quad +\lambda_e\alpha'_n(g_n(\lambda_e)f_{n+1}(\lambda_e) + f_n(\lambda_e)g_{n+1}(\lambda_e)))]/\lambda_i N_n, \\
e_n &= \lambda_e\overline{\mu}\epsilon_n[g_n(\lambda_e)f_{n+1}(\lambda_e) + f_n(\lambda_e)g_{n+1}(\lambda_e)]/M_n, \qquad (3.2.19)
\end{aligned}
$$

where

$$\begin{aligned} M_n &= [\{g_n(\lambda_e)(\lambda_i f_{n+1}(\lambda_i) + (n-1)f_n(\lambda_i))\} \\ &\quad +\overline{\mu}\{f_n(\lambda_i)(\lambda_e g_{n+1}(\lambda_e) - (n-1)g_n(\lambda_e))\}], \\ N_n &= [\{g_n(\lambda_e)((2n+1)\lambda_i f_n(\lambda_i) - 2(2n+1)f_{n+1}(\lambda_i)) \\ &\quad +\lambda_e g_{n+1}(\lambda_e)(2f_{n+1}(\lambda_i) - \lambda_i f_n(\lambda_i))\} \\ &\quad +\overline{\mu}\{f_{n+1}(\lambda_i)(g_n(\lambda_e)(2(2n+1) - \lambda_e^2) \\ &\quad -2\lambda_e g_{n+1}(\lambda_e))\}]. \end{aligned}$$

When the shape of the droplet is spherical, the discontinuity of the normal stress across the interface is manifested as the pressure difference equal to $\frac{2}{Ca^i}$, where $Ca^i = \frac{\mu^i U}{\sigma}$ is called the capillary number that represents the relative effect of viscous forces versus surface tension forces acting across an interface between two immiscible liquids. However in Section 3.4, when we assume that the sphere undergoes a deformation in the next level of approximation, we impose the additional boundary condition of the balance of normal stresses and surface tension forces to determine the shape of the interface.

3.3 Drag on the liquid sphere $r = 1$

When the liquid droplet remains spherical, we use the solution given in the previous section and calculate the dimensionless drag on the liquid sphere $r = 1$ due to the fluid in the region

$r > 1$ as follows.

$$\vec{\mathbf{D}} = 2\pi \left[\left(\frac{X + \overline{\mu} Y}{Z + \overline{\mu} W} \right) [\vec{\mathbf{q}}_0]_0 + \left(\frac{U + \overline{\mu} V}{Z + \overline{\mu} W} \right) [\nabla^2 \vec{\mathbf{q}}_0]_0 \right] \tag{3.3.1}$$

where

$$\begin{aligned}
X &= \lambda_e^3 \{\lambda_i f_1(\lambda_i) - 2 f_2(\lambda_i)\} g_2(\lambda_e), \\
Y &= \lambda_e^3 \{\lambda_e g_1(\lambda_e) + 2 g_2(\lambda_e)\} f_2(\lambda_i), \\
Z &= \{\lambda_i f_1(\lambda_i) - 2 f_2(\lambda_i)\} \{\lambda_e g_2(\lambda_e) - 3 g_1(\lambda_e)\}, \\
W &= \{2\lambda_e g_2(\lambda_e) - (6 - \lambda_e^2) g_1(\lambda_e)\} f_2(\lambda_i), \\
S &= 3\{f_2(\lambda_e) g_1(\lambda_e) + f_1(\lambda_e) g_2(\lambda_e)\} \\
&\quad \{\lambda_i f_1(\lambda_i) - 2 f_2(\lambda_i)\}, \\
T &= 2 f_2(\lambda_i) \{f_2(\lambda_e) g_1(\lambda_e) + f_1(\lambda_e) g_2(\lambda_e)\},
\end{aligned}$$

$$\begin{aligned}
U &= S - \frac{X}{\lambda_e^3}, \\
V &= T - \frac{Y}{\lambda_e^3},
\end{aligned}$$

$$[\vec{\mathbf{q}}_0]_0 = (2\alpha_1 + \frac{2}{3}\lambda_e \alpha_1')(A_{11}\hat{\mathbf{i}} + B_{11}\hat{\mathbf{j}} + A_{10}\hat{\mathbf{k}}),$$

$$[\nabla^2 \vec{\mathbf{q}}_0]_0 = \frac{2}{3}\lambda_e^3 \alpha_1' (A_{11}\hat{\mathbf{i}} + B_{11}\hat{\mathbf{j}} + A_{10}\hat{\mathbf{k}}).$$

Similarly the torque is found to be

$$\begin{aligned}
\vec{\mathbf{T}} &= \frac{8\pi}{3}\epsilon_1 \left[\frac{N}{\lambda_i g_1(\lambda_e) f_2(\lambda_i) - \overline{\mu}\lambda_e f_1(\lambda_i) g_2(\lambda_e)} \right] [\vec{\mathbf{q}}_0]_0, \\
&= 4\pi \left[\frac{N}{\lambda_i g_1(\lambda_e) f_2(\lambda_i) - \overline{\mu}\lambda_e f_1(\lambda_i) g_2(\lambda_e)} \right] [\nabla \times \vec{\mathbf{q}}_0]_0,
\end{aligned} \tag{3.3.2}$$

where

$$\begin{aligned} N &= \lambda_e\lambda_i f_2(\lambda_i)(f_2(\lambda_e)g_1(\lambda_e) + g_2(\lambda_e)f_1(\lambda_e)), \\ [\vec{\mathbf{q}}_0]_0 &= C_{11}\hat{\mathbf{i}} + D_{11}\hat{\mathbf{j}} + C_{10}\hat{\mathbf{k}}, \\ [\nabla \times \vec{\mathbf{q}}_0]_0 &= \frac{2}{3}\epsilon_1(C_{11}\hat{\mathbf{i}} + D_{11}\hat{\mathbf{j}} + C_{10}\hat{\mathbf{k}}). \end{aligned}$$

where $[\ ]_0$ denotes evaluation at the centre of the sphere.

Here we observe the following:

1. As $\overline{\mu} \to 0$, the formulae for both drag $\vec{\mathbf{D}}$ and torque $\vec{\mathbf{T}}$ reduce to those of the drag and torque on a rigid sphere of radius 1 respectively in an oscillatory flow. These formulae agree with those of Kim and Karrila [47].

$$\vec{\mathbf{D}}_R = 6\pi(J[\vec{\mathbf{q}}_0]_0 + K[\nabla^2\vec{\mathbf{q}}_0]_0),$$

where

$$\begin{aligned} J &= \left(1 + \lambda_e + \frac{\lambda_e^2}{3}\right), \\ K &= \frac{1}{\lambda_e^2}\left(e^{\lambda_e} - \left(1 + \lambda_e + \frac{\lambda_e^2}{3}\right)\right), \end{aligned}$$

and

$$\begin{aligned} \vec{\mathbf{T}}_R &= \frac{4\pi(f_2(\lambda_e)g_1(\lambda_e) + g_2(\lambda_e)f_1(\lambda_e))}{g_1(\lambda_e)}[\nabla \times \vec{\mathbf{q}}_0]_0, \\ &= 4\pi\frac{e^{\lambda_e}}{\lambda_e + 1}[\nabla \times \vec{\mathbf{q}}_0]_0. \end{aligned}$$

2. As $\overline{\mu} \to \infty$, the drag $\vec{\mathbf{D}}$ reduces to the drag on a shear-free sphere of radius 1 in an oscillatory flow given by

$$\vec{\mathbf{D}}_{SF} = 4\pi(L[\vec{\mathbf{q}}_0]_0 + M[\nabla^2\vec{\mathbf{q}}_0]_0),$$

where

$$\begin{aligned} L &= \left(1 + \lambda_e + \frac{\lambda_e^2}{2} + \frac{\lambda_e^3}{6}\right)\left(1 + \frac{\lambda_e}{3}\right)^{-1}, \\ M &= \left(\frac{e^{\lambda_e}}{\lambda_e^2} - \left(\frac{\lambda_e}{6} + \frac{1}{2} + \frac{1}{\lambda_e} + \frac{1}{\lambda_e^2}\right)\right)\left(1 + \frac{\lambda_e}{3}\right)^{-1}. \end{aligned}$$

The torque reduces to zero in this case.

The suffixes R and SF refer to the rigid and shear-free cases respectively.

In both the cases, in addition to the above limits, if both λ_e and $\lambda_i \to 0$, then the drag formula (3.3.1) reduces to the Faxén's [21] laws in rigid and shear-free cases in steady flows which are given as follows respectively.

$$\begin{aligned} \vec{\mathbf{D}}_{rigid} &= 6\pi[\vec{\mathbf{q}}_0]_0 + \pi[\nabla^2\vec{\mathbf{q}}_0]_0, \\ \vec{\mathbf{D}}_{shear-free} &= 4\pi[\vec{\mathbf{q}}_0]_0. \end{aligned}$$

Likewise, the torque formula (3.3.2) also reduces to the torque in rigid and shear-free cases respectively,

$$\begin{aligned} \vec{\mathbf{T}}_{rigid} &= 4\pi[\nabla \times \vec{\mathbf{q}_0}]_0, \\ \vec{\mathbf{T}}_{shear-free} &= \vec{\mathbf{0}}. \end{aligned}$$

3.4 The equation of the deformed interface

In this section, we assume that the shape of the liquid droplet undergoes a slight deformation about its mean position. Solving both the flow field and the equation of the surface of the deformed sphere simultaneously is mathematically intractable. Hence we adopt an iterative process which is similar to that employed by Hetsroni and Haber [38]. As a first approximation, we assumed that the liquid droplet retains a spherical shape and determined the flow field in Section 3.2 using the boundary conditions (3.2.13)-(3.2.18). Under these conditions, the surface tension adjusts itself to satisfy the condition of balance of normal stresses. Now when we assume that the shape is slightly deformed, in order to determine the equation of the deformed interface, we use the condition of balance of normal stresses and surface tension forces as follows (Hetsroni and Haber [38]).

$$T^i_{rr} - \overline{\mu} T^e_{rr} = \frac{1}{Ca^i}\left[\frac{1}{R_1} + \frac{1}{R_2}\right], \tag{3.4.1}$$

where $Ca^i = \frac{\mu^i U}{\sigma}$ and R_1 and R_2 are the principal radii of curvature. We assume that the shape of the deformed liquid sphere is given by $r = F(\theta, \phi, t)$ where $F(\theta, \phi, t) = a(1 + f(\theta, \phi)e^{-i\omega t})$ and $\max|f(\theta, \phi)| << 1$ such that the radius of the 'equivalent' spherical liquid drop is given by $|F(\theta, \phi, t)|$.

We use the Landau and Lifshitz [51] condition for unsteady periodic flow as

$$\begin{aligned}\frac{1}{R_1} + \frac{1}{R_2} &= \frac{2}{a} - \frac{2fe^{-i\omega t}}{a} \\ &\quad - \frac{e^{-i\omega t}}{a}\left[\frac{1}{\sin\theta}\frac{\partial}{\partial\theta}\left(\sin\theta\frac{\partial f}{\partial\theta}\right) + \frac{1}{\sin^2\theta}\frac{\partial^2 f}{\partial\phi^2}\right].\end{aligned} \tag{3.4.2}$$

We expand $f(\theta, \phi)$, which denotes the deformation of the sphere, in terms of spherical

harmonics as

$$f(\theta,\phi) = \sum_{n=1}^{\infty} G_n S_n(\theta,\phi), \tag{3.4.3}$$

where G_n's are constants to be determined. Hence the shape of the surface is given by

$$r = a(1+\sum_{n=1}^{\infty} G_n S_n(\theta,\phi)e^{-i\omega t}). \tag{3.4.4}$$

We now use the boundary condition (3.4.1) for determining the shape of the boundary. On substituting (3.4.2) and (3.4.3) into the dimensional form of the condition of balance of normal stresses and surface tension forces and reverting back to the non-dimensional form of the boundary condition (3.4.1), we get

$$T^i_{rr} - \overline{\mu} T^e_{rr} = \frac{1}{Ca^i}\left[2+\sum_{n=1}^{\infty}\{n(n+1)-2\}G_n S_n(\theta,\phi)\right]. \tag{3.4.5}$$

Substituting the values of T^e_{rr} and T^i_{rr} in (3.4.5), we solve for G_n $(n \neq 1)$ by using the orthogonality of Legendre polynomials. We obtain

$$\overline{\mu}P^e - P^i = \frac{2}{Ca^i}, \tag{3.4.6}$$

$$\begin{aligned} G_n = \frac{Ca^i}{(n^2+n-2)}[&\overline{\mu}\alpha_n(n+1)(\lambda_e^2-2n(n-1)) \\ &-2\overline{\mu}n(n+1)\alpha_n'((n-1)f_n(\lambda_e)+\lambda_e f_{n+1}(\lambda_e)) \\ &+n\overline{\mu}\beta_n(2(n+1)(n+2)-\lambda_e^2) \\ &-2\overline{\mu}\beta_n'((n-1)g_n(\lambda_e)-\lambda_e g_{n+1}(\lambda_e)) \\ &+(n+1)a_n(\lambda_i^2+2n) \\ &+2b_n n(n+1)((n-1)f_n(\lambda_i)+\lambda_i f_{n+1}(\lambda_i))], \end{aligned} \tag{3.4.7}$$

where P^e and P^i are constants of pressure. Following the above iterative method, the higher order (> 1) approximations for the surface equation of the deformed liquid sphere can be found out. For $n = 1$ in (3.4.5), we get an identity (3.4.6), indicating that the assumption that the liquid sphere retains its spherical shape is correct up to two terms in (3.4.5) irrespective of the surface tension. In other words, we obtain the condition of balance of normal stresses and surface tension forces manifested as the difference of pressures given by (3.4.6) as in the case of a sphere. This result is analogous to that of Hetsroni and Haber [38] who considered a steady flow. This also shows that when a creeping flow past a liquid sphere is considered, the assumption that the sphere maintains a spherical shape is true irrespective of the value of surface tension. This was also observed by Taylor and Acrivos [108] in steady creeping flows. Chisnell [11], who considered the unsteady motion of a liquid drop moving vertically under gravity showed that the solution satisfies the normal stress balance independent of the magnitude of the surface tension so that the spherical shape is retained. A similar result was obtained by Sy and Lightfoot [106]. The flow fields considered by Chisnell [11] correspond to the stream function of the form $\psi = \sin^2\theta f(r,t)$ which when expanded in a series form have terms up to $n = 1$. So the result obtained by us, that the spherical shape of the liquid sphere is retained for flow velocities which have terms only up to $n = 1$ in their series representation, agrees with Chisnell's [11] result. From (3.4.7) it is clear that the ratio of the viscosities $\overline{\mu}$ and the capillary number Ca^i affect the deformation. We now demonstrate the method to determine the shape of a deformed liquid sphere in the following example.

3.5 An example

Consider an unsteady basic flow in a dimensional form given by $\vec{\mathbf{q}} = e^{-i\omega t}G(y+1)\hat{\mathbf{i}}$, where G is the shear constant and ω is the frequency of oscillation. We choose the characteristic velocity U as Ga and obtain the non-dimensional form of the given velocity as $\vec{\mathbf{q}} = e^{-i\omega t}\frac{1}{a}(y+1)\hat{\mathbf{i}}$, corresponding to which the scalar functions are given by

$$\begin{aligned} A_0(r,\theta,\phi) &= \left(\frac{r}{a}S_1(\theta,\phi) + \frac{1}{6}r^2 S_2(\theta,\phi)\right), \\ B_0(r,\theta,\phi) &\equiv 0. \end{aligned}$$

The scalar functions $A^e(r,\theta,\phi)$ and $B^e(r,\theta,\phi)$ corresponding to the flow velocity can be represented in a series form as

$$\begin{aligned} A^e(r,\theta,\phi) &= \alpha_1 S_1(\theta,\phi) + \alpha_2 S_2(\theta,\phi) \\ &\quad + \sum_{n=1}^{2}(\beta_n r^{-n-1} + \beta_n' g_n(\lambda_e r))S_n(\theta,\phi), \\ B^e(r,\theta,\phi) &= 0, \\ A^i(r,\theta,\phi) &= \sum_{n=1}^{2}(a_n r^n + b_n f_n(\lambda_i r))S_n(\theta,\phi), \\ B^i(r,\theta,\phi) &= 0, \end{aligned}$$

where

$$\begin{aligned} \alpha_1 &= \frac{2}{a},\ \alpha_2 = \frac{1}{3a},\ \beta_1 = -\frac{2\delta}{\varsigma},\ \beta_1' = -\frac{2\varpi}{\varsigma},\ \beta_2 = -\frac{\lambda_e}{3}\frac{\kappa}{\eta}, \\ \beta_2' &= -\frac{1}{3}\frac{\gamma}{\eta}, \\ a_1 &= \frac{3\lambda_e^2 f_1(\lambda_i)g_1(\lambda_e)}{\lambda_i\varsigma}, b_1 = -\frac{3\lambda_e^2 g_1(\lambda_e)}{\lambda_i\varsigma}, \\ a_2 &= \frac{5\lambda_e^2 f_2(\lambda_i)g_2(\lambda_e)}{6\lambda_i\eta}, b_2 = -\frac{5\lambda_e^2 g_2(\lambda_e)}{3\lambda_i\eta}, \end{aligned}$$

$$
\begin{aligned}
\delta &= \lambda_e\{(\lambda_i f_1(\lambda_i) g_2(\lambda_e) - 2 f_2(\lambda_i) g_2(\lambda_e)) \\
&\quad +(f_2(\lambda_i) g_2(\lambda_e))\}, \\
\varpi &= 3(\lambda_i f_1(\lambda_i) - 2 f_2(\lambda_i)) + 3 f_2(\lambda_i), \\
\varsigma &= g_1(\lambda_e)(3\lambda_i f_1(\lambda_i) - 6 f_2(\lambda_i)) \\
&\quad +\lambda_e g_2(\lambda_e)(2 f_2(\lambda_i) - \lambda_i f_1(\lambda_i)) \\
&\quad +(0.5) f_2(\lambda_i)(g_1(\lambda_e)(6 - \lambda_e^2) - 2\lambda_e g_2(\lambda_e)), \\
\kappa &= (\lambda_i f_2(\lambda_i) g_3(\lambda_e) - 2 f_3(\lambda_i) g_3(\lambda_e)) \\
&\quad +f_3(\lambda_i) g_3(\lambda_e), \\
\gamma &= 5(\lambda_i f_2(\lambda_i) - 2 f_3(\lambda_i)) + 5 f_3(\lambda_i), \\
\eta &= g_2(\lambda_e)(5\lambda_i f_2(\lambda_i) - 10 f_3(\lambda_i)) \\
&\quad +\lambda_e g_3(\lambda_e)(2 f_3(\lambda_i) - \lambda_i f_2(\lambda_i)) \\
&\quad +(0.5)(f_3(\lambda_i)(g_2(\lambda_e)(10 - \lambda_e^2) - 2\lambda_e g_3(\lambda_e))), \\
S_1(\theta,\phi) &= \frac{P_1^1(\zeta)\cos\phi}{4},\ S_2(\theta,\phi) = \frac{P_2^2(\zeta)\sin 2\phi}{4},
\end{aligned}
$$

with $\lambda_e = \frac{1-i}{\sqrt{2}}$, $\lambda_i = \frac{1-i}{2}$.

By employing the method suggested in Section 3.4, we can obtain the shape of the droplet. In this example, the capillary number is defined as $Ca^i = \frac{\mu^i Ga}{\sigma}$. Figures 3.5.1 and 3.5.2 demonstrate the shapes of the deformed sphere at different values of ωt for $Ca^i = 0.055$ and $\overline{\mu} = 0.5$, which give a complete cycle of oscillations for $\omega t \in [0, 2\pi]$. We observe that at $\omega t = 0$ the shape of the liquid droplet is assumed to be non-spherical and this shape is attained again at $\omega t = 2\pi$. The value of Ca^i has been deliberately chosen to make the

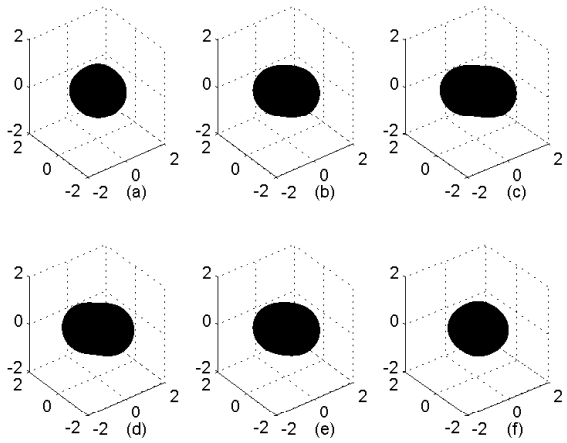

Figure 3.5.1: *(a)* $\omega t = 0$, *(b)* $\omega t = \frac{2\pi}{11}$, *(c)* $\omega t = \frac{4\pi}{11}$, *(d)* $\omega t = \frac{6\pi}{11}$, *(e)* $\omega t = \frac{8\pi}{11}$, *(f)* $\omega t = \frac{10\pi}{11}$

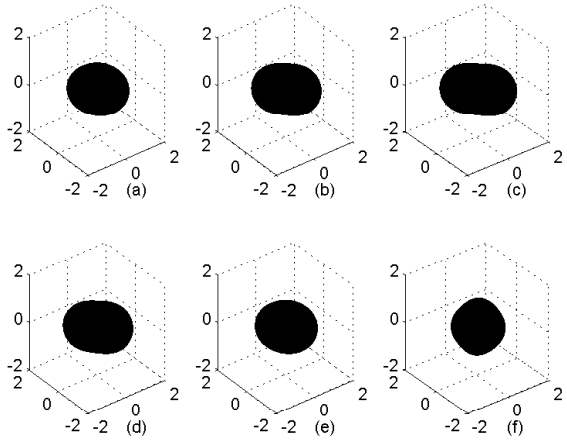

Figure 3.5.2: *(a)* $\omega t = \frac{12\pi}{11}$, *(b)* $\omega t = \frac{14\pi}{11}$, *(c)* $\omega t = \frac{16\pi}{11}$, *(d)* $\omega t = \frac{18\pi}{11}$, *(e)* $\omega t = \frac{20\pi}{11}$, *(f)* $\omega t = 2\pi$

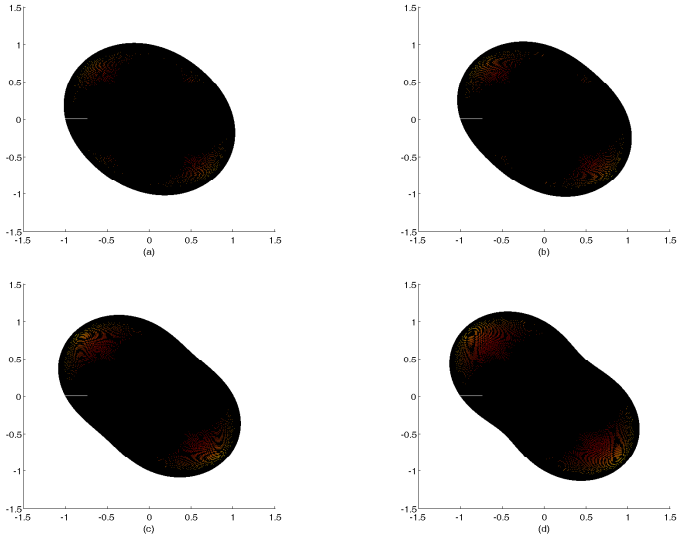

Figure 3.5.3: $Ca^i = 0.01$ *(a)* $\overline{\mu} = 2$, *(b)* $\overline{\mu} = 3.5$, *(c)* $\overline{\mu} = 6$, *(d)* $\overline{\mu} = 8$.

deviation from sphericity visible at different values of ωt. Figures 3.5.3 and 3.5.4 show the deformation of a liquid sphere for fixed capillary numbers Ca^i with varying ratio of viscosities $\overline{\mu}$. Figures 3.5.5 and 3.5.6 show how a liquid sphere deforms for a fixed ratio of viscosities $\overline{\mu}$ with varying capillary number Ca^i.

From these figures we observe that for a fixed capillary number, the deformation increases with increasing $\overline{\mu}$. When $\overline{\mu}$ is fixed, we find that the liquid sphere is spherical at low capillary numbers and has deviation from a spherical shape which increases as the capillary number increases.

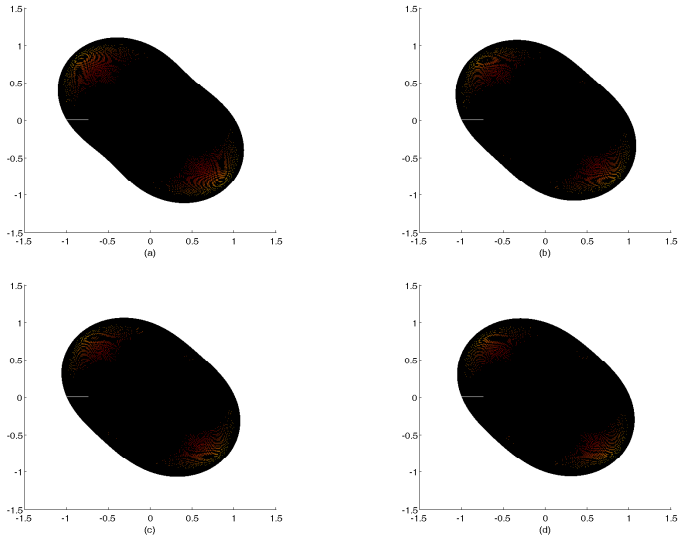

Figure 3.5.4: $Ca^i = 0.05$ *(a)* $\overline{\mu} = 0.05$, *(b)* $\overline{\mu} = 0.2$, *(c)* $\overline{\mu} = 0.5$, *(d)* $\overline{\mu} = 0.8$.

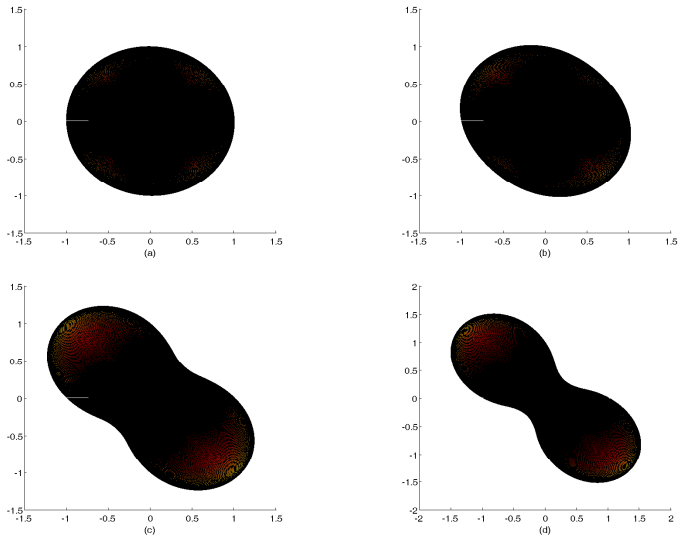

Figure 3.5.5: $\overline{\mu} = 2$ *(a)* $Ca^i = 0.001$, *(b)* $Ca^i = 0.01$, *(c)* $Ca^i = 0.05$, *(d)* $Ca^i = 0.09$.

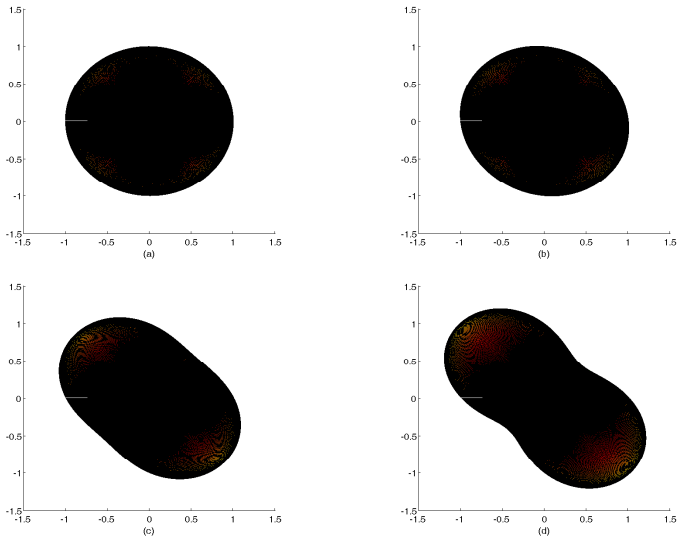

Figure 3.5.6: $\overline{\mu} = 0.5$ *(a)* $Ca^i = 0.001$, *(b)* $Ca^i = 0.01$, *(c)* $Ca^i = 0.05$, *(d)* $Ca^i = 0.09$.

3.6 Motion due to singularities inside a liquid sphere

We now assume the flow inside the liquid sphere to be generated due to a singularity in the region $r < 1$. Let the unperturbed flow be given by the scalar functions

$$A_0(r,\theta,\phi) = \sum_{n=1}^{\infty}(H_n r^{-n-1} + I_n g_n(\lambda_i r))S_n(\theta,\phi), \tag{3.6.1}$$

$$B_0(r,\theta,\phi) = \sum_{n=1}^{\infty}(L_n g_n(\lambda_i r))T_n(\theta,\phi). \tag{3.6.2}$$

Here $\mu_o = \mu^i$ and $\lambda_0 = \lambda_i$. Then the perturbed flow generated in the region $r < 1$ is

$$\begin{aligned} A^i(r,\theta,\phi) = \sum_{n=1}^{\infty}&(H_n r^{-n-1} + I_n g_n(\lambda_i r) \\ &+ J_n r^n + K_n f_n(\lambda_i r))S_n(\theta,\phi), \end{aligned} \tag{3.6.3}$$

$$B^i(r,\theta,\phi) = \sum_{n=1}^{\infty}(L_n g_n(\lambda_i r) + R_n f_n(\lambda_i r))T_n(\theta,\phi). \tag{3.6.4}$$

The perturbed flow outside the liquid sphere $r > 1$ is

$$A^e(r,\theta,\phi) = \sum_{n=1}^{\infty}(C_n r^{-n-1} + D_n g_n(\lambda_e r))S_n(\theta,\phi), \tag{3.6.5}$$

$$B^e(r,\theta,\phi) = \sum_{n=1}^{\infty}(Q_n g_n(\lambda_e r))T_n(\theta,\phi). \tag{3.6.6}$$

We use the boundary conditions (3.2.13)-(3.2.18) to determine the unknown coefficients J_n, K_n, R_n, C_n, D_n and Q_n in terms of the known coefficients H_n, I_n and L_n.

$$\begin{aligned}
R_n &= [L_n(g_n(\lambda_e(\lambda_e g_{n+1}(\lambda_i) - (n-1)g_n(\lambda_i)) \\
&\quad +\lambda_e\overline{\mu}g_n(\lambda_i)((n-1)g_n(\lambda_e) - g_{n+1}(\lambda_e)))]/U_n, \\
Q_n &= [L_n\lambda_i(g_n(\lambda_i)f_{n+1}(\lambda_i) + f_n(\lambda_i)g_{n+1}(\lambda_i))]/U_n, \\
C_n &= [-(\lambda_i g_n(\lambda_e)(\lambda_i I_n(g_n(\lambda_i)f_{n+1}(\lambda_i) + f_n(\lambda_i)g_{n+1}(\lambda_)) \\
&\quad +f_n(\lambda_i)(H_n(2n+1))))]/V_n, \\
D_n &= [(\lambda_i(\lambda_i I_n(g_n(\lambda_i)f_{n+1}(\lambda_i) + f_n(\lambda_i)g_{n+1}(\lambda_i)) \\
&\quad +f_n(\lambda_i)(H_n(2n+1))))]/V_n, \\
J_n &= [H_n((\lambda_e g_{n+1}(\lambda_e)(2\lambda_i f_{n+1}(\lambda_i) + 2f_n(\lambda_i)\lambda_i^2 f_n(\lambda_i)) \\
&\quad +(2n+1)g_n(\lambda_e)(2\lambda_i f_{n+1}(\lambda_i) - 2(2n+1)f_n(\lambda_i) \\
&\quad -\lambda_i^2 f_n(\lambda_i)) - \lambda_i\lambda_e^2 g_n(\lambda_e)f_{\lambda_i}) \\
&\quad +\overline{\mu}(g_n(\lambda_e)(2n+1)(\lambda_e^2 f_n(\lambda_i)
\end{aligned}$$

$$
\begin{aligned}
& +2(2n+1)f_n(\lambda_i) - 2\lambda_i f_{n+1}(\lambda_i)) \\
& -2\lambda_e g_{n+1}(\lambda_e)(\lambda_i f_{n+1}(\lambda_i) + (2n+1)f_n(\lambda_i)))) \\
& +I_n(2\lambda_e\lambda_i g_{n+1}(\lambda_e)(f_{n+1}(\lambda_i)g_n(\lambda_i) \\
& +f_n(\lambda_i)g_{n+1}(\lambda_i)) \\
& -\lambda_i(2(2n+1)+\lambda_e^2)g_n(\lambda_e)(f_{n+1}(\lambda_i)g_n(\lambda_i) \\
& +f_n(\lambda_i)g_{n+1}(\lambda_i)))]/\lambda_i V_n, \\
K_n &= [H_n(2n+1)((g_n(\lambda_e)(\lambda_e^2 - 2(2n+1)) \\
& -2\lambda_e g_{n+1}(\lambda_e)) + 2\overline{\mu}(\lambda_e g_{n+1}(\lambda_e) \\
& +(2n+1)g_n(\lambda_e))) \\
& +I_n((g_n(\lambda_e)\lambda_i(\lambda_e^2 g_{n+1}(\lambda_i) \\
& +2(2n+1)g_{n+1}(\lambda_i)\lambda_i(2n+1)g_n(\lambda_i)) \\
& -2\lambda_e\lambda_i g_{n+1}(\lambda_e)(g_{n+1}(\lambda_i) \\
& +\lambda_i g_n(\lambda_i))) + 2\overline{\mu}(\lambda_i g_{n+1}(\lambda_i)(\lambda_e g_{n+1}(\lambda_e) \\
& -(2n+1)g_n(\lambda_e))))]/\lambda_i V_n.
\end{aligned}
$$

where

$$
\begin{aligned}
U_n &= (\lambda_e g_{n+1}(\lambda_e) - (n-1)f_n(\lambda_i)g_n(\lambda_e)) \\
& +\overline{\mu}g_n(\lambda_e)(\lambda_i f_{n+1}(\lambda_i) + (n-1)f_n(\lambda_i)), \\
V_n &= [(\lambda_e g_{n+1}(\lambda_e)(\lambda_i - 2\lambda_e f_{n+1}(\lambda_i))) \\
& +\overline{\mu}\lambda_e g_{n+1}(\lambda_e)(2f_{n+1}(\lambda_i) + g_n(\lambda_e)f_{n+1}(\lambda_i) \\
& (\lambda_e^2 - 2(2n+1)))].
\end{aligned}
$$

By a similar analysis as in Section 3.4, we determine the equation of the deformed surface of the interface by using the condition of the balance of normal stresses and surface tension forces. However we now make an interesting observation in the following two singularity driven flows.

1. Oscillating Stokeslet at the origin : The scalar functions which give the flow due to an oscillating Stokeslet at the origin of strength $\frac{F}{8\pi}$ directed towards the positive x-axis are given by
$$A_0 = \frac{F}{8\pi}\left\{-\frac{4}{\pi}g_1(R) + \frac{2}{R^2}\right\}\sin\theta\cos\phi, \quad B_0 \equiv 0.$$

2. Oscillating rotlet at the origin : The scalar functions corresponding to a oscillating rotlet of strength $\frac{F}{4\pi}$ located at the origin and directed towards the positive y-axis are given by
$$A_0 \equiv 0, \quad B_0 = \frac{F}{\pi}\left\{\frac{\lambda_i^2}{\pi}g_1(R)\right\}\sin\theta\cos\phi,$$

where $R = \lambda_i r$. In both these singularity driven flows, the sphere retains its spherical shape as we obtain an identity in these two cases given by the condition (3.4.6), as these two cases correspond to $n = 1$, indicating that the assumption the liquid sphere retains its spherical shape is correct up to two terms in equation (3.4.5). We now give an example of a singularity driven flow in the following section where deformation of the liquid sphere is possible.

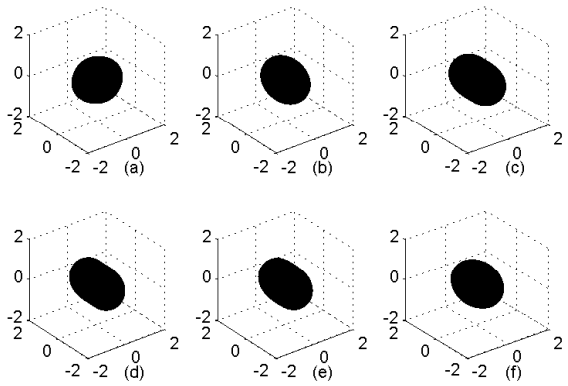

Figure 3.6.1: *(a)* $\omega t = 0$, *(b)* $\omega t = \frac{2\pi}{11}$, *(c)* $\omega t = \frac{4\pi}{11}$, *(d)* $\omega t = \frac{6\pi}{11}$, *(e)* $\omega t = \frac{8\pi}{11}$, *(f)* $\omega t = \frac{10\pi}{11}$

An example to find the shape of the deformed sphere: We consider an unperturbed flow which is given by the scalar functions

$$\begin{aligned} A_0(r,\theta,\phi) &= \frac{18\sin^2\theta\cos 2\phi}{r^3}, \\ &= \frac{6S_2(\theta,\phi)}{r^3}, \\ B_0 &\equiv 0. \end{aligned} \tag{3.6.7}$$

Figures 3.6.1 and 3.6.2 show the shapes of the deformed sphere for $Ca^i = 0.0016$ and $\overline{\mu} = 0.5$ at different values of ωt in the interval $[0, 2\pi]$. The value of Ca^i has been chosen to demonstrate a slight deviation from sphericity in this singularity driven internal flow.

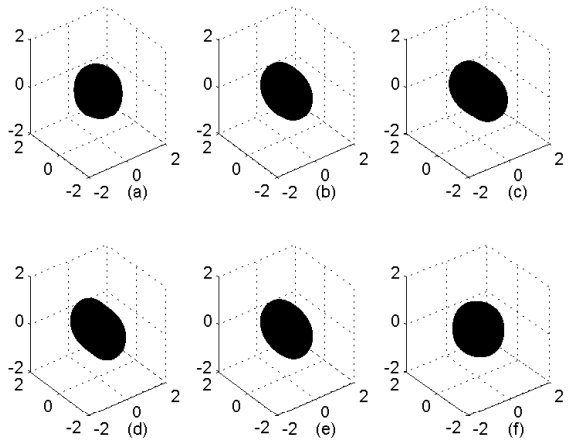

Figure 3.6.2: *(a)* $\omega t = \frac{12\pi}{11}$, *(b)* $\omega t = \frac{14\pi}{11}$, *(c)* $\omega t = \frac{16\pi}{11}$, *(d)* $\omega t = \frac{18\pi}{11}$, *(e)* $\omega t = \frac{20\pi}{11}$, *(f)* $\omega t = 2\pi$

3.7 Conclusions

The problem of an arbitrary, oscillatory Stokes flow past a fluid particle immersed in another immiscible fluid of a different viscosity has been studied. We determined the drag and torque on the liquid sphere, which reduce to the drag and torque on a rigid sphere and a shear free sphere in the limiting cases $\overline{\mu} \to 0$ and $\overline{\mu} \to \infty$ respectively. We also extended the study to consider an oscillatory Stokes flow generated by internal singularities inside a liquid sphere. We have used an iterative procedure to determine the shape of the deformed liquid sphere by following the approach of Hetsroni and Haber [38]. We were also able to show that the assumption that the liquid sphere retains its spherical shape for flow velocities which have only terms up to $n = 1$ in their series representations is correct. This agrees with the result

of Chisnell [11]. This was found to be true in both the external and internal singularity driven flows. Hence in a singularity driven flow due to an oscillating Stokeslet at the origin as well as in a flow due to an oscillating rotlet at the origin, the droplet is found to retain its spherical shape. If the droplet is assumed to remain spherical and the deformation is not taken into account, the oscillations are not visible as they are in Figures 3.5.1-3.6.2, because of spherical symmetry. We have also illustrated how the ratio of viscosities and capillary number play an important role in determining the shape of the deformed surface, i.e., deviation from a spherical shape.

Chapter 4

Flow generated due to a Stokeslet inside a spherical container with slip-stick boundary conditions

4.1 Introduction and mathematical formulation

Some experiments conducted by Helmholtz and Piotrowsky [37] suggested that some slipping may take place at the surface of contact, when certain fluids are in contact with the surface of a solid. When the velocity of the fluid is small compared to the solid, it is assumed that the tangential force exerted by the solid upon the fluid acts in the same direction as that of the relative velocity and is proportional to it. The constant of proportionality,

which is the ratio of the tangential force to the relative velocity is called 'the coefficient of sliding friction'. The corresponding boundary conditions are termed as 'slip-stick boundary conditions' and are given by equations (1.2.2) in Chapter 1. Such boundary conditions are more general and allow us to deduce a wide choice of boundary conditions ranging from no-slip to perfect-slip conditions. One of the key observations in both experimental [70] and theoretical [33, 40] investigations on bounded Stokes flows is that the flow characteristics are sensitive to the geometry and fluid parameters, and drastic changes in the fluid motion can occur due to small perturbations of these parameters. Two-dimensional flows in cylindrical domains - modelled by point singularities such as Stokeslet, rotlet, and so on together with no-slip boundary conditions - exhibit eddy patterns for a certain range in the parameter space [17, 93], especially for some specific positions. For a single cylindrical fluid domain the eddies are created if the singularity generating the motion is away from the center. The three-dimensional models in spherical domains [91, 99] with a Stokeslet at the center with no-slip boundary conditions confirms the assertion that the eddy patterns are dependent on the geometry and flow parameters. Hackborn et al. [27] and Usha and Nigam [111] have studied the singularity driven flows in a rigid spherical cavity. Ranger [91] and Meleshko et al. [67] independently considered the flow generated by a rotlet inside a cylinder using no-slip boundary conditions.

One of the earliest researchers who studied the problem of Stokes flow past a sphere with slip-stick boundary conditions was Basset [5] (see also, [32]), who considered the motion of a sphere of radius a, moving with a uniform velocity along a straight line in a viscous fluid, with the assumption that there is some slipping at the surface of the sphere. Basset [5]

illustrated the impact of slip on the Stokes solution for the flow past an isolated sphere. Thereafter, Lamb [50] obtained the result of Basset [5] by using his general solution of Stokes equations for a uniform flow past a sphere in a viscous, incompressible fluid employing slipping at the surface. Schmitz et al. [98] gave a general solution of the Stokes equations using the approach of cartesian tensors. Using the solution developed by them, they considered the problem of an incompressible, arbitrary, incident Stokes flow past a stationary sphere with slip-stick boundary conditions, and gave a solution in cartesian co-ordinates. But as in the case of Lamb's solution [50], it may not always be possible to sum up the series solution even in simple cases. Padmavathi et al. [75] considered a general solution of Stokes equations and gave a general method for the problem of Stokes flow past a sphere with slip-stick boundary conditions, which was obtained in a closed form and also obtained the Faxén's [21] laws for drag and torque on the sphere. There have been numerous studies on flows exterior to the bounding surface with slip [20, 75] in view of their applications in engineering like micro device technology (see the recent work [4, 56], and references therein) and the interest in these studies is growing in the modern era. Several flow related features including the drag coefficient have been discussed in order to demonstrate the slip effect [4, 56]. Later Palaniappan and Daripa [81], considered the two dimensional Stokes flow generated by different line singularities inside a circular cylinder using the slip-stick boundary conditions and observed some interesting flow patterns. However, the problem of a general non-axisymmetric motion generated by singularities inside a spherical cavity with slip-stick boundary conditions does not seem to have been disussed so far although the problem is mathematically tractable. Based on the results of Helmholtz and Piotrowsky [37], it

is more appropriate to study this problem assuming that some slipping takes place at the surface of contact of the fluid with the solid spherical boundary.

Consider the Stokes flow generated due to the presence of a Stokeslet of strength $\vec{\mathbf{F}}$, placed at the origin, inside a spherical container of radius a. The mathematical statement of this problem is

$$\mu\nabla^2\vec{\mathbf{q}} = \nabla p - \vec{\mathbf{F}}\delta(\vec{\mathbf{r}}), \tag{4.1.1}$$

$$\nabla\cdot\vec{\mathbf{q}} = 0, \tag{4.1.2}$$

where $\delta(\vec{\mathbf{r}})$ is the Dirac-delta function. By using the non-dimensional variables as in Section 1.3 in Chapter 1, with $L = a$, we obtain the non-dimensional form of equations (4.1.1)-(4.1.2) as follows.

$$\nabla^2\vec{\mathbf{q}} = \nabla p - \vec{\mathbf{F}}\delta(\vec{\mathbf{r}}), \tag{4.1.3}$$

$$\nabla\cdot\vec{\mathbf{q}} = 0. \tag{4.1.4}$$

where $\vec{\mathbf{F}}$ is the non-dimensional strength.

The solution to the problem (4.1.3) and (4.1.4) can be written as

$$\vec{\mathbf{q}} = \vec{\mathbf{F}}\cdot\left[\frac{\delta_{ij}}{r} + \frac{\vec{\mathbf{r}}\otimes\vec{\mathbf{r}}}{r^3}\right] + \vec{\mathbf{q}}_G. \tag{4.1.5}$$

Here the first term is the famous *Green's function* (also known as Oseen tensor) for the unbounded domain due to a Stokeslet and is singular at the origin. The term $\vec{\mathbf{q}}_G$ is a suitable solution of the Stokes equations, regular at the origin, to be added in order to satisfy the boundary conditions at the container surface.

Suppose we consider the slip-stick boundary conditions (Section 1.2, Chapter 1), on $r = 1$, which are given in a non-dimensional form as follows.

$$q_r(1,\theta,\phi) = 0, \tag{4.1.6}$$

$$q_\theta(1,\theta,\phi) = -\overline{\lambda}T_{r\theta}(1,\theta,\phi), \tag{4.1.7}$$

$$q_\phi(1,\theta,\phi) = -\overline{\lambda}T_{r\phi}(1,\theta,\phi), \tag{4.1.8}$$

where $\overline{\lambda}$ is the non-dimensional slip coefficient and $T_{r\theta}$, $T_{r\phi}$ are the non-dimensional tangential stresses as given in Section 1.2 in Chapter 1.

We employ the representation of the solution of the steady Stokes equations for the velocity and pressure proposed by Palaniappan et al.[79] as given in Section 1.1 of Chapter 1. In the absence of any rigid boundaries, suppose the unperturbed flow is given by the velocity $\vec{\mathbf{q}}_0$ and pressure p_0 where

$$\vec{\mathbf{q}}_0 = \nabla \times \nabla \times (\mathbf{r}A_0) + \nabla \times (\mathbf{r}B_0), \tag{4.1.9}$$

$$p_0 = P_0 + \frac{\partial}{\partial r}(r\nabla^2 A_0), \tag{4.1.10}$$

$$\nabla^4 A_0 = 0, \tag{4.1.11}$$

$$\nabla^2 B_0 = 0. \tag{4.1.12}$$

where P_0 is a constant. Then the scalar functions A_0 and B_0 can be expanded in terms of spherical harmonics as follows

$$A_0 = \sum_{n=1}^{\infty}(\alpha_n r^{-n-1} + \alpha'_n r^{-n+1})S_n(\theta,\phi), \tag{4.1.13}$$

$$B_0 = \sum_{n=1}^{\infty}\chi_n r^{-n-1}T_n(\theta,\phi), \tag{4.1.14}$$

where

$$S_n(\theta,\phi) = \sum_{n=1}^{\infty} P_n^m(\zeta)(A_{nm}\cos m\phi + B_{nm}\sin m\phi), \tag{4.1.15}$$

$$T_n(\theta,\phi) = \sum_{n=1}^{\infty} P_n^m(\zeta)(C_{nm}\cos m\phi + D_{nm}\sin m\phi), \tag{4.1.16}$$

$\alpha_n, \alpha_n', \chi_n, A_{nm}, B_{nm}, C_{nm}, D_{nm}$ are known constants. In the presence of a sphere of radius 1, we assume the modified flow $(\vec{\mathbf{q}}, p)$ in the region $r < 1$ to be given by the scalar functions A and B as follows

$$A = \sum_{n=1}^{\infty}(\alpha_n r^{-n-1} + \alpha_n' r^{-n+1} + \beta_n r^n + \beta_n' r^{n+2})S_n(\theta,\phi), \tag{4.1.17}$$

$$B = \sum_{n=1}^{\infty}(\chi_n r^{-n-1} + \sigma_n r^n)T_n(\theta,\phi), \tag{4.1.18}$$

where the unknown constants β_n, β_n' and σ_n are to be determined from the slip-stick boundary conditions (4.1.6)-(4.1.8). For $\overline{\lambda} \neq 1$, the boundary conditions on $r = 1$, in terms of A and B, are as follows

$$A = 0, \tag{4.1.19}$$

$$\frac{\partial A}{\partial r} = -\overline{\lambda}\frac{\partial^2 A}{\partial r^2}, \tag{4.1.20}$$

$$B = -\left(\frac{\overline{\lambda}}{1-\overline{\lambda}}\right)\left[\frac{\partial B}{\partial r}\right]. \tag{4.1.21}$$

For $\overline{\lambda} = 1$, the boundary conditions are

$$A = 0, \tag{4.1.22}$$

$$\frac{\partial A}{\partial r} = -\frac{\partial^2 A}{\partial r^2}, \tag{4.1.23}$$

$$\frac{\partial B}{\partial r} = 0. \tag{4.1.24}$$

Using the boundary conditions (4.1.19)-(4.1.21), we solve for the three unknown constants in terms of α_n, α'_n and χ_n when $\overline{\lambda} \neq 1$ as follows:

$$\beta_n = -\frac{\alpha_n(2n+3) + \alpha'_n(1+2\overline{\lambda})(2n+1)}{M_n}, \tag{4.1.25}$$

$$\beta'_n = \frac{\alpha_n(1-2\overline{\lambda})(2n+1) + \alpha'_n(2n-1)}{M_n}, \tag{4.1.26}$$

$$\sigma_n = -\frac{(1-\overline{\lambda}(n+2))\chi_n}{(1+\overline{\lambda}(n-1))}, \tag{4.1.27}$$

where $M_n = 2(1+(2n+1)\overline{\lambda})$.

However, when $\overline{\lambda} = 1$, the solution obtained using the boundary conditions (4.1.22)-(4.1.24) agrees with the solution given by (4.1.25)-(4.1.27) in the limit $\overline{\lambda} \to 1$. We now give the solution in the form of a sphere theorem as follows.

Theorem: If the flow of a viscous, incompressible fluid in the absence of rigid boundaries be denoted by $A_0(r,\theta,\phi)$ and $B_0(r,\theta,\phi)$, which are biharmonic and harmonic respectively, the singularities of these functions being at a distance lesser than 1 from the origin and if $A_0 \sim o(1)$, $B_0 \sim o\left(\frac{1}{r^2}\right)$ as $r \to \infty$, and if now the flow be considered inside the sphere $r = 1$, then the modified flow in the interior of the sphere with slip-stick boundary conditions (4.1.6)-(4.1.8) on $r = 1$ for $\overline{\lambda} \neq 0$ is given by

$$\begin{aligned} A(r,\theta,\phi) = {} & A_0(r,\theta,\phi) - rA_0\left(\frac{1}{r},\theta,\phi\right) + (1-r^2)\left[\frac{1}{8\overline{\lambda}r^{\frac{1}{2\overline{\lambda}}-\frac{1}{2}}}\right. \\ & \left.\times\left(\int_\infty^{\frac{1}{r}} R^{-\frac{1}{2\overline{\lambda}}-\frac{3}{2}}\left(\nabla^2 A_0 - R^4\nabla^2\left(\frac{A_0}{R^2}\right)\right)dR\right)\right], \end{aligned} \tag{4.1.28}$$

$$
\begin{aligned}
B(r,\theta,\phi) &= B_0(r,\theta,\phi) + \frac{1}{r}B_0(r,\theta,\phi) - \left(\frac{2}{\overline{\lambda}} - 3\right) \\
&\quad \times \int_{\infty}^{\frac{1}{r}} R^{-\frac{1}{\lambda}-1} B_0 dR. \qquad (4.1.29)
\end{aligned}
$$

When $\overline{\lambda} \to \infty$, equations (4.1.28) and (4.1.29) reduce to

$$
\begin{aligned}
A(r,\theta,\phi) &= A_0(r,\theta,\phi) - \frac{r}{a}A_0(\frac{a^2}{r},\theta,\phi), \\
B(r,\theta,\phi) &= B_0(r,\theta,\phi) + \frac{1}{r}B_0(\frac{1}{r},\theta,\phi) - 3r\int_{\infty}^{\frac{1}{r}} RB_0 dR, \qquad (4.1.30)
\end{aligned}
$$

which agree with the result obtained by Palaniappan et al. [78] corresponding to shear-free boundary conditions. However equations (4.1.28)-(4.1.29) are invalid when $\overline{\lambda} = 0$. The solution obtained when $\overline{\lambda} = 0$ in (4.1.19)-(4.1.21) using (4.1.25)-(4.1.27) gives rise to the following closed form which agrees with the sphere theorem due to Palaniappan et al. [79].

$$
\begin{aligned}
A(r,\theta,\phi) &= A_0(r,\theta,\phi) - \left[\frac{r^2+1}{2r}\right] A_0\left(\frac{1}{r},\theta,\phi\right) \\
&\quad + \left[(r^2-1)\right] \frac{\partial}{\partial r} A_0\left(\frac{1}{r},\theta,\phi\right) \\
&\quad - \left[\frac{r^2(r^2-1)^2}{4}\right] \nabla^2\left(r^{-1} A_0\left(\frac{1}{r},\theta,\phi\right)\right), \qquad (4.1.31) \\
B(r,\theta,\phi) &= B_0(r,\theta,\phi) - \frac{1}{r} B_0\left(\frac{1}{r},\theta,\phi\right). \qquad (4.1.32)
\end{aligned}
$$

Drag and Torque: The drag $\vec{\mathbf{D}}$ and torque $\vec{\mathbf{T}}$ experienced by the sphere on the boundary $r = 1$ are given by

$$
\begin{aligned}
\vec{\mathbf{D}} &= -\int_0^{\pi}\int_0^{2\pi} [T_{rr}\hat{\mathbf{e}_r} + T_{r\theta}\hat{\mathbf{e}_\theta} + T_{r\phi}\hat{\mathbf{e}_\phi}]_{r=1} \sin\theta d\theta d\phi, \qquad (4.1.33) \\
\vec{\mathbf{T}} &= -\int_0^{\pi}\int_0^{2\pi} [rT_{r\theta}\hat{\mathbf{e}_\phi} - rT_{r\phi}\hat{\mathbf{e}_\theta}]_{r=1} \sin\theta d\theta d\phi, \qquad (4.1.34)
\end{aligned}
$$

respectively. Hence the drag experienced by the sphere of radius 1 is found to be

$$\vec{\mathbf{D}} = -8\pi\alpha_1'(A_{11}\hat{\mathbf{i}} + B_{11}\hat{\mathbf{j}} + A_{10}\hat{\mathbf{k}}). \tag{4.1.35}$$

Similarly the torque is

$$\vec{\mathbf{T}} = -8\pi\chi_1(C_{11}\hat{\mathbf{i}} + D_{11}\hat{\mathbf{j}} + C_{10}\hat{\mathbf{k}}). \tag{4.1.36}$$

It is interesting to observe that the drag and torque are independent of the slip parameter $\overline{\lambda}$. Hence the formula for drag and torque are the same for all the boundary conditions ranging from no-slip to perfect-slip.

Examples:

4.1.1 A Stokeslet at the origin $(0, 0, 0)$:

Consider a Stokeslet of strength $\frac{F}{8\pi}$, located at the origin and whose axis is directed towards $\hat{\mathbf{i}}$. The corresponding scalar functions A_0 and B_0 are

$$A_0(r, \theta, \phi) = \frac{F}{8\pi}\sin\theta\cos\phi, \tag{4.1.37}$$

$$B_0(r, \theta, \phi) = 0. \tag{4.1.38}$$

The perturbed flow generated inside $r = 1$ for slip-stick boundary conditions (4.1.19)-(4.1.21) is given by (4.1.28)-(4.1.29) as follows.

$$A(r, \theta, \phi) = \frac{F}{8\pi}\left[1 - \frac{3(1+2\overline{\lambda})}{2(1+3\overline{\lambda})}r + \frac{1}{2(1+3\overline{\lambda})}r^3\right]\sin\theta\cos\phi, \tag{4.1.39}$$

$$B(r, \theta, \phi) = 0. \tag{4.1.40}$$

4.1.2 A Stokeslet located at $(0,0,c)$, $c<1$:

Consider a Stokeslet of strength $\frac{F}{8\pi}$, whose axis is directed towards $\hat{\mathbf{i}}$ and located at $(0,0,c), c<1$. The corresponding scalar functions A_0 and B_0 are

$$\begin{aligned} A_0(r,\theta,\phi) &= \frac{F}{8\pi}\sum_{n=1}^{\infty}\left[\frac{c^{n-1}}{n(2n-1)r^{n-1}} - \frac{(n+3)c^{n+1}}{n(n+1)(2n+3)r^{n+1}}\right]P_n^1(\zeta)\cos\phi, \\ B_0(r,\theta,\phi) &= \frac{F}{4\pi}\sum_{n=1}^{\infty}\left[\frac{c^n}{n(n+1)r^{n+1}}\right]P_n^1(\zeta)\sin\phi. \end{aligned}$$

In this case, the perturbed flow generated inside $r=1$ for slip-stick boundary conditions (4.1.19)-(4.1.21) is given by

$$\begin{aligned} A(r,\theta,\phi) &= \frac{F}{8\pi}\sum_{n=1}^{\infty}\left[\frac{\alpha_n}{r^{n+1}} + \frac{\alpha_n'}{r^{n-1}}\right. \\ &\quad - \left(\frac{\alpha_n(2n+3)+\alpha_n'(1+2\overline{\lambda})(2n+1)}{M_n}\right)r^n \\ &\quad \left. + \left(\frac{\alpha_n(1-2\overline{\lambda})(2n+1)+\alpha_n'(2n-1)}{M_n}\right)r^{n+2}\right]P_n^1(\zeta)\cos\phi, \\ B(r,\theta,\phi) &= \frac{F}{4\pi}\sum_{n=1}^{\infty}\frac{c^n}{n(n+1)}\left[\frac{1}{r^{n+1}} - \frac{(1-\overline{\lambda}(n+2))r^n}{(1+\overline{\lambda}(n-1))}\right]P_n^1(\zeta)\sin\phi, \end{aligned} \tag{4.1.41}$$

where $\alpha_n = -\frac{(n+3)c^{n+1}}{n(n+1)(2n+3)}$, $\alpha_n' = \frac{c^{n-1}}{n(2n-1)}$, $M_n = 2(1+\overline{\lambda}(2n+1))$. So the drag force acting on a sphere of unit radius is

$$\vec{\mathbf{D}} = -F\hat{\mathbf{i}}. \tag{4.1.42}$$

This shows that the drag is independent of the location of the Stokeslet. Similarly the torque experienced by the sphere is

$$\vec{\mathbf{T}} = cF\hat{\mathbf{j}}. \tag{4.1.43}$$

The expression (4.1.43) shows that the torque depends on the location of the Stokeslet. Hence the torque due to a Stokeslet located at the origin is zero.

Stagnation points: It turns out that for a Stokeslet induced slip flow problem (4.1.3)-(4.1.4) with (4.1.6)-(4.1.8) in a spherical container, the flow fields can be obtained in a rather simple method. By superposing suitable solutions of Stokes equations with appropriate behavior at the origin one finds the solution to (4.1.3)-(4.1.4) satisfying (4.1.6)-(4.1.8) (where $\vec{\mathbf{F}} = \frac{F}{8\pi}\hat{\mathbf{i}}$) as

$$q_r = \frac{F}{8\pi}\left[\frac{2}{r} - \frac{3(1+2\overline{\lambda})}{1+3\overline{\lambda}} + \frac{r^2}{1+3\overline{\lambda}}\right]\sin\theta\cos\phi, \tag{4.1.44}$$

$$q_\theta = \frac{F}{8\pi}\left[\frac{1}{r} - \frac{3(1+2\overline{\lambda})}{1+3\overline{\lambda}} + \frac{2r^2}{1+3\overline{\lambda}}\right]\cos\theta\cos\phi, \tag{4.1.45}$$

$$q_\phi = \frac{F}{8\pi}\left[-\frac{1}{r} + \frac{3(1+2\overline{\lambda})}{1+3\overline{\lambda}} - \frac{2r^2}{1+3\overline{\lambda}}\right]\sin\phi. \tag{4.1.46}$$

The last two terms in the above three expressions correspond to $\vec{\mathbf{q}}_G$. In the limit $\overline{\lambda} \to 0$, the above solution reduces to the Stokeslet flow in a no-slip container [91, 99] and for $\overline{\lambda} \to \infty$ it yields the solution for a shear-free boundary set up. It follows from the vanishing of (4.1.44)-(4.1.46) that there is a circle of stagnation points, in the meridian plane $\phi = \frac{\pi}{2}$ and $\phi = \frac{3\pi}{2}$, centered at the origin and radius given by the roots of the cubic (algebraic) equation

$$2r^3 - 3(1+2\overline{\lambda})r + (1+3\overline{\lambda}) = 0. \tag{4.1.47}$$

It is found that all the three roots of the above equation are real for $\overline{\lambda} > 0$ and one of them lies in the flow domain $r < 1$. For $\overline{\lambda} = 0$, the radius of the stagnation circle is $\frac{1}{2}(-1 \pm \sqrt{3})$ which is the radius of the stagnation circle for the no-slip case which agrees with the result

of Shail [99] who corrected the value previously given by Ranger [91]. We also observed that when $\phi = 0$ or π, $\theta = \frac{\pi}{2}$ and $r = 1$, the velocity components (4.1.44)-(4.1.46) vanish thus showing that $(1, 0, 0)$ and $(-1, 0, 0)$ are also the stagnation points for any value of $\overline{\lambda}$.

4.2 Axisymmetric case

When the flow is axisymmetric, $q_\phi = 0$ and the stream function $\psi_0(r, \theta)$ and the scalar functions A_0 and B_0 have the following relations.

$$A_0 = A_0(r, \theta),\ B_0 \equiv 0,\ \frac{\psi_0(r, \theta)}{r \sin\theta} = \frac{\partial A_0(r, \theta)}{\partial \theta}.$$

Here $\psi_0(r, \theta)$ is the stream function corresponding to the unperturbed velocity of the flow. In terms of the stream function $\psi(r, \theta)$ corresponding to the velocity of the flow in the presence of a sphere of unit radius, the boundary conditions are obtained from (4.1.6)-(4.1.8) as follows.

$$\psi(1, \theta) = 0, \tag{4.2.1}$$

$$\frac{\partial \psi(1, \theta)}{\partial r} = -\left(\frac{\overline{\lambda}}{1 - 2\overline{\lambda}}\right) \frac{\partial^2 \psi(1, \theta)}{\partial r^2}. \tag{4.2.2}$$

This agrees with the slip-stick boundary conditions given by Tophøj et al. [109]. For $\overline{\lambda} = \frac{1}{2}$ the boundary conditions are

$$\psi(1, \theta) = 0, \tag{4.2.3}$$

$$\frac{\partial^2 \psi(1, \theta)}{\partial r^2} = 0. \tag{4.2.4}$$

We observe that the vorticity in terms of the stream function is given by

$$\vec{\Omega} = \Omega\hat{\mathbf{e}}_\phi, \tag{4.2.5}$$

where $\Omega = \frac{D^2\psi}{r\sin\theta}$. But

$$\left(\frac{D^2\psi}{r\sin\theta}\right)_{r=1}\hat{\mathbf{e}}_\phi = \frac{1}{\sin\theta}\frac{\partial^2\psi(1,\theta)}{\partial r^2}\hat{\mathbf{e}}_\phi. \tag{4.2.6}$$

Hence the condition in (4.2.4) has a deeper implication that the vorticity on the boundary vanishes at $\overline{\lambda} = \frac{1}{2}$, indicating flow '*separation*'. We define the points of vanishing vorticity as separation points.

Suppose

$$\psi_0(r,\theta) = \sum_{n=1}^{\infty}[A_n r^{-n} + B_n r^{-n+2}]P_n^1(\zeta)\sin\theta. \tag{4.2.7}$$

Then in the presence of a sphere $r = 1$, let the stream function be given as follows.

$$\psi(r,\theta) = \sum_{n=1}^{\infty}[A_n r^{-n} + B_n r^{-n+2} + C_n r^{n+1} + D_n r^{n+3}]P_n^1(\zeta)\sin\theta, \tag{4.2.8}$$

where C_n and D_n are the unknowns to be determined from the boundary conditions. Using the boundary conditions (4.2.1)-(4.2.2), we solve for the two unknown constants in terms of A_n and B_n for $\overline{\lambda} \neq \frac{1}{2}$ as follows.

$$C_n = -\frac{A_n(2n+3) + B_n(1+2\overline{\lambda})(2n+1)}{M_n}, \tag{4.2.9}$$

$$D_n = \frac{A_n(1-2\overline{\lambda})(2n+1) + B_n(2n-1)}{M_n}, \tag{4.2.10}$$

where $M_n = 2(1 + (2n+1)\overline{\lambda})$. However, when $\overline{\lambda} = \frac{1}{2}$, the solution obtained using the boundary conditions (4.2.3)-(4.2.4) agrees with the solution given by (4.2.9)-(4.2.10) in the

limit $\overline{\lambda} \to \frac{1}{2}$. So this solution is valid for all $\overline{\lambda} \geq 0$. The solution can also be expressed in a closed form in terms of ψ_0 for $\overline{\lambda} \neq 0$ as follows.

$$\begin{aligned}\psi(r,\theta) &= \psi_0(r,\theta) - r^3\psi_0\left(\frac{1}{r},\theta\right) - (1-r^2) \\ &\quad \times \left[\frac{1}{8\overline{\lambda} r^{\frac{1}{2\overline{\lambda}}-\frac{1}{2}}} \int_\infty^{\frac{1}{r}} R^{-\frac{1}{2\overline{\lambda}}-\frac{3}{2}} \left(D^2\psi_0 - R^4 D^2\left(\frac{\psi_0}{R^2}\right)\right) dR\right]. \qquad (4.2.11)\end{aligned}$$

Examples:

4.2.1 An axisymmetric Stokeslet located at $(0,0,0)$:

Consider a Stokeslet of strength $\frac{F}{8\pi}$, whose axis is directed towards $\hat{\mathbf{k}}$ and located at $(0,0,0)$. The corresponding stream function is

$$\psi_0(r,\theta) = \frac{F}{8\pi} r \sin^2\theta. \qquad (4.2.12)$$

From (4.2.9)-(4.2.10), the perturbed flow generated inside a sphere $r = 1$ is given by the following stream function

$$\psi(r,\theta) = \frac{F}{8\pi}\left[r - \frac{3(1+2\overline{\lambda})}{2(1+3\overline{\lambda})} r^2 + \frac{1}{2(1+3\overline{\lambda})} r^4\right] \sin^2\theta. \qquad (4.2.13)$$

Here the drag is equal to $-F\hat{\mathbf{k}}$. The torque in this case is equal to zero.

4.2.2 An axisymmetric Stokeslet located at $(0,0,c)$, $c < 1$:

Consider a Stokeslet of strength $\frac{F}{8\pi}$, whose axis is directed towards $\hat{\mathbf{i}}$ and located at $(0,0,c)$. The corresponding stream function of the perturbed flow generated inside a

sphere $r = 1$ is

$$\psi_0(r,\theta) = \frac{F}{8\pi}\frac{r^2\sin^2\theta}{R_1}, \tag{4.2.14}$$

$$= \frac{F}{8\pi}\sum_{n=1}^{\infty}\left[\frac{A_n}{r^n}+\frac{B_n}{r^{n-2}}\right]P_n^1(\zeta)\sin\theta. \tag{4.2.15}$$

where $A_n = -\frac{c^{n+1}}{(2n+3)}$, $B_n = \frac{c^{n-1}}{(2n-1)}$ as in (4.2.7).

From (4.2.9)-(4.2.10), the perturbed flow is given by the following stream function

$$\begin{aligned}\psi(r,\theta) = \frac{F}{8\pi}\sum_{n=1}^{\infty}\Bigg[&\frac{A_n}{r^n}+\frac{B_n}{r^{n-2}}\\ &-\left(\frac{A_n(2n+3)+B_n(1+2\overline{\lambda})(2n+1)}{M_n}\right)r^{n+1}\\ &+\left(\frac{A_n(1-2\overline{\lambda})(2n+1)+B_n(2n-1)}{M_n}\right)r^{n+3}\Bigg]P_n^1(\zeta)\sin\theta.\end{aligned} \tag{4.2.16}$$

For $\overline{\lambda} \neq 0$, the solution can be written in a closed form as follows.

$$\begin{aligned}\psi(r,\theta) = \psi_0(r,\theta) &- \frac{1}{c}\frac{r^2\sin^2\theta}{R_2} - (1-r^2)\\ &\times\left[\frac{(1-c^2)}{4\overline{\lambda}r^{\frac{1}{2\overline{\lambda}}-\frac{1}{2}}}\int_{\infty}^{\frac{1}{r}}\left(R^{-\frac{1}{2\overline{\lambda}}+\frac{1}{2}}\frac{\sin^2\theta}{\overline{R_1}^3}\right)dR\right],\end{aligned} \tag{4.2.17}$$

where $R_2 = (r^2+c'^2-2rc'\cos\theta)^{\frac{1}{2}}$, $\overline{R_1} = (R^2+c^2-2Rc\cos\theta)^{\frac{1}{2}}$ with $c' = \frac{1}{c}$.

Here the drag is equal to $-F\hat{\mathbf{k}}$. The torque in this case is equal to zero.

We will now elaborate on these examples in detail in the following discussion. In particular, we will discuss some physical phenomenon associated with them like stagnation points and separation points.

Stokeslet at the origin: If the singularity is at the center of two dimensional configurations, the resulting systems possess high symmetry and the flow structure remains the same in most cases. The purpose of this note is to demonstrate that for a simple configuration of a Stokes flow in a spherical container - generated by a Stokeslet positioned at the center of the container - the use of slip-stick boundary conditions at the wall reveals that the eddy patterns do exist, but only for very small values of the slip parameter. Now the problem of a general Stokeslet located at an arbitrary point in a no-slip spherical container was first found by Oseen [74] and later by several others [35, 47, 99] on various occasions. Maul and Kim [63] presented the solution in the form of Stokes flow image singularities for both axisymmetric and non-axisymmetric Stokeslets. The solution for a Stokeslet at the origin can be extracted from these studies and was discussed earlier by Ranger [91] independently as the zero Reynolds number limit of the flow due to a Landau source at the center of a sphere. In fact, Ranger [91] used his solution to compute the first few terms of the perturbation expansion in powers of Reynolds number to illustrate the dominance of diffusion of vorticity over convection in the nonlinear regime. However, the slip flow problem with a Stokeslet in a container bounded by a spherical wall does not seem to have been discussed so far although the problem is mathematically tractable. The question addressed here is whether the slip has an impact on the flow structure. For a Stokeslet situated at the center of the spherical container in any direction, the flow is axially symmetric and therefore one can utilize the stream function formulation representing the flow. The velocity components for axisymmetric flow are connected to the stream function by (1.1.28)-(1.1.30) (Section 1.1 in Chapter 1). Using (4.1.6)-(4.1.8), the modified stream function $\psi(r, \theta)$ satisfying

slip-stick boundary conditions inside the sphere $r = 1$ is given as in (4.2.13). The velocity components corresponding to the stream function $\psi(r, \theta)$ are given as follows.

$$q_r(r,\theta) = \frac{F}{8\pi}\left[-\frac{2}{r} + \frac{3(1+2\overline{\lambda})}{1+3\overline{\lambda}} - \frac{1}{1+3\overline{\lambda}}r^2\right]\cos\theta, \tag{4.2.18}$$

$$q_\theta(r,\theta) = \frac{F}{8\pi}\left[\frac{1}{r} - \frac{3(1+2\overline{\lambda})}{1+3\overline{\lambda}} + \frac{2}{1+3\overline{\lambda}}r^2\right]\sin\theta, \tag{4.2.19}$$

$$q_\phi(r,\theta) = 0. \tag{4.2.20}$$

For $\overline{\lambda} \to 0$, the above yields Ranger's solution [91] for a rigid container. The vanishing of (4.2.18)-(4.2.20) indicates that there is a circle of stagnation points at $\theta = \frac{\pi}{2}$, centred at the origin and the radius of the circle is given by the roots of the cubic polynomial

$$2r^3 - 3r(1+2\overline{\lambda}) + (1+3\overline{\lambda}) = 0. \tag{4.2.21}$$

The velocity components (4.2.18)-(4.2.20) also vanish when $\theta = 0$ or π and $r = 1$, indicating that $(0, 0, 1)$ and $(0, 0, -1)$ are also the stagnation points for all values of $\overline{\lambda}$. From (4.2.13), the vorticity $\Omega = D^2\psi$ is given by

$$\Omega = \left[\frac{5}{1+3\overline{\lambda}} - \frac{2}{r^3}\right] r\sin\theta \tag{4.2.22}$$

and on the spherical container it becomes $\Omega = \frac{3(1-2\overline{\lambda})}{(1+3\overline{\lambda})}\sin\theta$. It follows that the vorticity vanishes for $\overline{\lambda} = \overline{\lambda}_c = \frac{1}{2}$, indicating the flow separation at the wall of the container $r = 1$. More importantly the vanishing of vorticity in the flow domain can be understood by the following algebraic equation

$$r^3 - \frac{2(1+3\overline{\lambda})}{5} = 0 \tag{4.2.23}$$

which always has one real root for $r \leq 1$. Note that for a no-slip spherical container, the vorticity does not vanish at the wall and consequently there is no separation. Further, for

$\overline{\lambda} < \overline{\lambda}_c$, $\Omega > 0$ and for $\overline{\lambda} < \overline{\lambda}_c$, $\Omega < 0$. The locations of the point of zero vorticity in the flow domain for various values of $\overline{\lambda}$ are provided in Table 4.2.1. It is clear that the stagnation points and the points of zero vorticity co-exist in the flow domain for $\overline{\lambda} < 0.5$. However for $\overline{\lambda} \geq 0.5$, only the stagnation points occur inside the container. Table 4.2.1 shows the roots for various values of the slip parameter $\overline{\lambda}$ starting with $\overline{\lambda} = 0$ (no-slip case). Here r_{stag}, r_{sep} refer to the stagnation and separation points respectively. It is seen that the radius of the stagnation circle increases with increasing $\overline{\lambda}$ and nearly approaches 0.5 as $\overline{\lambda} \to \infty$. Clearly the slip parameter affects the location of the stagnation points. The streamlines are plotted for some values of the slip parameter $\overline{\lambda}$ and the flow topologies are depicted in Figures 4.2.1 and 4.2.2.

For $\overline{\lambda} = 0$ which corresponds to the no-slip case, a pair of symmetric eddies attached to the container wall appear as shown in Figure 4.2.1 (a). As we vary $\overline{\lambda}$, the streamline topologies show a variety of flow patterns. First, the closed streamlines close to the location of the Stokeslet start opening up for a very small $\overline{\lambda}$ as seen from Figure 4.2.1 (b). A slight increase of the slip parameter opens additional streamlines leading to the generation of slender eddies close to the wall (see Figure 4.2.1 (c,d)). Further increase in $\overline{\lambda}$ pushes more fluid towards the wall making the slender eddies thinner and thinner as depicted in Figure 4.2.2 (a)-(c). As $\overline{\lambda}$ approaches 0.5, all the eddies completely disappear and the streamlines become flat and parallel to the axis (that is a dividing streamline) as can be seen in Figure 4.2.2 (d). We have noted that with further increase in $\overline{\lambda}$ beyond 0.5, the eddy patterns remain very similar to the one in Figure 4.2.2 (d). Now from Table 4.2.1 we observe that for $0 \leq \overline{\lambda} < 0.5$ the stagnation point r_{stag} and the point of zero vorticity r_{sep} co-exist in the fluid domain $r < 1$.

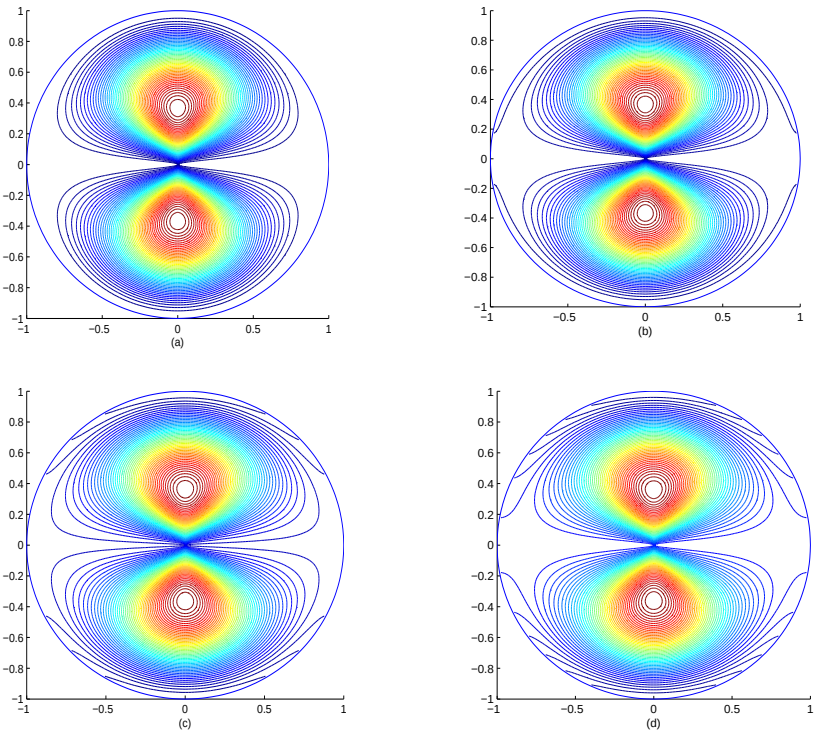

Figure 4.2.1: *Streamline topologies for the Stokeslet flow in a spherical container for different values of* λ*: (a)* $\overline{\lambda} = 0$*, (b)* $\overline{\lambda} = 0.00042$*, (c)* $\overline{\lambda} = 0.0016$*, (d)* $\overline{\lambda} = 0.0027$

This is precisely the range in which the eddy patterns occur in the spherical container. We have also given the plots for the vorticity in Figure 4.2.3. It is observed that the vortex contours become fewer (thinner) near $r = 1$ at $\overline{\lambda} = 0.5$. There is no vorticity contour on $r = 1$ at $\overline{\lambda} = 0.5$. As $\overline{\lambda}$ increases, the vorticity patterns change and remain steady, i.e. the same as $\overline{\lambda} = 10$ thereafter.

$\overline{\lambda}$	r_{stag}	r_{sep}	
0	0.3660	0.7368	No-slip (Ref. [93, 99])
0.001	0.3664	0.7375	
0.1	0.3955	0.8041	
0.5	0.4463	1	
5	0.4921	–	
20	0.4992	–	

Table 4.2.1. *Locations of the stagnation points r_{stag} and the points of zero vorticity r_{sep} for various $\overline{\lambda}$*

Therefore, one can conjecture that the co-existence of a stagnation point and a point of zero vorticity in the interior of the flow is a necessary condition for the eddy patterns to occur in the case of Stokeslet induced flow in a spherical slip container. The fact that phenomenal changes in the flow pattern occur for small values of the slip parameter suggests that care must be taken while choosing the values for the slip; otherwise, significant flow patterns may not be captured in bounded flows. Flows at small Knudson numbers Kn (ratio of the free mean path of the molecules to the characteristic gas-flow length) in micro-channels are of great interest in fabrication technology. A knowledge of the flow passing a spherical object moving in a micro-tube [115] is essential in designing biomedical and cooling devices. The exact analysis requires a more comprehensive investigation [115], but approximate results can be gained through Stokeslet solutions [9]. We now apply the Stokeslet solution to the derivation of an approximate expression for the drag on a particle situated at $(x, y, z) = (0, 0, 0)$ which translates without rotation parallel to the x-axis with

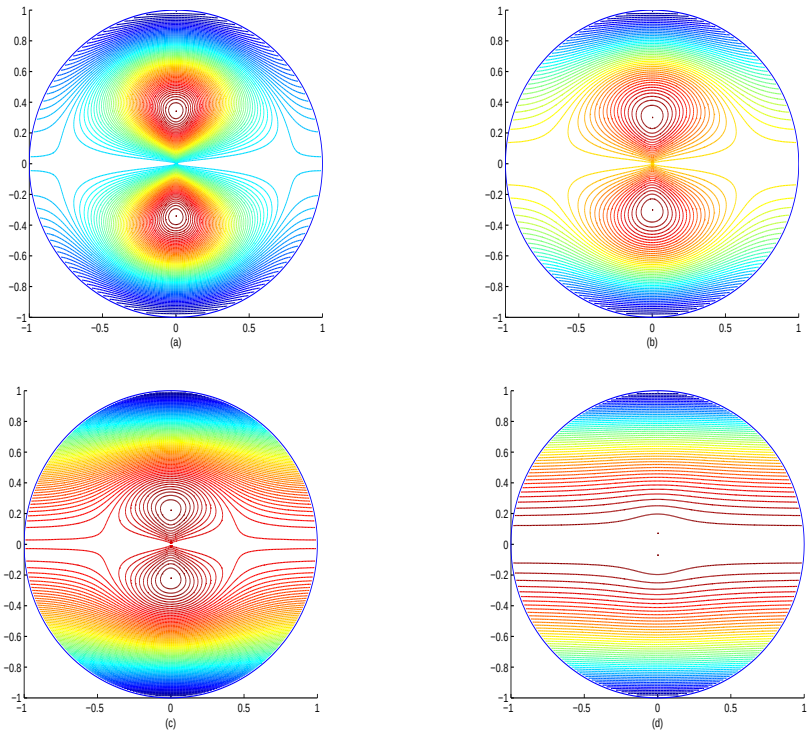

Figure 4.2.2: *Streamline topologies for the Stokeslet flow in a spherical container for different values of* λ*: (a)* $\overline{\lambda} = 0.0085$*, (b)* $\overline{\lambda} = 0.03$*, (c)* $\overline{\lambda} = 0.095$*, (d)* $\overline{\lambda} = 0.5$

velocity $U\hat{\mathbf{i}}$. The axis of translation is assumed to be a principal axis of resistance of the particle. Let $F\hat{\mathbf{i}}$ and $F_\infty\hat{\mathbf{i}}$ denote the viscous drag forces on the slip particle for the bounded motion and motion in an everywhere infinite fluid. If a_s denotes a typical dimension and h measures the distance of a suitable center, say Q, of the translating body from the slip

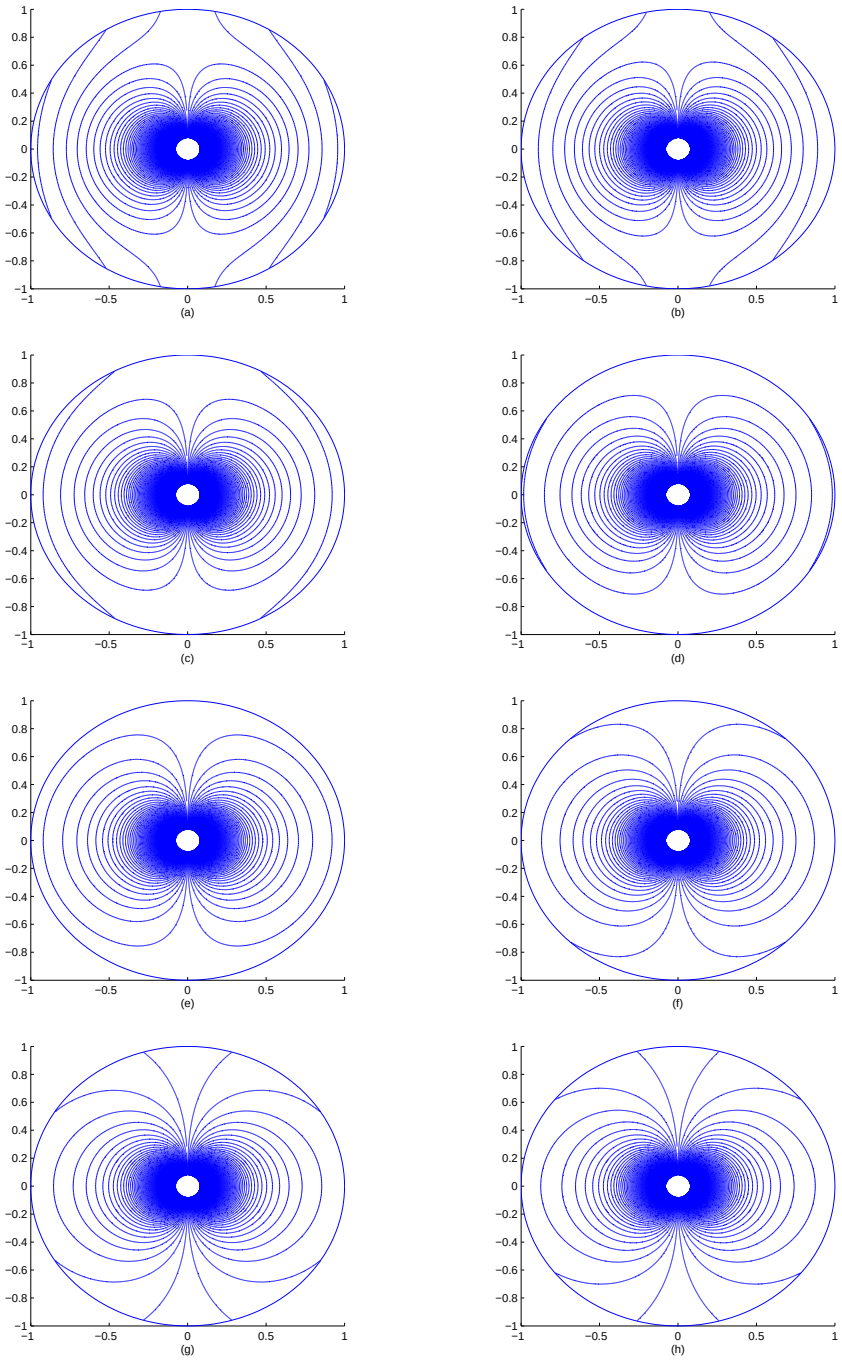

Figure 4.2.3: *Vorticity plots for an axisymmetric flow due to a Stokeslet located at* $(0,0,0)$ *for different values of* $\overline{\lambda}$*: (a)* $\overline{\lambda}=0$*, (b)* $\overline{\lambda}=0.03$*, (c)* $\overline{\lambda}=0.2$*, (d)* $\overline{\lambda}=0.3$*, (e)* $\overline{\lambda}=0.5$*, (f)* $\overline{\lambda}=1$*, (g)* $\overline{\lambda}=10$*, (h)* $\overline{\lambda}=100$

spherical container, then according to Brenner [9]

$$\frac{F}{F_\infty} = \frac{1}{1 + k_1(F_\infty/6\pi\mu U h)} + O(\epsilon^2), \tag{4.2.24}$$

where $\epsilon = a_s/h$, and the constant factor k_1 is defined by

$$k_1 = -\frac{3}{4}[\vec{\mathbf{q}} * (\vec{\mathbf{Q}}) \cdot \hat{\mathbf{i}}], \tag{4.2.25}$$

$\vec{\mathbf{q}} * (\vec{\mathbf{Q}})$ being the regular part of the Stokeslet velocity field evaluated at the center $Q(0,0,0)$. Using (4.2.18)-(4.2.20), the drag factor for a moving particle in a slip spherical container is

$$k_1 = \frac{9}{4}\left(\frac{1+2\overline{\lambda}}{1+3\overline{\lambda}}\right). \tag{4.2.26}$$

The k_1 factor decreases monotonically for increasing $\overline{\lambda}$. When $\overline{\lambda} = 0$, $k_1 = \frac{9}{4}$ agreeing with the results in [9, 99] for a particle at the center of a no-slip container. When $\overline{\lambda} \to \infty$, $k_1 = \frac{3}{2}$ yielding the results for a particle at the center of a shear-free sphere.

Stokeslet located away from the origin: Consider an off-centred Stokeslet located at $(0,0,c)$, of strength $\frac{F}{8\pi}$ and directed towards $\hat{\mathbf{i}}$. The perturbed flow inside the sphere is given as in equation (4.2.17) for $\overline{\lambda} \neq 0$. We note that for $\overline{\lambda} = 0$, all the points on $r = 1$ are stagnation points due to the no-slip conditions on $r = 1$. The velocity components corresponding to the modified stream function are given as follows.

$$q_r = \frac{F}{8\pi}\left(\frac{-2\cos\theta}{(r^2+c^2-2rc\cos\theta)^{\frac{1}{2}}} + \frac{cr\sin^2\theta}{(r^2+c^2-2rc\cos\theta)^{\frac{3}{2}}}\right)$$

$$
\begin{aligned}
&+\left(\frac{2c'\cos\theta}{(r^2+c'^2-2rc'\cos\theta)^{\frac{1}{2}}}-\frac{c'^2r\sin^2\theta}{(r^2+c'^2-2rc'\cos\theta)^{\frac{3}{2}}}\right)\\
&-\left[\frac{(1-r^2)(1-c^2)}{4\overline{\lambda}r^{\frac{1}{2\overline{\lambda}}+\frac{3}{2}}}\int_{\frac{1}{r}}^{\infty}\left\{\frac{2R^{-\frac{1}{2\overline{\lambda}}+\frac{1}{2}}\cos\theta}{(R^2+c^2-2Rc\cos\theta)^{\frac{3}{2}}}-\frac{3cR^{-\frac{1}{2\overline{\lambda}}+\frac{3}{2}}\sin^2\theta}{(R^2+c^2-2Rc\cos\theta)^{\frac{5}{2}}}\right\}dR\right],\\
q_\theta \;=\;& \frac{F}{8\pi}\left(\frac{2\sin\theta}{(r^2+c^2-2rc\cos\theta)^{\frac{1}{2}}}-\frac{r\sin\theta(r-c\cos\theta)}{(r^2+c^2-2rc\cos\theta)^{\frac{3}{2}}}\right)\\
&-\left(\frac{2c'\sin\theta}{(r^2+c'^2-2rc'\cos\theta)^{\frac{1}{2}}}-\frac{c'r\sin\theta(r-c'\cos\theta)}{(r^2+c'^2-2rc'\cos\theta)^{\frac{3}{2}}}\right)\\
&+\left(\frac{(1-r^2)(1-c^2)\sin\theta}{4\overline{\lambda}c^3(r^2+c'^2-2rc'\cos\theta)^{\frac{3}{2}}}\right)\\
&+\left\{-\frac{2(1-c^2)}{4\overline{\lambda}r^{\frac{1}{2\overline{\lambda}}-\frac{1}{2}}}+\left(-\frac{1}{2\overline{\lambda}}+\frac{1}{2}\right)\frac{(1-r^2)(1-c^2)}{4\overline{\lambda}r^{\frac{1}{2\overline{\lambda}}+\frac{3}{2}}}\right\}\left(\int_{\frac{1}{r}}^{\infty}\frac{R^{-\frac{1}{2\overline{\lambda}}+\frac{1}{2}}\sin\theta}{(R^2+c^2-2Rc\cos\theta)^{\frac{3}{2}}}dR\right),\\
q_\phi \;=\;& 0, \qquad (4.2.27)
\end{aligned}
$$

where $c'=\frac{1}{c}$.

We now show that irrespective of the location of the off-centred Stokeslet and the value of the slip parameter $\overline{\lambda}\neq 0$, the stagnation points are at $(0,0,1)$ and $(0,0,-1)$. It is found from the expressions of the velocity components in (4.2.27) that the tangential component of the velocity vanishes whenever $\theta=0$ or π. The no-flux condition at the impermeable wall implies that the normal component of velocity is zero at $r=1$ as given in (4.1.6) and again since the tangential component of the velocity vanishes on the z-axis this indicates that $(0,0,1)$ and $(0,0,-1)$ are the two stagnation points for all values of $\overline{\lambda}$ and for all locations of the Stokeslet.

θ	r_{sep}	θ	r_{sep}
0.2	0.8096/0.8068	1.8	0.3056/0.7088
0.4	0.8012/0.804	2.0	0.3588/0.6976
0.6	0.79/0.7928	2.2	0.6864
0.8	0.4484/0.7788	2.4	0.6808
1.0	0.3952/0.762	2.6	0.5212/0.6752
1.2	0.748	2.8	0.6696
1.4	0.734	3.0	0.5744/0.6668
1.6	0.72		

Table 4.2.2. Locations of the separation points for $\overline{\lambda} = 0$ for a Stokeslet located at $(0, 0, 0.3)$

θ	r_{sep}	θ	r_{sep}
0.2	0.9468	1.8	0.902/0.3056
0.4	0.944	2.0	0.8964/0.3588
0.6	0.9384	2.2	0.8908
0.8	0.9328/0.4456	2.4	0.8852
1.0	0.9272/0.3952	2.6	0.8824/0.5212
1.2	0.9188	2.8	0.8824
1.4	0.9132	3.0	0.8796/0.5716
1.6	0.9076		

Table 4.2.3. Locations of the separation points for $\overline{\lambda} = 0.3$ for a Stokeslet located at $(0, 0, 0.3)$

θ	r_{sep}	θ	r_{sep}
0.8	0.4484	2.0	0.3588
1.0	0.3952	2.6	0.5212
1.8	0.3056	3.0	0.5716

Table 4.2.4. Locations of the separation points for $\overline{\lambda} = 0.5, 1, 10$ *for a Stokeslet located at* $(0, 0, 0.3)$

θ	r_{sep}	θ	r_{sep}
0.8	0.748	2.0	0.598
1.0	0.66	2.6	0.866
1.8	0.51	3.0	0.95

Table 4.2.5. Locations of the separation points for $\overline{\lambda} = 0.5, 10, 100$ *for a Stokeslet located at* $(0, 0, 0.5)$

θ	r_{sep}	θ	r_{sep}
1.0	0.934	2.0	0.8476
1.8	0.7204		

Table 4.2.6. Locations of the separation points for $\overline{\lambda} = 0.5, 10, 100$ *for a Stokeslet located at* $(0, 0, 0.7)$

θ	r_{sep}
1.0	0.9432

Table 4.2.7. Locations of the separation points for $\overline{\lambda} = 0.5, 10, 100$ *for a Stokeslet located at* $(0, 0, 0.9)$

Tables 4.2.2-4.2.3 shows that for different values of $\overline{\lambda}$, the separation points also change. However, this happens upto $\overline{\lambda} = 0.5$, beyond which we find the same sets of separation points. Tables 4.2.4-4.2.7 give the sets of separation points for different locations of the Stokeslet. From these tables we observe that in each case, the sets of separation points remain the same for all values of $\overline{\lambda} > 0.5$. The vorticity on the boundary $r = 1$ also vanishes for $\overline{\lambda} = \frac{1}{2}$ irrespective of the position of the Stokeslet. We found in the case of an axisymmetric flow due to an off-centred Stokeslet located at $(0, 0, 0.3)$ that the stagnation points and the points of zero vorticity always co-exist and hence the eddy patterns in the flow domain always exist for all values of $\overline{\lambda}$ as is evident from Figures 4.2.4. Figures 4.2.4 (a)-(e) depict how the eddy patterns change with $\overline{\lambda}$ between 0 and 0.5. We found analytically and numerically in this case that there are only two stagnation points in the flow domain. Further we do not find any more points of zero vorticity for $\overline{\lambda} > 0.5$ as observed from Table (4.2.4). From Figure 4.2.4 (e)-(h), we find that the flow patterns remain the same thereafter. We verified this for different locations of Stokeslet inside the sphere and observed the same phenomenon for different values of c. Hence we conjecture that the existence of both the stagnation and the separation points ensure the existence of eddy patterns.

Stokeslet reversal: For a Stokeslet of strength $\frac{F}{8\pi}$ located at $(0, 0, c)$, $c < 1$, and whose axis is directed towards $\hat{\mathbf{k}}$, the stream function corresponding to the unperturbed flow is given in Example 4.2.2 as

$$\psi_0(r, \theta) = \frac{F}{8\pi} \frac{r^2 \sin^2 \theta}{R_1}. \tag{4.2.28}$$

Now the stream function due to a Stokeslet located inside a rigid sphere of radius 1 (corre-

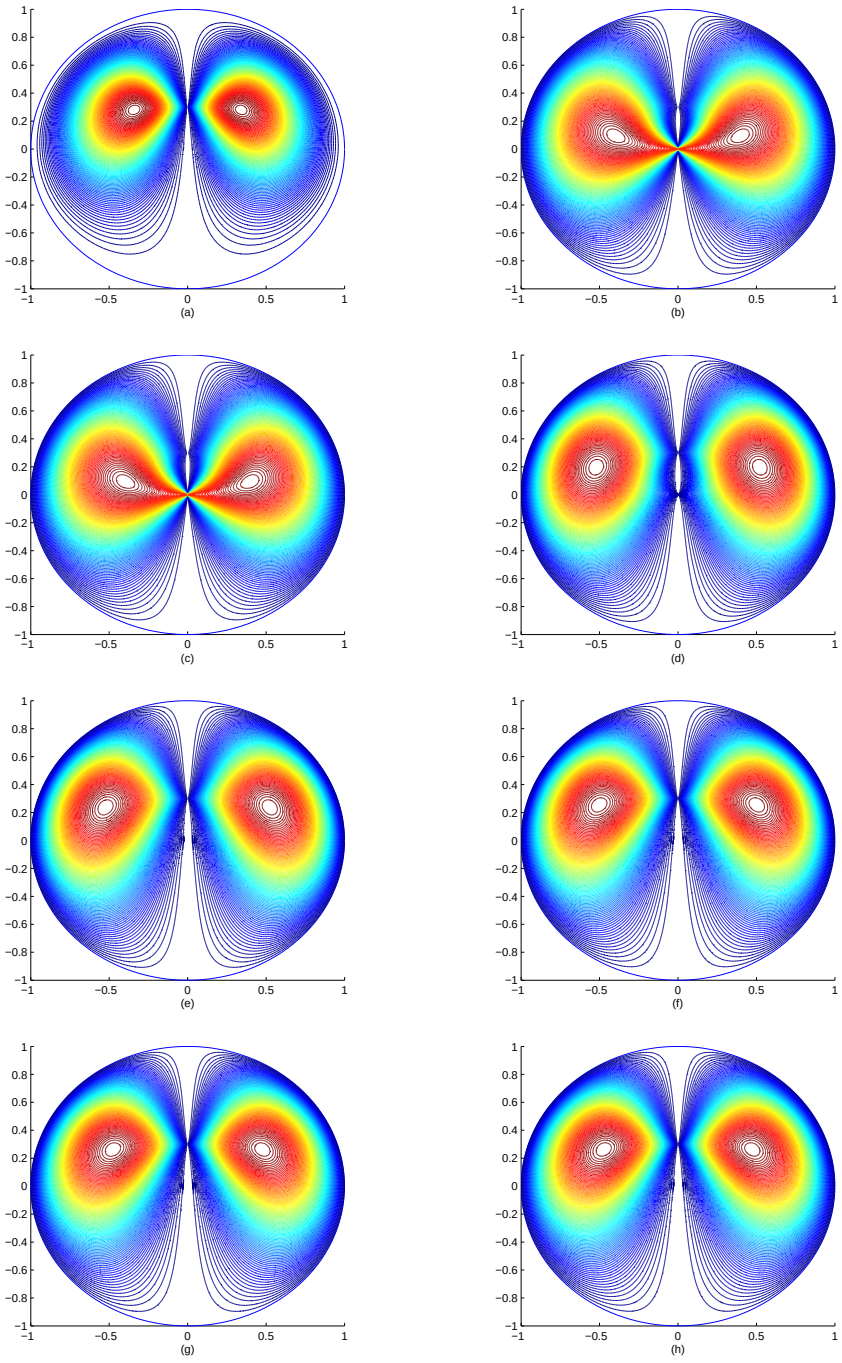

Figure 4.2.4: *Contour plots for an axisymmetric flow due to a Stokeslet located at* $(0, 0, 0.3)$ *for different values of* $\overline{\lambda}$*: (a)* $\overline{\lambda} = 0$*, (b)* $\overline{\lambda} = 0.17$*, (c)* $\overline{\lambda} = 0.2$*, (d)* $\overline{\lambda} = 0.3$*, (e)* $\overline{\lambda} = 0.5$*, (f)* $\overline{\lambda} = 1$*, (g)* $\overline{\lambda} = 10$*, (h)* $\overline{\lambda} = 100$

sponding to $\overline{\lambda} = 0$) is given by Collin's sphere theorem [15] as

$$\begin{aligned}\psi(r,\theta) &= \psi_0(r,\theta) + \frac{F}{8\pi}\left(\frac{c'^3 - 3c'}{2}\right)\frac{r^2\sin^2\theta}{R_2} \\ &+\frac{F}{8\pi}(c'^2(c'^2-1))\frac{r^2\sin^2\theta(r\cos\theta - c')}{R_2^3} \\ &+\frac{F}{8\pi}\left(\frac{c'(c'^2-1)^2}{4}\right)\frac{2r^2\sin^2\theta}{R_2^3},\ c' = \frac{1}{c}. \end{aligned} \tag{4.2.29}$$

The image comprises of a Stokeslet and higher order singularities namely, a Stresslet and a degenerate Quadrupole at $(0,0,c')$ of strengths $\frac{F}{8\pi}\frac{(c'^3-3c')}{2}$, $\frac{F}{8\pi}c'^2(c'^2-1)$, $\frac{F}{8\pi}\frac{c'(c'^2-1)^2}{4}$ respectively, agreeing with the result of Maul and Kim [63]. In fact, if the original Stokeslet is very close to the spherical wall, i.e., if $c = 1-\epsilon$ and $c' = \frac{1}{c} \simeq 1+\epsilon$, where $\epsilon \ll 1$, then the coefficient (the strength) of the image Stokeslet $\frac{F}{8\pi}(\frac{c'^3-3c'}{2})$ becomes equal to $-\frac{F}{8\pi}$, thus indicating that the Stokeslet in the image is equal in magnitude, but opposite in direction to the original Stokeslet. For $c' < \sqrt{3}$, the sign of the coefficient of the image Stokeslet is opposite to that of the given Stokeslet whereas for $c' > \sqrt{3}$ the sign is the same as that of the given Stokeslet. As the location $(0,0,c)$ $(0 < c < 1)$ of the given Stokeslet varies, if there is a critical value of c at which the strength of the image Stokeslet vanishes, then this phenomena is called as '*Stokeslet reversal*'. Since there is a reversal of the orientation of the image Stokeslet as c passes through this critical value, this phenomena is termed as Stokeslet reversal. This means that the strength of the image Stokeslet changes sign as c passes through this critical value. Maul and Kim [63] considered the problem of Stokes flow generated due to a Stokeslet inside a rigid sphere and found the critical value of c to be equal to $\frac{1}{\sqrt{3}}$. When the Stokeslet is inside a shear-free sphere, the image consists of another

Stokeslet at the inverse point. Then the stream function in the presence of the sphere is

$$\psi(r,\theta) = \frac{F}{8\pi}\frac{r^2\sin\theta}{R_1} - \frac{F}{8\pi}c'\frac{r^2\sin\theta}{R_2}. \tag{4.2.30}$$

So we do not find any c' for which the image Stokeslet vanishes unless $c' = 0$ which is impractical. Hence there is no Stokeslet reversal in the shear-free case. We try to check whether the Stokeslet reversal phenomenon can be observed in the case of slip-stick boundary conditions. Consider the closed form of the stream function for the slip-stick boundary conditions given by (4.2.1)-(4.2.2) for a given undisturbed flow $\psi_0(r,\theta)$ given by (4.2.14) as follows.

$$\psi(r,\theta) = \psi_0(r,\theta) + Image(\psi_0(r,\theta)), \tag{4.2.31}$$

where

$$\begin{aligned} Image(\psi_0(r,\theta)) &= -\frac{1}{c}\frac{r^2\sin^2\theta}{R_2} - (1-r^2) \\ &\quad \times \left[\frac{(1-c^2)}{4\overline{\lambda}r^{\frac{1}{2\overline{\lambda}}-\frac{1}{2}}}\int_\infty^{\frac{1}{r}}\left(R^{-\frac{1}{2\overline{\lambda}}+\frac{1}{2}}\frac{\sin^2\theta}{\overline{R_1}^3}\right)dR\right], \end{aligned}$$

for $\overline{\lambda} \neq 0$ from (4.2.17).

Due to the presence of the improper integral in $Image(\psi_0(r,\theta))$ and therefore in (4.2.17), it is not possible to come to any definite conclusion about Stokeslet reversal, as the image singularities cannot be identified easily from the closed form. We require to determine the strength of the image Stokeslet and check where it would vanish. By adopting the method given in the Appendices 4.1 and 4.2 we find that the strength of the image Stokeslet at $(0,0,c')$ is given as $\frac{F}{8\pi}\left(\frac{c'^3-3(1+2\overline{\lambda})c'}{2(1+3\overline{\lambda})}\right)$. Unlike in the no-slip case, the strength of the image

Stokeslet is never equal in magnitude to the given Stokeslet, no matter how much ever close the given Stokelset is to the spherical wall. This is because $\frac{F}{8\pi}\left(\frac{c'^3-3(1+2\overline{\lambda})c'}{2(1+3\overline{\lambda})}\right) \simeq -\frac{F}{8\pi}(1+3\overline{\lambda}(1+\epsilon))$ whenever $c \simeq 1-\epsilon$. However, for $c' > \sqrt{3(1+2\overline{\lambda})}$ or $c < \frac{1}{\sqrt{3(1+2\overline{\lambda})}}$ the image Stokeslet is directed opposite to that of the direction of the given Stokeslet inside the sphere $r = 1$ and at the '*critical*' value of $c = \frac{1}{\sqrt{3(1+2\overline{\lambda})}}$ or $c' = \sqrt{3(1+2\overline{\lambda})}$, the image Stokeslet vanishes. Apparently one can see that for the no-slip case, i.e., for $\overline{\lambda} = 0$, $c = \frac{1}{\sqrt{3}}$. The streamlines for a Stokeslet at different locations and for different values of $\overline{\lambda}$ in a sphere of unit radius are given in the Figures 4.2.4.

By a similar analysis in the case of a non-axisymmetric Stokeslet, as given in Example 4.1.2, using A and B given as in (4.1.41), the Stokeslet reversal is found to be absent in the non-axisymmetric case when the Stokeslet is located at $(0, 0, c)$ and directed towards $\hat{\mathbf{i}}$ since the coefficient of the image Stokeslet $\frac{F}{8\pi}\frac{(c'^3+3(1+2\overline{\lambda})c')}{4(1+3\overline{\lambda})}$ never vanishes for any value of c'.

4.3 Conclusions

The problem of Stokes flow generated inside a rigid sphere with slip-stick boundary conditions has been studied by considering a singularity generated flow due to a Stokeslet. We have given a closed form solution for the perturbed flow (in both axisymmetric and non-axisymmetric cases) and calculated the drag on the sphere. We showed that the drag is independent of the location of the Stokeslet and that only the torque depends on the location of a non-axisymmetric Stokeslet. In fact, we observe that torque due to a Stokeslet located at the origin is zero. However, the torque is always zero in axisymmetric flows. We

concluded in the axisymmetric case that the stagnation and separation points change with the slip parameter $\overline{\lambda}$. We observed that the co-existence of both separation and stagnation points in the flow domain lead to the formation of the eddies in the case of an axisymmetric Stokes flow due to a Stokeslet at the origin. We showed analytically that for an axisymmetric flow due to an off-centred Stokeslet there are only two stagnation points. We also observed that the set of separation points do not change for $\overline{\lambda} \geq 0.5$. Unlike the flow due to a Stokeslet at the origin where the eddy patterns vanish for $\overline{\lambda} > 0.5$, the eddy patterns in the flow due to an off-centred Stokeslet exist for all values of $\overline{\lambda}$. In fact, we conjecture that the eddy patterns do not change for $\overline{\lambda} > 0.5$ because of the co-existence of the same sets of the stagnation points and the separation points in the flow domain. In fact, the eddy patterns remain the same for all $\overline{\lambda} > 0.5$ for the same reason. We also showed the existence of 'Stokeslet reversal' phenomenon in an axisymmetric flow which indicates that the strength of the image Stokeslet reverses its sign depending on the location of the given Stokeslet. We found that the strength of the image Stokeslet vanishes at $\sqrt{3(1+2\overline{\lambda})}$, $\overline{\lambda}$ being the slip parameter. It is evident that the Stokeslet reversal is dependent on the slip parameter $\overline{\lambda}$. We do not find any evidence of Stokeslet reversal in the following cases.

- Axisymmetric flow inside a sphere due to a Stokeslet located at the origin with slip-stick boundary conditions.
- Axisymmetric flow inside a sphere due to an off-centred Stokeslet with shear-free boundary conditions.
- Non-axisymmetric flow due to an off-centred Stokeslet with slip-stick boundary con-

ditions.

Appendix 4.1

Consider an axisymmetric Stokes flow due to a Stokeslet of strength $\frac{F}{8\pi}$, located at $(0,0,C)$ $C>1$ and directed towards $\hat{\mathbf{k}}$. The corresponding stream function is

$$\psi_0 = \frac{F}{8\pi}\sum_{n=1}^{\infty}[\alpha_n r^{n+1}+\alpha_n' r^{n+3}]\sin\theta P_n^1(\zeta), \tag{4.3.1}$$

where $\alpha_n = \frac{C^{-n}}{(2n-1)}$, $\alpha_n' = -\frac{C^{-n-2}}{(2n+3)}$.

The modified stream function ψ in the presence of a sphere of unit radius satisfying the slip-stick boundary conditions (1.2.6) is given as follows [75].

$$\psi = \psi_0+\psi_0^+, \tag{4.3.2}$$

where ψ_0^+ is the image of ψ_0 in the presence of a sphere of radius 1, given by

$$\begin{aligned}\psi_0^+ = \frac{F}{8\pi}\sum_{n=1}^{\infty}\Bigg[&\left(\frac{\alpha_n(2n-1)+\alpha_n'(1-2\overline{\lambda})(2n+1)}{2(1+\overline{\lambda}(2n+1))}\right)r^{-n}\\ &-\left(\frac{\alpha_n(1+2\overline{\lambda})(2n+1)+\alpha_n'(2n+3)}{2(1+\overline{\lambda}(2n+1))}\right)r^{-n+2}\Bigg]\sin\theta P_n^1(\zeta).\end{aligned} \tag{4.3.3}$$

Let $C'=\frac{1}{C}$ so that $(0,0,C')$ is the location of the inverse point with respect to the sphere of radius 1. Then observe that the series of ψ_0^+ is valid in the region $C'<r<1$.

Appendix 4.2

Suppose we have a Stokeslet enclosed in a small sphere $B(\vec{\mathbf{r}}, \delta)$, centred around the location of the Stokeslet, which in turn is assumed to be contained in another sphere $B(\vec{\mathbf{0}}, R)$ centred at the origin, where $\vec{\mathbf{0}} = (0, 0, 0)$ and $\vec{\mathbf{r}} = (x, y, z)$. Then the drag on both the spheres is the same provided there are no other singularities in the region enclosed between $B(\vec{\mathbf{0}}, R)$ and $B(\vec{\mathbf{r}}, \delta)$. This can be proved easily from Stokes' equation which is $T_{ij,j} = 0$, where $T_{ij,j}$, $i, j = 1, 2, 3$, are the contravariant derivatives of the components of the stress tensor. From this, we have

$$\int_{B(\vec{\mathbf{0}},R)-B(\vec{\mathbf{r}},\delta)} T_{ij,j} dV \quad = \quad 0, \tag{4.3.4}$$

where dV is the measure of an infinitesimally small volume in this annular region (Refer Batchelor [3], pp 238-240). By Gauss-divergence theorem

$$\int_{\partial B(\vec{\mathbf{0}},R)} T_{ij,j}.\hat{\mathbf{n}}_R dS \quad = \quad \int_{\partial B(\vec{\mathbf{r}},\delta)} T_{ij,j}.\hat{\mathbf{n}}_\delta dS = 8\pi M, \tag{4.3.5}$$

where $\hat{\mathbf{n}}_R$ and $\hat{\mathbf{n}}_\delta$ are the outward drawn unit normals to the surfaces of the spheres $B(\vec{\mathbf{0}}, R)$ and $B(\vec{\mathbf{r}}, \delta)$ respectively and M being the strength of the Stokeslet. Equation (4.3.5) shows that the drag on the boundary $\partial B(\vec{\mathbf{0}}, R)$ is same as the drag on the boundary $\partial B(\vec{\mathbf{r}}, \delta)$ and is equal to $8\pi M$. Equation (4.3.5) denotes the formulae to compute the drag on a sphere. It is known that for a Stokes flow past a sphere, the drag is equal to the strength of the Stokeslet at the inverse point inside the sphere so that both the forces from outside and within the sphere balance and the sphere $r = 1$ becomes a streamsurface. Using this result in the present context, where the image Stokeslet is located at $(0, 0, c')$, we employ the following

method to find the strength of the image Stokeslet which is present in $Image(\psi_0(r,\theta))$ in equation (4.2.31) which is same as (4.2.17). The stream function ψ given in (4.2.31) or (4.2.17) can be expressed in the form of an infinite series which is given by (4.2.16), that is valid in the region $c < r < 1$, and is expressed as follows.

$$\begin{aligned}
\psi(r,\theta) &= \psi_0 + \psi_0^-, \\
&= \frac{F}{8\pi}\sum_{n=1}^{\infty}\Big[A_n r^{-n} + B_n r^{-n+2} \\
&\quad - \left(\frac{A_n(2n+3) + B_n(1+2\overline{\lambda})(2n+1)}{M_n}\right) r^{n+1} \\
&\quad + \left(\frac{A_n(1-2\overline{\lambda})(2n+1) + B_n(2n-1)}{M_n}\right) r^{n+3}\Big] P_n^1(\zeta)\sin\theta, \qquad (4.3.6)
\end{aligned}$$

where

$$\psi_0 = \frac{F}{8\pi}\sum_{n=1}^{\infty}\left[A_n r^{-n} + B_n r^{-n+2}\right] P_n^1(\zeta)\sin\theta, \qquad (4.3.7)$$

$$\begin{aligned}
\psi_0^- &= -\frac{F}{8\pi}\left[\frac{A_n(2n+3) + B_n(1+2\overline{\lambda})(2n+1)}{M_n}\right) r^{n+1} \\
&\quad + \left(\frac{A_n(1-2\overline{\lambda})(2n+1) + B_n(2n-1)}{M_n}\right) r^{n+3}\Big] P_n^1(\zeta)\sin\theta, \qquad (4.3.8)
\end{aligned}$$

$A_n = -\frac{c^{n+1}}{(2n+3)}$, $B_n = \frac{c^{n-1}}{(2n-1)}$, $c' = \frac{1}{c} > 1$. Here ψ_0^- denotes the image of ψ_0 located at $(0,0,c')$ which is the same as $Image(\psi_0(r,\theta))$ in (4.2.17). Now let $\vec{\mathbf{r}} = \vec{\mathbf{c}}'$, where $\vec{\mathbf{c}}' = (0,0,c')$. Observe that the image of ψ_0, i.e. ψ_0^-, consists of singularities like a Stokeslet at $(0,0,c')$. In order to check for Stokeslet reversal, we have to find whether there is a value of $c < 1$ for which the strength of the Stokeslet which is present in ψ_0^- at the inverse point vanishes.

Computation of the strength M of the image Stokeslet: Consider the singularities corresponding to the stream function ψ_0^- located at $(0,0,c')$ in $\mathbb{R}^3$. Let us consider an imaginary

sphere $B(\vec{\mathbf{r}}, \delta)$ where $\vec{\mathbf{r}} = (0, 0, c')$ located inside the imaginary sphere $B(\vec{\mathbf{0}}, R)$. As discussed previously, the drag on $\partial B(\vec{\mathbf{0}}, R)$ is same as the drag on $\partial B(\vec{\mathbf{r}}, \delta)$ which is given by $8\pi M$ where M is the strength of the Stokeslet at $(0, 0, c')$ (which is present in the image of ψ_0). In fact, the sign of M gives the orientation of the Stokeslet. To find the strength of the image Stokeslet, we look at the series representation of ψ_0^- that is valid in the region $c' < r < R$ and find the coefficient of $r \sin^2\theta$ i.e., M from it (Refer Batchelor [3] pp 238-240). We can show that such a series representation of ψ_0^- which is valid in the region $c' < r < R$, is given by ψ_0^+ where $C = c$ in equation (4.3.3). Note that the series representation of ψ_0^+ which is given in (4.3.3) is obtained by replacing n by $-n-1$ and also $\overline{\lambda}$ by $-\overline{\lambda}$ in (4.3.8). These replacements are justified by the facts that $\chi_1 = r^n \sin\theta P_n^1(\zeta)$ and $\chi_2 = r^{-n-1} \sin\theta P_n^1(\zeta)$ both satisfy $D^2\chi_i = 0$ $i = 1, 2$ (Refer Batchelor [3] pp 121-122) and also $\lim\limits_{r \to c'-} \psi_0^- = \lim\limits_{r \to c'+} \psi_0^+$. From (4.3.3), the coefficient of $r \sin^2\theta$ is then found to be

$$\frac{F}{8\pi} \left(\frac{c'^3 - 3(1 + 2\overline{\lambda})c'}{2(1 + 3\overline{\lambda})} \right), \tag{4.3.9}$$

which is the strength M of the image Stokeslet at $(0, 0, c')$.

Chapter 5

Stokes flow past an arbitrary shaped body with slip-stick boundary conditions

5.1 Introduction

The two dimensional problem of a viscous, incompressible flow past an arbitrarily shaped body with no-slip boundary conditions was discussed by Bourot [8], Hellou and Coutanceau [36] using the method of least squares. Later, Lecoq [53] studied the problem of an axisymmetric Stokes flow past an arbitrary shaped body with no-slip boundary conditions. Payne and Pell [82] considered an axisymmetric Stokes flow past an arbitrary shaped rigid particle

and gave a formula to compute the drag in terms of the stream function. The solution proposed by Palaniappan et al. [79] which is in terms of two scalar functions A and B was used in an effective manner for solving many boundary value problems involving spherical boundaries using the two scalar functions which play the role of the stream function. But there has been no general formula for the corresponding problem of a non-axisymmetric Stokes flow in the presence of a rigid body of arbitrary shape. However there have been some attempts to discuss Stokes flow past rigid bodies having non-spherical shapes. The earliest such attempts were by Oberbeck [73] and G.B.Jefferey [41] who discussed the motion of ellipsoidal particles in a viscous fluid where the solution was given in terms of certain improper integrals. Kim and Arunachalam [46] derived the general solution for Stokes flow past an ellipsoid by using a representation of the solution in terms of ellipsoidal harmonics. Kim and Karilla [47] also discussed the Stokes flow past oblate and prolate spheroidal particles using the Green's function technique. Chwang and Wu [13] also used the method of singularities to discuss the method of solution for arbitrary body shapes, in particular for the special case of prolate spheroids. More recently, Vafaes and Dassios [112] discussed the problem of low Reynolds number flow of a swarm of ellipsoidal particles using an ellipsoidal-in-cell model using ellipsoidal harmonics. The approach of modelling the particle as a collection of small spheres was used by Blawzdziewicz [7]. But most of these methods either involve the complicated ellipsoidal coordinates or improper integrals. Recently Radha et al. [88] solved the problem of an arbitrary axisymmetric Stokes flow past a body of arbitrary shape with no-slip boundary conditions using the complete general solution due to Palaniappan et

al. [79]. They gave an approximate analytical solution using the method of least squares. In this chapter, we have adopted their technique to suggest an analytic but approximate solution for the problem of Stokes flow of a viscous, incompressible fluid past a body of arbitrary shape satisfying the slip-stick boundary conditions. The method has been demonstrated for the example of a singularity driven flow due to a Stokeslet located outside an ellipsoid with different slip parameters. The effect of the slip parameter on physical quantities like the drag and the torque have been discussed. We also discuss the convergence of the method for different values of the slip parameter.

5.2 Mathematical formulation and method of solution

Previously, Padmavathi et al. [75] discussed the motion of a viscous, incompressible fluid past a sphere using slip-stick boundary conditions in a non-axisymmetric Stokes flow by employing the complete general solution of Stokes equations proposed by Palaniappan et al. [79]. In this chapter, we consider the non-dimensional steady Stokes equations as given in equations (1.3.3)-(1.3.4) governing the flow of a viscous, incompressible fluid past an arbitrarily shaped body Ω using slip-stick boundary conditions. We suggest a method to obtain a solution which is analytic but approximate and demonstrate the method by an example. The motivation for this method is from the work of Radha et al. [88] who proposed a method to find an approximate analytical soution of Stokes equations past a rigid body

Ω of arbitrary shape, whose boundary is denoted by $\partial\Omega$ satisfying the no-slip conditions on the boundary. They demonstrated their method with the example of a uniform flow past a rigid body made up of two intersecting spheres. The method proposed by Radha et al. [88] can be extended to non-axisymmetric flows as follows. Let $(\vec{\mathbf{q}}_0, p_0)$ denote the unperturbed flow in the absence of a rigid body and be expressed in terms of the solution due to Palaniappan et al. [79] as follows

$$\vec{\mathbf{q}}_0 = \nabla \times \nabla \times (\vec{\mathbf{r}} A_0) + \nabla \times (\vec{\mathbf{r}} B_0), \tag{5.2.1}$$

$$p_0 = P_0 + \frac{\partial}{\partial r}(r\nabla^2 A_0), \tag{5.2.2}$$

where P_0 is a constant and A_0, B_0 are the corresponding scalar functions satisfying $\nabla^4 A_0 = 0$, $\nabla^2 B_0 = 0$.

In the presence of a rigid body Ω, let the disturbance be denoted by $(\vec{\mathbf{q}}_1, p_1)$ and the perturbed flow be given by $(\vec{\mathbf{q}}, p)$ where

$$\vec{\mathbf{q}} = \vec{\mathbf{q}}_0 + \vec{\mathbf{q}}_1, \tag{5.2.3}$$

$$p = p_0 + p_1, \tag{5.2.4}$$

such that $(\vec{\mathbf{q}}_1, p_1) \to (0, 0)$ as $r \to \infty$. Let the scalar functions corresponding to $(\vec{\mathbf{q}}, p)$ and $(\vec{\mathbf{q}}_1, p_1)$ be denoted by (A, B) and (A_1, B_1) respectively in the solution due to Palaniappan et al. [79], where A_1 and A are biharmonic functions and B_1 and B are harmonic functions as in (5.2.1)-(5.2.2). Let us assume that we can expand each of A_0, B_0, A_1 and B_1 as a

series in terms of spherical harmonics as follows.

$$\begin{aligned}
A_0 &= \left[\sum_{n=1}^{\infty}\sum_{m=0}^{n}\{(\alpha_{nm}r^n+\gamma_{nm}r^{n+2})\cos m\phi+(\beta_{nm}r^n+\delta_{nm}r^{n+2})\sin m\phi\}P_n^m(\zeta)\right],\\
B_0 &= \left[\sum_{n=1}^{\infty}\sum_{m=0}^{n}\{(\chi_{nm}\cos m\phi+\eta_{nm}\sin m\phi)\,r^n\}\,P_n^m(\zeta)\right],\\
A_1 &= \left[\sum_{n=1}^{\infty}\sum_{m=0}^{n}\left\{\left(\frac{A_{nm}}{r^{n+1}}+\frac{C_{nm}}{r^{n-1}}\right)\cos m\phi+\left(\frac{B_{nm}}{r^{n+1}}+\frac{D_{nm}}{r^{n-1}}\right)\sin m\phi\right\}P_n^m(\zeta)\right],\\
B_1 &= \left[\sum_{n=1}^{\infty}\sum_{m=0}^{n}\left\{(E_{nm}\cos m\phi+F_{nm}\sin m\phi)\,\frac{1}{r^{n+1}}\right\}P_n^m(\zeta)\right]. \qquad (5.2.5)
\end{aligned}$$

Here α_{nm}, β_{nm}, γ_{nm}, δ_{nm}, χ_{nm}, η_{nm} are known constants corresponding to the given flow $(\vec{\mathbf{q}}_0, p_0)$ and A_{nm}, B_{nm}, C_{nm}, D_{nm}, E_{nm}, F_{nm} are to be determined from the boundary conditions. Thus we have

$$\begin{aligned}
A &= A_0 + A_1,\\
B &= B_0 + B_1.
\end{aligned}$$

In spherical polar coordinates, the no-slip condition $\vec{\mathbf{q}} = 0$ on the boundary is the same as satisfying $q_r = q_\theta = q_\phi = 0$ on the boundary $\partial\Omega$ of the rigid body Ω. Instead of applying the no-slip condition $\vec{\mathbf{q}} = 0$ on the boundary $\partial\Omega$, Radha et al. [88] adopted the condition that

$$I = \int_{\partial\Omega} |\vec{\mathbf{q}}|^2 dS = 0. \qquad (5.2.6)$$

This condition (5.2.6) can be rewritten as

$$I = \int_{\partial\Omega} (q_r^2 + q_\theta^2 + q_\phi^2) dS = 0.$$

As $\vec{\mathbf{q}}$ is a continuous function of (r, θ, ϕ) and $(q_r^2 + q_\theta^2 + q_\phi^2)$ being a non negative quantity, one can conclude that $I = \int_{\partial\Omega}(q_r^2+q_\theta^2+q_\phi^2)dS = 0$ if and only if $(q_r^2+q_\theta^2+q_\phi^2) \equiv 0$ and hence $q_r = q_\theta = q_\phi = 0$, i.e., $\vec{\mathbf{q}} = 0$ on $\partial\Omega$. From (5.2.5), we observe that A_1 and B_1 are given by infinite series. So in order to compute the solution approximately, we truncate the series of A_1 and B_1 upto N terms and denote the resulting terms as A_1^N and B_1^N respectively which are given as follows.

$$\begin{aligned} A_1^N &= \left[\sum_{n=1}^{N}\sum_{m=0}^{n}\left\{\left(\frac{A_{nm}}{r^{n+1}}+\frac{C_{nm}}{r^{n-1}}\right)\cos m\phi + \left(\frac{B_{nm}}{r^{n+1}}+\frac{D_{nm}}{r^{n-1}}\right)\sin m\phi\right\}P_n^m(\zeta)\right], \\ B_1^N &= \left[\sum_{n=1}^{N}\sum_{m=0}^{n}\left\{(E_{nm}\cos m\phi + F_{nm}\sin m\phi)\,\frac{1}{r^{n+1}}\right\}P_n^m(\zeta)\right]. \end{aligned} \tag{5.2.7}$$

Suppose we denote by (A_N, B_N), the approximation thus obtained of the scalar functions (A, B). Then the approximate solution is given by $\vec{\mathbf{q}}_N$ where

$$\vec{\mathbf{q}}_N = \nabla \times \nabla \times (\vec{\mathbf{r}}A_N) + \nabla \times (\vec{\mathbf{r}}B_N). \tag{5.2.8}$$

where

$$A_N = A_0 + A_1^N, \tag{5.2.9}$$

$$B_N = B_0 + B_1^N. \tag{5.2.10}$$

Hence, instead of (5.2.6), we can adopt an alternate condition that

$$I_N = \int_{\partial\Omega} |\vec{\mathbf{q}}_N|^2 dS = 0, \tag{5.2.11}$$

and try to minimize the integral in (5.2.11) in order to obtain an approximate analytic solution. This results in a system of linear non-homogeneous equations which can be solved

for the unknown constants. Using the afore mentioned technique, Radha et al. [88] solved the problem of an axisymmetric flow, namely, a uniform flow past a rigid body made up of two intersecting rigid spheres.

We now try to adopt this technique for slip-stick boundary conditions which can be used for bodies of arbitrary shape. The slip-stick boundary conditions for a general boundary $\partial\Omega$ are given as follows.

$$\vec{\mathbf{q}}.\hat{\mathbf{n}}|_{\partial\Omega} = 0, \tag{5.2.12}$$

$$\vec{\mathbf{q}}.\hat{\mathbf{t}}_1|_{\partial\Omega} = \overline{\lambda}\vec{\mathbf{T}}^{\hat{\mathbf{n}}}.\hat{\mathbf{t}}_1|_{\partial\Omega}, \tag{5.2.13}$$

$$\vec{\mathbf{q}}.\hat{\mathbf{t}}_2|_{\partial\Omega} = \overline{\lambda}\vec{\mathbf{T}}^{\hat{\mathbf{n}}}.\hat{\mathbf{t}}_2|_{\partial\Omega}, \tag{5.2.14}$$

where $[\hat{\mathbf{n}}, \hat{\mathbf{t}}_1, \hat{\mathbf{t}}_2]$ are the local orthonormal basis vectors on the surface of the particle $\partial\Omega$. We can rewrite these conditions on the boundary $\partial\Omega$ as

$$\begin{aligned} q_n|_{\partial\Omega} &= 0, \\ q_{t_1}|_{\partial\Omega} &= \overline{\lambda}T_{t_1}|_{\partial\Omega}, \\ q_{t_2}|_{\partial\Omega} &= \overline{\lambda}T_{t_2}|_{\partial\Omega}, \end{aligned}$$

using the notation in Section 1.2 in Chapter 1, where $\vec{\mathbf{q}} = q_n\hat{\mathbf{n}} + q_{t_1}\hat{\mathbf{t}}_1 + q_{t_2}\hat{\mathbf{t}}_2$ and T_{t_1}, T_{t_2} are the tangential stresses. The conditions (5.2.12)-(5.2.14) reduce to no-slip conditions when $\overline{\lambda} = 0$ and to shear-free conditions when $\overline{\lambda} \to \infty$. Since $\overline{\lambda}$ takes the values from 0 to ∞ for slip-stick boundary conditions, we introduce a parameter $\beta = \frac{\overline{\lambda}}{1+\overline{\lambda}}$, so that $\beta = 0$ when $\overline{\lambda} = 0$ and $\beta \to 1$ when $\overline{\lambda} \to \infty$. In other words, the domain of slip parameter $[0, \infty)$ has

been scaled down to $[0,1)$ by using the transformation $\beta = \frac{\overline{\lambda}}{1+\overline{\lambda}}$. We use the following form of slip-stick boundary conditions in terms of β as

$$q_n|_{\partial\Omega} = 0, \tag{5.2.15}$$

$$(1-\beta)q_{t_1}|_{\partial\Omega} = \beta T_{t_1}|_{\partial\Omega}, \tag{5.2.16}$$

$$(1-\beta)q_{t_2}|_{\partial\Omega} = \beta T_{t_2}|_{\partial\Omega}. \tag{5.2.17}$$

We express the equation of the surface as $r = f(\theta,\phi)$ in spherical polar co-ordinates (r,θ,ϕ) (refer Section 1.2 of Chapter 1).

Motivated by the work of Radha et al. [88], we adopt their technique to reformulate the slip-stick boundary conditions (5.2.15)-(5.2.17) on the boundary $\partial\Omega$ as requiring the fulfillment of the condition that

$$I = \int_{\partial\Omega} [q_n^2 + ((1-\beta)q_{t1} - \beta T_{t1})^2 + ((1-\beta)q_{t2} - \beta T_{t2})^2] dS = 0, \tag{5.2.18}$$

instead of the boundary conditions (5.2.15)-(5.2.17).

Since the solution, in terms of A and B, is given as an infinite series when expressed in spherical polar coordinates (r,θ,ϕ), we impose an alternate condition that

$$I_N = \int_{\partial\Omega} \{(q_n^N)^2 + ((1-\beta)q_{t1}^N - \beta T_{t1}^N)^2 + ((1-\beta)q_{t2}^N - \beta T_{t2}^N)^2\} dS = 0, \tag{5.2.19}$$

where the superscript N indicates that the flow quantities have been truncated upto $n = N$ in the series representation of the solution (refer Appendix 5.1). The number of arbitrary constants occuring in (5.2.7) which are to be determined using the boundary conditions (5.2.15)-(5.2.17) are $3N(N+3)$ namely A_{nm}, B_{nm}, C_{nm}, D_{nm}, E_{nm}, F_{nm}, where $n =$

$1, 2, ..., N,\ m = 0, 1, ..., n$. Clearly, I_N being non-negative, the existence of an infimum of I_N is guaranteed. Hence, we find the minimum value of I_N by applying the following conditions.

$$\frac{\partial I_N}{\partial A_{ij}} = 0, \qquad \frac{\partial I_N}{\partial B_{ij}} = 0, \qquad \frac{\partial I_N}{\partial C_{ij}} = 0, \tag{5.2.20}$$

$$\frac{\partial I_N}{\partial D_{ij}} = 0, \qquad \frac{\partial I_N}{\partial E_{ij}} = 0, \qquad \frac{\partial I_N}{\partial F_{ij}} = 0, \tag{5.2.21}$$

$i = 1$ to N and $j = 0$ to i. These equations form a linear system of non-homogeneous equations involving A_{ij}, B_{ij}, C_{ij}, D_{ij}, E_{ij} and F_{ij}. We now present an example to illustrate this method.

5.2.1 Consider the Stokes flow of a viscous, incompressible fluid past an ellipsoid given by $x^2 + \frac{y^2}{0.75^2} + \frac{z^2}{0.5^2} = 1$, induced due to a Stokeslet of unit strength located at $(0, 0, 0.75)$ and whose axis lies along the positive x-axis. We assume the slip parameter value β to be equal to $\frac{1}{3}$ in this example. By using the method suggested for slip-stick boundary conditions, we have calculated (A_1^N, B_1^N) for $N = 1, 2, ..., 9$ (refer to Appendices 5.1 and 5.2). For $N = 9$, we obtain

$$\begin{aligned}
A_1^N &= [\{(2.11805r^{-2} - 3.02799)P_1(\zeta) + (93.2183r^{-3} - 45.0989r^{-1})P_2(\zeta) \\
&- (0.44899r^{-4} - 1.28621r^{-2})P_3(\zeta) - (17.0513r^{-5} - 9.19796r^{-3})P_4(\zeta) \\
&+ (0.0747035r^{-6} - 0.185572r^{-4})P_5(\zeta) + (0.404749r^{-7} - 6.13047r^{-5})P_6(\zeta) \\
&- (0.00525081r^{-8} - 0.00501518r^{-6})P_7(\zeta) + (0.227785r^{-9} - 1.4524r^{-7})P_8(\zeta)
\end{aligned}$$

$$
\begin{aligned}
&- (0.000396663r^{-10} - 0.00288658r^{-8})P_9(\zeta)\} \times 10^{-12} \\
&+ \{(1.51287r^{-2} - 47.2512)P_1^1(\zeta) - (0.681361r^{-3} - 1.99339r^{-1})P_2^1(\zeta) \\
&- (0.224696r^{-4} - 1.16619r^{-2})P_3^1(\zeta) - (0.00745753r^{-5} - 0.160097r^{-3})P_4^1(\zeta) \\
&+ (0.0165318r^{-6} - 0.0412963r^{-4})P_5^1(\zeta) - (0.00187356r^{-7} - 0.0109095r^{-5})P_6^1(\zeta) \\
&- (0.00146645r^{-8} - 0.00419457r^{-6})P_7^1(\zeta) - (0.000197909r^{-9} - 0.00107501r^{-7})P_8^1(\zeta) \\
&- (0.0000102052r^{-10} - 0.000117647r^{-8})P_9^1(\zeta)\} \cos\phi \times 10^{-2} \\
&+ \{(1.1913r^{-3} - 0.292837r^{-1})P_2^2(\zeta) - (0.000329272r^{-4} - 0.000749726r^{-2})P_3^2(\zeta) \\
&- (0.130568r^{-5} - 0.266977r^{-3})P_4^2(\zeta) + (0.0000229244r^{-6} - 0.0000468854r^{-4})P_5^2(\zeta) \\
&+ (0.00494434r^{-7} - 0.00545668r^{-5})P_6^2(\zeta) \\
&+ (0.00025619r^{-9} - 0.00173157r^{-7})P_8^2(\zeta)\} \cos 2\phi \times 10^{-10} \\
&- \{(23.8926r^{-4} - 163.919r^{-2})P_3^3(\zeta) - (6.6041r^{-5} - 8.53223r^{-3})P_4^3(\zeta) \\
&- (2.89022r^{-6} - 10.1164r^{-4})P_5^3(\zeta) - (0.272567r^{-7} - 1.70785r^{-5})P_6^3(\zeta) \\
&+ (0.121787r^{-8} - 0.317812r^{-6})P_7^3(\zeta) + (0.0183889r^{-9} - 0.0796786r^{-7})P_8^3(\zeta) \\
&- (0.000726217r^{-10} - 0.00274236r^{-8})P_9^3(\zeta)\} \cos 3\phi \times 10^{-6} \\
&- \{(0.0235396r^{-5} - 0.0400253r^{-3})P_4^4(\zeta) - (0.00121001r^{-7} - 0.00317844r^{-5})P_6^4(\zeta) \\
&- (0.0000255744r^{-9} - 0.000145017r^{-7})P_8^4(\zeta)\} \cos 4\phi \times 10^{-10} \\
&- \{(2.76227r^{-6} + 0.528823r^{-4})P_5^5(\zeta) + (0.0355246r^{-7} + 0.576805r^{-5})P_6^5(\zeta) \\
&+ (0.149749r^{-8} - 0.513836r^{-6})P_7^5(\zeta) + (0.00614185r^{-9} - 0.0330422r^{-7})P_8^5(\zeta)
\end{aligned}
$$

$$
\begin{aligned}
&- (0.00154886r^{-10} - 0.00291031r^{-8})P_9^5(\zeta)\} \cos 5\phi \times 10^{-8} \\
&+ \{(1.02088r^{-7} - 0.604942r^{-5})P_6^6(\zeta)\} \cos 6\phi \times 10^{-15} \\
&- \{(1.18818r^{-8} - 8.08031r^{-6})P_7^7(\zeta) + (0.0453238r^{-9} - 0.171543r^{-7})P_8^7(\zeta) \\
&- (0.0205875r^{-10} - 0.0707192r^{-8})P_9^7(\zeta)\} \cos 7\phi \times 10^{-11} \\
&+ \{(7.07611r^{-10} - 23.5485r^{-8})P_9^9(\zeta)\} \cos 9\phi \times 10^{-15} \\
&+ \{(1.37581r^{-2} - 0.305558)P_1^1(\zeta) + (7.37886r^{-3} - 0.101122r^{-1})P_2^1(\zeta) \\
&- (0.0470325r^{-4} - 0.0419817r^{-2})P_3^1(\zeta) - (0.134944r^{-5} - 0.810666r^{-3})P_4^1(\zeta) \\
&+ (0.0048352r^{-6} - 0.00716801r^{-4})P_5^1(\zeta) - (0.0419146r^{-7} - 0.247987r^{-5})P_6^1(\zeta) \\
&- (0.000253244r^{-8})P_7^1(\zeta) - (0.00138792r^{-9} - 0.00866634r^{-7})P_8^1(\zeta) \\
&+ (0.000123917r^{-8})P_9^1(\zeta)\} \sin\phi \times 10^{-12} \\
&- \{(0.660201r^{-4} - 1.6685r^{-2})P_3^3(\zeta) + (5.09897r^{-5} - 13.0666r^{-3})P_4^3(\zeta) \\
&- (0.0164012r^{-6} - 0.0405661r^{-4})P_5^3(\zeta) - (0.208962r^{-7} - 0.531209r^{-5})P_6^3(\zeta) \\
&+ (0.00146903r^{-9} - 0.00519343r^{-7})P_8^3(\zeta)\} \sin 3\phi \times 10^{-13} \\
&+ \{(1.8438r^{-6} - 3.74806r^{-4})P_5^5(\zeta) \\
&+ (4.03409r^{-7} - 7.21168r^{-5})P_6^5(\zeta)\} \sin 5\phi \times 10^{-16}] \\
B_1^N &= [\{16.5989r^{-2}P_1^1(\zeta) - 0.672204r^{-3}P_2^1(\zeta) - 18.1963r^{-4}P_3^1(\zeta) \\
&+ 0.0883978r^{-5}P_4^1(\zeta) + 3.89238r^{-6}P_5^1(\zeta) - 0.0103824r^{-7}P_6^1(\zeta) \\
&- 0.545346r^{-8}P_7^1(\zeta) + 0.000623896r^{-9}P_8^1(\zeta) + 0.0383653r^{-10}P_9^1(\zeta)\} \cos\phi
\end{aligned}
$$

$$
\begin{aligned}
&+ \{1.73625r^{-3}P_2^2(\zeta)\}\cos 2\phi \\
&+ \{2.60764r^{-4}P_3^3(\zeta) + 0.0146756r^{-5}P_4^3(\zeta) + 0.338524r^{-6}P_5^3(\zeta) \\
&- 0.000941878r^{-7}P_6^3(\zeta) - 0.0428656r^{-8}P_7^3(\zeta) + 0.00248631r^{-10}P_9^3(\zeta)\}\cos 3\phi \\
&- \{0.00487845r^{-6}P_5^5(\zeta) - 0.000312676r^{-7}P_7^5(\zeta)\}\cos 5\phi] \times 10^{-12} \\
&- \{132.538r^{-2}P_1^1(\zeta) - 5.74295r^{-3}P_2^1(\zeta) - 2.58214r^{-4}P_3^1(\zeta) \\
&- 0.236345r^{-5}P_4^1(\zeta) - 0.0388528r^{-6}P_5^1(\zeta) - 0.0347912r^{-7}P_6^1(\zeta) \\
&- 0.00854601r^{-8}P_7^1(\zeta) + 0.000591397r^{-9}P_8^1(\zeta) \\
&+ 0.0000351253r^{-10}P_9^1(\zeta)\}\sin\phi \times 10^{-3} \\
&- \{0.0400477r^{-3}P_2^2(\zeta) + 2.61287r^{-4}P_3^2(\zeta) - 0.00103875r^{-5}P_4^2(\zeta) \\
&+ 0.661265r^{-6}P_5^2(\zeta) + 0.0000257138r^{-7}P_6^2(\zeta) - 0.0557074r^{-8}P_7^2(\zeta) \\
&+ 0.00139546r^{-10}P_9^2(\zeta)\}\sin 2\phi \times 10^{-11} \\
&+ \{1975.53r^{-4}P_3^3(\zeta) + 143.257r^{-5}P_4^2(\zeta) + 2.61809r^{-6}P_5^2(\zeta) \\
&- 1.64987r^{-7}P_6^2(\zeta) - 0.0233622r^{-8}P_7^2(\zeta) - 0.229851r^{-9}P_8^2(\zeta) \\
&- 0.0539956r^{-10}P_9^2(\zeta)\}\sin 3\phi \times 10^{-7} \\
&+ \{0.0124402r^{-5}P_4^4(\zeta) + 6.31057r^{-6}P_5^4(\zeta) + 0.583585r^{-8}P_7^4(\zeta)\}\sin 4\phi \times 10^{-13} \\
&- \{8.34703r^{-6}P_5^5(\zeta) + 3.0247r^{-5}P_6^5(\zeta) + 0.037821r^{-7}P_7^5(\zeta) \\
&- 0.0125032r^{-9}P_8^5(\zeta) - 0.000660397r^{-10}P_9^5(\zeta)\}\sin 5\phi \times 10^{-8} \\
&- \{0.0125032r^{-8}P_7^6(\zeta)\}\sin 6\phi \times 10^{-16} \\
&- \{2.89462r^{-8}P_7^7(\zeta) - 0.634302r^{-9}P_8^7(\zeta) - 0.0114386r^{-10}P_9^7(\zeta)\}\sin 7\phi \times 10^{-11} \\
&+ \{4.39749r^{-10}P_9^9(\zeta)\}\sin 9\phi \times 10^{-15}.
\end{aligned}
$$

Using the approximate analytical solution obtained we have computed the drag experienced by the ellipsoid and the minimum value of I_N for different values of N. We have tabulated the corresponding values for $\beta = \frac{1}{3}$ in Table 5.2.1. It is observed from Table 5.2.1 that I_N decreases from 3.81746 when $N = 1$ to 0.0946 when $N = 9$. From this observation we can conclude that I_N can be made further smaller and closer to zero by increasing N. We also computed the approximate but analytical solutions for different values of the slip parameter β and noticed that I_N decreases to zero as N increases (refer Figure 5.2.1). Further, we have computed the drag experienced by the body and the torque, for different values of slip parameter β in order to understand the effect of β on the drag and the torque. Figures 5.2.2 and 5.2.3 depict that the magnitude of the drag experienced by the body and the torque decrease as the value of the slip parameter β increases.

N	I_N	$Drag$	$Torque$	N	I_N	$Drag$	$Torque$
1	3.81746	$9.8117\hat{\mathbf{i}}$	$1.19351\hat{\mathbf{j}}$	6	0.143811	$11.7351\hat{\mathbf{i}}$	$3.26464\hat{\mathbf{j}}$
2	3.29739	$10.3724\hat{\mathbf{i}}$	$1.26688\hat{\mathbf{j}}$	7	0.129522	$11.7527\hat{\mathbf{i}}$	$3.2632\hat{\mathbf{j}}$
3	1.99579	$11.5728\hat{\mathbf{i}}$	$1.28068\hat{\mathbf{j}}$	8	0.110037	$11.7533\hat{\mathbf{i}}$	$3.32911\hat{\mathbf{j}}$
4	0.606072	$11.4789\hat{\mathbf{i}}$	$3.25043\hat{\mathbf{j}}$	9	0.0945999	$11.8755\hat{\mathbf{i}}$	$3.33104\hat{\mathbf{j}}$
5	0.295513	$11.6886\hat{\mathbf{i}}$	$3.27444\hat{\mathbf{j}}$				

Table 5.2.1: Convergence of the solution and the corresponding drag for $\beta=\frac{1}{3}$.

Figure 5.2.1 shows that the convergence of the integrals I_N to 0 as $N \to \infty$ is slower with increasing values of the slip parameter β. We also observe from Figures 5.2.2 and 5.2.3 that the magnitude of the drag and that of the torque decrease with increasing β.

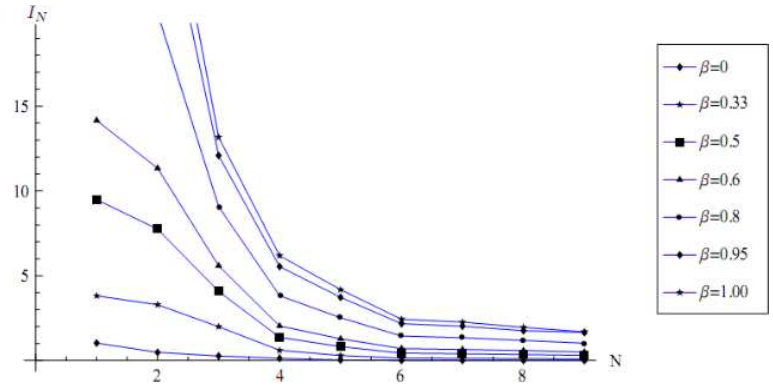

Figure 5.2.1: *Convergence of I_N for different values of slip parameter β.*

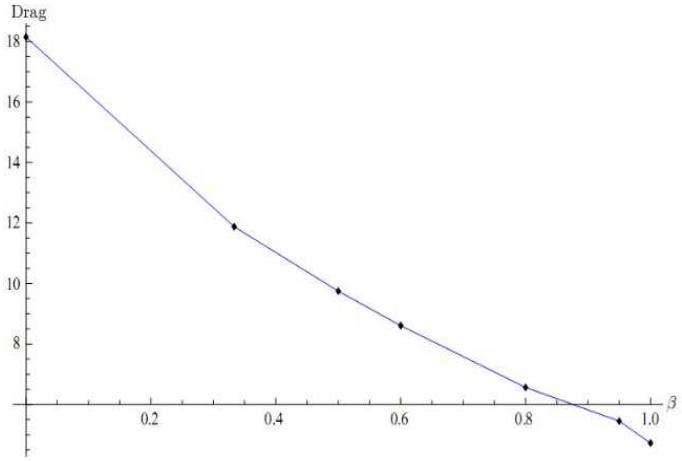

Figure 5.2.2: *Variation in the magnitude of the drag for different values of slip parameter β.*

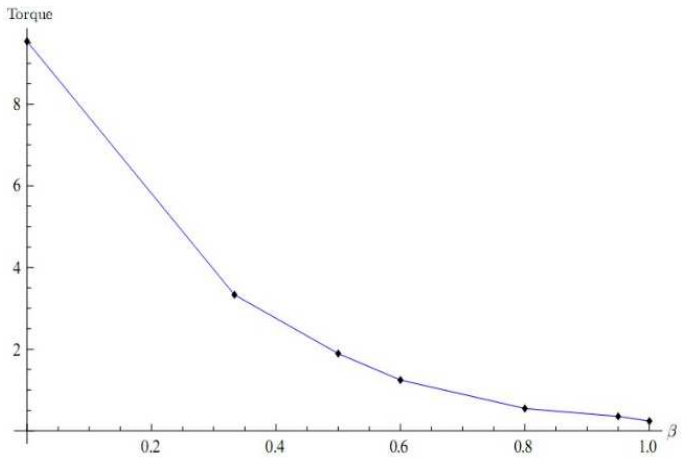

Figure 5.2.3: *Variation in the magnitude of the torque for different values of slip parameter* β.

5.3 Conclusions

In this chapter, we propose a method to obtain an analytic but approximate solution by modifying the method proposed by Radha et al. [88] and adopting it for slip-stick boundary conditions to study the flow due to an arbitrary Stokes flow past an arbitrary shaped body whose surface is given by $r = f(\theta, \phi)$. In particular, we considered flow generated due to the presence of a Stokeslet outside an ellipsoid in a viscous, incompressible Stokes flow. We observed the convergence of the sequence of approximate solutions with increasing 'N' by computing I_N at each stage and showed that $I_N \to 0$ as N increases. An advantage of this method over other methods like finite difference or finite element methods is that in the latter methods the velocity and pressure are known only at a finite number of points on

the surface unlike in this method, where the solution is known in the entire domain, even though approximately. Hence this method enables us to find the physical quantities like drag and torque more accurately as their computation involves calculating the derivatives of velocities. The method also matches with the exact solutions if the surface is a perfect sphere. We observed that the integrals I_N converge to 0 as $N \to \infty$ faster if the slip parameter β is small. We also observed that the magnitude of the drag and that of the torque decreases as $\beta \to 1$. This technique can be used for any problem pertaining to Stokes flow past any body of arbitrary shape satisfying slip-stick boundary conditions.

Appendix 5.1

Consider the approximate solution $\vec{\mathbf{q}}_N$ given by (5.2.8)-(5.2.10). Then

$$\begin{aligned} q_n^N &= \vec{\mathbf{q}}_N.\hat{\mathbf{n}}, \\ q_{t_1}^N &= \vec{\mathbf{q}}_N.\hat{\mathbf{t}}_1, \\ q_{t_2}^N &= \vec{\mathbf{q}}_N.\hat{\mathbf{t}}_2, \end{aligned}$$

are the corresponding components of normal and tangential velocities. The corresponding pressure is given by

$$p^N = \frac{\partial}{\partial r}(r\nabla^2 A_N).$$

where A_N is given as in equation (5.2.9). Similarly, the tangential components of the stress are given by

$$\begin{aligned} T_{t_1}^N &= \vec{\mathbf{T}}_N^{\hat{\mathbf{n}}}.\hat{\mathbf{t}}_1, \\ T_{t_2}^N &= \vec{\mathbf{T}}_N^{\hat{\mathbf{n}}}.\hat{\mathbf{t}}_2, \end{aligned}$$

where $\vec{\mathbf{T}}_N^{\hat{\mathbf{n}}} = \mathbf{T}_N.\hat{\mathbf{n}}$, $\mathbf{T}_N$ being the stress tensor of rank 2 whose components are computed with the components of $\vec{\mathbf{q}}_N$ and p^N as in (1.2.4).

Appendix 5.2

Suppose the rigid body is an ellipsoid defined by $\frac{x^2}{a^2} + \frac{y^2}{b^2} + \frac{z^2}{c^2} = 1$, then the equation of the rigid body in spherical polar coordinates is $r = f(\theta, \phi)$, where we have

$$\begin{aligned} f(\theta,\phi) &= \frac{abc}{(b^2c^2\sin^2\theta\cos^2\phi + a^2c^2\sin^2\theta\sin^2\phi + a^2b^2\cos^2\theta)^{\frac{1}{2}}} \\ \frac{\partial f}{\partial\theta} &= -\frac{abcZ_1}{(b^2c^2\sin^2\theta\cos^2\phi + a^2c^2\sin^2\theta\sin^2\phi + a^2b^2\cos^2\theta)^{\frac{3}{2}}}, \\ \frac{\partial f}{\partial\phi} &= -\frac{abcZ_2}{(b^2c^2\sin^2\theta\cos^2\phi + a^2c^2\sin^2\theta\sin^2\phi + a^2b^2\cos^2\theta)^{\frac{3}{2}}}, \\ Z_1 &= (b^2c^2\sin\theta\cos\theta\cos^2\phi + a^2c^2\sin\theta\cos\theta\sin^2\phi - a^2b^2\cos\theta\sin\theta), \\ Z_2 &= (a^2c^2\sin^2\theta\sin\phi\cos\phi - b^2c^2\sin^2\theta\sin\phi\cos\phi). \end{aligned}$$

The element of surface area is

$$dS = \left[f^2\sin^2\theta\left\{f^2 + \left(\frac{\partial f}{\partial\theta}\right)^2\right\} + f^2\left(\frac{\partial f}{\partial\phi}\right)^2\right]^{\frac{1}{2}}.$$

Chapter 6

Summary

In this chapter, we summarize the main results of the thesis.

Chapter 2: A steady, incompressible Stokes flow past a sphere coated with a viscous fluid of viscosity μ^i immersed in an immiscible viscous fluid of a different viscosity μ^e is considered. It is assumed that the spherical shape of the coating is retained under the condition that the surface tension forces are large enough to balance the viscous forces. The boundary conditions employed here are the vanishing of the normal velocities, the continuity of the tangential velocities and stresses respectively at the interface of the two fluids and the no-slip condition on the rigid surface of the sphere. The representation of velocity $\vec{\mathbf{q}}$ and pressure p of Stokes equations given in [79] has been used as in equations (2.2.3)-(2.2.4) and a method of obtaining the modified flow field in the presence of the coated sphere has been discussed. The expressions for the drag $\vec{\mathbf{D}}_c$ and torque $\vec{\mathbf{T}}_c$ experienced by the coated

sphere were derived similar to Faxén's laws [21]. An immediate result is that, if the flow is harmonic or purely biharmonic then the magnitude of the drag on the coated sphere is lesser compared to the magnitude of the drag on the rigid sphere of radius equal to that of the coated sphere. Suppose ϵ is the thickness of the coating on a sphere of unit radius, then the drag on the coated sphere is found to be

$$\begin{aligned}\vec{\mathbf{D}}_c = 6\pi &\left[1+\epsilon\left(1-\frac{\overline{\mu}}{4}\right)+O(\epsilon^2)\right][\vec{\mathbf{q}}_0]_0 \\ &+\pi\left[1+3\epsilon\left(1-\frac{\overline{\mu}}{4}\right)+O(\epsilon^2)\right][\nabla^2\vec{\mathbf{q}}_0]_0,\end{aligned} \tag{2.3.14}$$

which shows that when the ratio of the viscosities $\overline{\mu} = \frac{\mu^e}{\mu^i}$ is greater than 4 and if the unperturbed flow is either harmonic or purely biharmonic, then the magnitude of the drag on the coated sphere is less than the maginitude of the drag on an uncoated rigid sphere of unit radius. It is demonstrated by an example that this result does not hold true in the case of a general flow. The optimum thickness of the coating required for the drag to be minimum has been computed. In a similar manner, it can be concluded that the magnitude of the torque on the coated sphere increases when $\overline{\mu} < 1$ and reduces when $\overline{\mu} > 1$ compared to the torque experienced by an uncoated sphere of unit radius. Nevertheless, the magnitude of torque is always found to decrease compared to that on a rigid sphere of radius equal to that of the coated sphere. The expression for the drag is also computed for the axisymmetric case. The chapter ends with two examples of flows due to a Stokeslet and a potential doublet respectively. The drag on the coated sphere has been computed using the expression derived earlier in this chapter. The results of Chapter 2 can be found in Choudhuri et al. [12].

Chapter 3: An oscillatory flow of a fluid of viscosity μ^e past a liquid sphere of viscosity μ^i is considered. We employ Venkatlaxmi's [113, 114] solution of velocity and pressure as given in equations (3.2.5)-(3.2.6) for the unsteady Stokes equations (3.2.3)-(3.2.4). The liquid sphere is assumed to be of spherical shape as the zeroth approximation. We solve for the flow field using the boundary conditions of vanishing of normal velocities, continuity of tangential velocities and stresses. The expressions for the drag and torque have been derived akin to Faxén's laws [21]. As limiting cases, the following results have been obtained:

1. As $\overline{\mu} \to 0$, where $\overline{\mu} = \frac{\mu^e}{\mu^i}$, the formulae for drag and torque on the liquid sphere reduce to those on a rigid sphere of the same radius in an oscillating flow, agreeing with the formulae due to Kim and Karrila [47].

2. As $\overline{\mu} \to \infty$, the drag and torque on the liquid sphere reduce to those on a shear-free sphere of the same radius in an oscillating flow.

3. In addition to the preceeding two limiting cases, if both λ_1, $\lambda_2 \to 0$ where λ_1, λ_2 correspond to the frequencies of the velocities outside and inside the liquid sphere respectively, then the drag and torque reduce to Faxén's laws [21] in rigid and shear-free cases in steady flow.

The sphere is then assumed to undergo a slight deformation from its spherical shape. On the lines of Hetsroni and Haber [38], the equation of the surface of the deformed sphere has been computed upto the first order approximation using the boundary condition that the jump in the normal stresses across the surface is balanced by the surface tension forces. The

method of determining the equation of the surface of the deformed sphere is demonstrated by examples for singularity driven flows both outside and inside the fluid spheres. Another important result is that we verified the fact that the spherical shape of the liquid sphere is retained for flow velocities which have terms only upto $n = 1$ in the series representation of the solution, thereby agreeing with the result of Chisnell [11] who considered a uniform flow. We observe that the two parameters which play an important role in deformation of the spherical shape of the fluid sphere are the ratio of viscosities $\overline{\mu}$ and the capillary number.

Chapter 4: A viscous, incompressible fluid flow due to a singularity located inside a spherical container centred at the origin is considered using slip-stick boundary conditions

$$q_r(1, \theta, \phi) = 0, \tag{4.1.6}$$

$$q_\theta(1, \theta, \phi) = -\overline{\lambda} T_{r\theta}(1, \theta, \phi), \tag{4.1.7}$$

$$q_\phi(1, \theta, \phi) = -\overline{\lambda} T_{r\phi}(1, \theta, \phi), \tag{4.1.8}$$

$\overline{\lambda}$ being the slip parameter, q_r, q_θ, q_ϕ being the velocity components and $T_{r\theta}$, $T_{r\phi}$ being the components of stress in spherical polar coordinates (r, θ, ϕ). Such boundary conditions find their use in diverse fields of engineering such as micro device technology. As $\overline{\lambda} \to 0$, the no-slip boundary conditions are retrieved and when $\overline{\lambda} \to \infty$, the shear-free boundary conditions are obtained. We found the modified flow field inside the sphere by giving the solution in a closed form as a sphere theorem in terms of two scalar functions A and B corresponding to the solution proposed by Palaniappan et al. [79] as follows.

Theorem If the flow of a viscous, incompressible fluid in the absence of rigid boundaries be denoted by $A_0(r,\theta,\phi)$ and $B_0(r,\theta,\phi)$, which are biharmonic and harmonic respectively, the singularities of these functions being at a distance lesser than 1 from the origin and if $A_0 \sim o(1)$, $B_0 \sim o\left(\frac{1}{r^2}\right)$ as $r \to \infty$, and if now the flow be considered inside the sphere $r = 1$, then the modified flow in the interior of the sphere satisfying slip-stick boundary conditions (4.1.6)-(4.1.8) ($\lambda \neq 0$) on $r = 1$ is given by

$$A(r,\theta,\phi) = A_0(r,\theta,\phi) - rA_0\left(\frac{1}{r},\theta,\phi\right) + (1-r^2)\left[\frac{1}{8\overline{\lambda}r^{\frac{1}{2\overline{\lambda}}-\frac{1}{2}}} \times \left(\int_{\infty}^{\frac{1}{r}} R^{-\frac{1}{2\overline{\lambda}}-\frac{3}{2}}\left(\nabla^2 A_0 - R^4\nabla^2\left(\frac{A_0}{R^2}\right)\right)dR\right)\right], \tag{4.1.28}$$

$$B(r,\theta,\phi) = B_0(r,\theta,\phi) + \frac{1}{r}B_0(r,\theta,\phi) - \left(\frac{2}{\overline{\lambda}} - 3\right) \times \int_{\infty}^{\frac{1}{r}} R^{-\frac{1}{\overline{\lambda}}-1}B_0 dR. \tag{4.1.29}$$

The expression for drag has been obtained from which we concluded that the drag is independent of the size of the sphere. The axisymmetric flows inside a unit sphere due to a Stokeslet located at the origin and also away from it have been analysed in detail separately. Firstly, we found the stagnation and the separation points in the flow domain of a flow due to a Stokeslet located at the origin. An important observation while finding the stagnation points is that when $\overline{\lambda} = 0$, the radius of stagnation circle which is equal to $\frac{1}{2}(-1+\sqrt{3})$ for the no-slip case matches with the one obtained by Shail [99]. It is also seen that as $\overline{\lambda} \to \infty$, the radius of the stagnation circle approaches 0.5, hence proving that the slip parameter plays a role in the location of the stagnation points. We then computed the points of zero

vorticity. We observed that for $0 \leq \overline{\lambda} < 0.5$ the stagnation points and the points of zero vorticity co-exist in the fluid domain. The figures which demonstrate the flow patterns also show that the range of slip paramater $\overline{\lambda}$ in which the eddy patterns occur in the spherical container is $[0, 0.5)$. Secondly, we concluded both analytically and numerically that there are only two stagnation points in the flow domain of a flow due to an off-centred Stokeslet for non-zero values of slip parameter $\overline{\lambda}$. We also found that for a given location of a Stokeslet the set of separation points remains the same for all values of $\overline{\lambda} > 0.5$. We conjecture that the co-existence of stagnation points and points of zero vorticity in the interior of the flow is a necessary condition for the eddy patterns to occur in the case of a Stokeslet induced flow in a spherical container. We found that the axisymmetric flow generated due to a Stokeslet located away from the origin always produced eddies because the stagnation and separation points co-exist for all values of $\overline{\lambda}$. Another result obtained is that when $\overline{\lambda} = \frac{1}{2}$, the vorticity on the boundary always vanishes.

We discussed another important phenomenon in this chapter called '*Stokeslet reversal*'.

Stokeslet reversal: As the location $(0, 0, c)$ $(0 < c < 1)$ of the given Stokeslet varies, if there is a critical value of c at which the strength of the image Stokeslet vanishes, then this phenomena is called as '*Stokeslet reversal*'. Since we found that there is a reversal of the orientation of the image Stokeslet as c passes through this critical value, this phenomena is termed as Stokeslet reversal. This means that the strength of the image Stokeslet changes sign as c passes through this critical value.

Maul and Kim [63] studied the phenomenon for a flow generated due to a Stokeslet inside

a rigid spherical container. We discuss the phenomenon of Stokeslet reversal in the general case of slip-stick boundary conditions. It was found that this phenomenon does not occur for a non-axisymmetric flow due to a Stokeslet located at $(0, 0, c), c \neq 0$. However for an axisymmetric flow with slip-stick boundary conditions, it is found that the Stokeslet, if located at $c = \frac{1}{\sqrt{3(1+2\overline{\lambda})}}$, makes the strength of the image Stokeslet vanish. As a limiting case, if $\overline{\lambda} \to 0$ the location of the Stokeslet inside the sphere is found to be at $\frac{1}{\sqrt{3}}$ which agrees with the result of Maul and Kim [63]. In particular, for an axisymmetric flow due to a Stokeslet located at the origin, there is no Stokeslet reversal. We also did not find any evidence of Stokeslet reversal in the case of an axisymmetric flow due to a Stokeslet inside a sphere with shear-free boundary conditions and also in the case of a non-axisymmetric flow due to a Stokeslet with slip-stick boundary conditions.

Chapter 5: A viscous, incompressible Stokes flow past a body of arbitrary shape satisfying slip-stick boundary conditions is considered, where we adopt a method proposed by Radha et al. [88] for slip-stick boundary conditions. The velocity of the fluid is expressed as

$$\vec{\mathbf{q}} = q_n \hat{\mathbf{n}} + q_{t1} \hat{\mathbf{t}}_1 + q_{t2} \hat{\mathbf{t}}_2,$$

where $[\hat{\mathbf{n}}, \hat{\mathbf{t}}_1, \hat{\mathbf{t}}_2]$ are the local orthnormal basis, q_n, q_{t1}, q_{t2} are the velocity components of the velocity on the surface of the particle $\partial\Omega$. The slip-stick boundary conditions for a general boundary $\partial\Omega$ are given as follows.

$$\begin{aligned} q_n|_{\partial\Omega} &= 0, \\ q_{t1}|_{\partial\Omega} &= \overline{\lambda} T_{t1}|_{\partial\Omega}, \\ q_{t2}|_{\partial\Omega} &= \overline{\lambda} T_{t2}|_{\partial\Omega}, \end{aligned}$$

where T_{t1} and T_{t2} are the tangential stresses. In the limits $\overline{\lambda} \to 0$ and $\overline{\lambda} \to \infty$, we obtain the rigid and shear-free boundary conditions respectively. Suppose $\beta = \frac{\overline{\lambda}}{1+\overline{\lambda}}$, we restate the boundary conditions as

$$q_n|_{\partial\Omega} = 0, \tag{5.2.15}$$

$$(1-\beta)q_{t1}|_{\partial\Omega} = \beta T_{t1}|_{\partial\Omega}, \tag{5.2.16}$$

$$(1-\beta)q_{t2}|_{\partial\Omega} = \beta T_{t2}|_{\partial\Omega}. \tag{5.2.17}$$

The representation of the solution of Stokes equation due to Palaniappan et al. [79] has been used and A and B are expressed as an infinite series in terms of spherical harmonics. Motivated by the work of Radha et al. [88], we restate the slip-stick boundary conditions as satisfying

$$I = \int_{\partial\Omega} [\{q_n\}^2 + \{(1-\beta)q_{t1} - \beta T_{t1}\}^2 + \{(1-\beta)q_{t2} - \beta T_{t2}\}^2] dS = 0. \tag{5.2.18}$$

But since it is computationally difficult to use the infinite series solution, we truncate the series upto N terms and replace the condition (5.2.18) by

$$I_N = \int_{\partial\Omega} [\{q_n^N\}^2 + \{(1-\beta)q_{t1}^N - \beta T_{t1}^N\}^2 + \{(1-\beta)q_{t2}^N - \beta T_{t2}^N\}^2] dS = 0, \tag{5.2.19}$$

where q_n^N, q_{t1}^N, q_{t2}^N, T_{t1}^N, T_{t2}^N are the velocity and tangential stress components computed by truncating the corresponding series upto N terms. We employ the method of least squares to find the minimum value of I_N. In particular, we demonstrate this method for a non-axisymmetric Stokes flow past an ellipsoid given by $x^2 + \frac{y^2}{0.75^2} + \frac{z^2}{0.5^2} = 1$, where the flow is generated by a Stokeslet whose axis is directed towards $\hat{\mathbf{i}}$ and located outside the

ellipsoid. This method can be applied for bodies of arbitrary shape. Although the solution is approximate, it is better than a solution obtained by numerical methods like finite difference methods as the solution is given in an analytic form which is valid in the entire domain. Hence, this method enables us to find the physical quantities like the drag and the torque more accurately as their computation involves calculating the derivatives of the velocity. We demonstrate in this example, the convergence of the sequence of approximate solutions to the original solution with increasing N by computing I_N at each stage. An interesting result obtained by us is that the magnitude of the drag and torque reduce as the slip parameter β increases.

Bibliography

[1] Almansi, E., "Sail 'integrazione dell' equazione differenziale $\Delta^{2n} = 0$", Ann. Math. Pura Appl. Ser., **III(2)**, 1-51 (1897).

[2] Andersen, J.L., Solomentsev, Y., "Hydrodynamic effects of surface layers on colloidal particles", Chem. Engg. Comm., **148-50**, 291-314 (1996).

[3] Batchelor, G.K., *An introduction to Fluid Dynamics*, Cambridge University Press, 1996.

[4] Barber, R.W., Emerson, D.R., "Numerical simulation of low Reynolds number slip flow past a confined microsphere", **23**rd International Symposium on Rarefied Gas Dynamics, Whistler, Canada, 20-25 (2002).

[5] Basset, A.B., *A treatise on hydrodynamics with numerous examples*, Vol.**2**, Dover, New York, 1961.

[6] Blake, J.R. and Chwang, A.T., "Fundamental singularities of viscous flows", J. Engg. Mathematics, **8(1)**, 23-29 (1974).

[7] Blawzdziewicz, J., Wajnnyb, E., Given, J.A., Hubbard, J.B., "Sharp scalar and tensor bounds on the hydrodynamic friction and mobility of arbitrarily shaped bodies in Stokes flow", Phys. of Fluids, **17**, 0336021-9 (2005).

[8] Bourot, J.M., "On the numerical computation of the optimum profile in Stokes flow", J. Fluid Mech., **65**, 513-515 (1974).

[9] Brenner, H., "Effect of finite boundaries on the Stokes resistance of an arbitrary particle", J. Fluid Mech., **63**, 35-48 (1962).

[10] Burgers, J.M., "Second report on Viscosity and Plasticity", Kon. Ned. Akad. Wet. Verhand, **16**, 113-184 (1938).

[11] Chisnell, R.F., "The unsteady motion of a drop moving vertically under gravity", J. Fluid Mech., **176**, 443-464 (1987).

[12] Choudhuri, D., Sri Padmavati, B., "A study of an arbitrary Stokes flow past a fluid coated sphere in a fluid of a different viscosity", ZAMP, **61(2)**, 317-328 (2010).

[13] Chwang, A.T., Wu, T., Yao-Tsu, "Hydrodynamics of low Reynolds number flow, Part 1, Rotation of Axisymmetric prolate bodies", J. Fluid Mech., **63(3)**, 607-622 (1974); "Singularity method for Stokes flow", J. Fluid Mech. **67(4)**, 787-815 (1975).

[14] Coimbra, C.F.M., Rangel, R.H., "General solution of the particle momentum equation in unsteady Stokes flow" (English summary), J. Fluid Mech., **370**, 53-72 (1998).

[15] Collins, W.D., "A note on Stokes's stream-function for the slow steady motion of viscous fluid before plane and spherical boundaries", Mathematika, **1(2)**, 125-130 (1954).

[16] Cox, R.G. "The motion of long slender bodies in a viscous fluid, Part I, General theory", J. Fluid Mech., **44**, 791-810 (1970).

[17] Daripa, P., Palaniappan, D., "Singularity induced exterior and interior Stokes flows", Phys. Fluids, **13**, 3134-3154 (2001).

[18] Dimitrikapoulos, P., Higdon, J.J.L., "Displacement of fluid droplets from solid surface in low-Reynolds-number shear flows", J. Fluid Mech., **336**, 351-378 (1997).

[19] Dohara Nariyoshi, "The unsteady flow around an oscillating sphere in a viscous fluid", J. Phys. Soc. of Japan, **51(12)**, 4095-4103 (1982).

[20] Einzel, D., Panzer, P., Liu, M., "Boundary conditions for fluid flow: Curved or rough surfaces", Phys. Rev. Lett., **64**, 2269 (1990).

[21] Faxén, H., "Der widerstandgegen die bewegung einer starren kugel in einer zähen flüssigkeit die zwischen zwei parallelen ebenen wänden eingeschlossen ist", Ann. Phys., **68**, 89-119 (1922); "Der widerstandgegen die bewegung einer starren kugel in einer zähen flüssigkeit die zwischen zwei parallelen ebenen wänden eingeschlossen ist", Arkiv für Matematik Astromi Och. Fysik, **18(29)**, 1-52 (1924).

[22] Feng, J., Joseph, D.D., "The unsteady motion of solid bodies in creeping flows", J. Fluid Mech., **303**, 83-102 (1995).

[23] Fuentes, Y.O., Kim, S., Jeffrey, D.J., "Mobility functions for two unequal viscous drops in Stokes flow: I Axisymmetric motions", Phys. Fluids A, **31(9)**, 2445-2455 (1988).

[24] Fuentes, Y.O., Kim, S., Jeffrey, D.J., "Mobility functions for two unequal viscous drops in Stokes flow: II Asymmetric motions", Phys. Fluids A, **1(1)**, 61-76 (1988).

[25] Gupalo, P.Yu., Ryazantsev, Yu., Chalyuk, A.T., "Flow past a sphere coated by a liquid film for small Reynolds number", Fluid Dyn., **9(5)**, 673-682 (1974).

[26] Goldstein, S., *Modern Developments in Fluid Dynamics*, Dover Publications, New York, First edition, 1965.

[27] Hackborn, W., O'Neill, M.E., Ranger, K.B., "The structure of an asymmetric Stokes flow", Quart. J. Mech. appl. Math., **39(1)**, 1-14 (1986).

[28] Hadamard, J.S., "Mécanique-Mouvement lent d'une sphère liquide et visqueuse dans un liquide visqueux", C. Rend. Acad. Sci., **152**, 1735-1738 (1911).

[29] Hadamard, J.S., "Hydrodynamique-Sur une question relative aux liquides visqueux", C. Rend. Acad. Sci., **154**, 109 (1912).

[30] Hancock, G.J., "The self propulsion of microscopic organisms through liquids", Proc. R. Soc. London , **A217**, 96-121 (1953).

[31] Hancock, G.J., Grey, J., "The propulsion of sea urchin spermatozoa", J. Exp. Biol., **22**, 802-814 (1955).

[32] Happel, J., Brenner, H., *Low Reynolds number Hydrodynamics*, The Hague: Martinus Nijhof (1983).

[33] Hashimoto, H., Sano, O., "Stokeslets and eddies in creeping flows", Ann. Rev. Fluid Mech., **12**, 335-363 (1980).

[34] Sano, T. "Unsteady flow past a sphere at low Reynolds number", J. Fluid Mech., **112**, 433-441 (1981).

[35] Hasimoto, H., "Sphere theorem for the Stokes flow", Phys. Fluids, **9**, 1838-1840 (1997).

[36] Hellou, M., Coutanceau, M., "Cellular Stokes flow induced by rotation of a cylinder in a closed channel", J. Fluid Mech., **236**, 557-577 (1992).

[37] Helmholtz, Piotrowsky, Sitzungs. der k.k.Acad.der Wiss.zu Wien, Wissenschaft, Abhand, **Vol.1**, 172 (1882).

[38] Hetsroni, G., Haber, S., "The flow in and around a droplet or bubble submerged in an unbounded arbitrary velocity field", Rheol. Acta, **9**, 488-496 (1970).

[39] Higdon, J.J.L, "A hydrodynamic analysis of flagellar propulsion", J. Fluid Mech., **90(4)**, 685-711 (1979).

[40] Jeffrey, D.J., Sherwood, J.D., "Streamline patterns and eddies in low-Reynolds-number flows", J. Fluid Mech., **96**, 315-334 (1980).

[41] Jeffery, G.B., "The motion of ellipsoidal particles immersed in a viscous fluid", Proc. R. Soc. London A, **102**, 161-179 (1922).

[42] Johnson, R.E., "Stokes flow past a sphere coated with a thin fluid film", J. Fluid Mech., **110**, 217-238 (1981).

[43] Kawano, S., Hasimoto, H., Suyama, T., "Heat and fluid flow of two immiscible liquid layers in vertical cylindrical container (application to device for sequential production of solid spherical shells in liquid-liquid-gas system)", JSME Int. J. Ser.B, **39**, 246-256 (1996).

[44] Kawano, S., Hasimoto, H., Ihara, A., Shin, K., "Sequential production of mm-sized spherical shells in liquid-liquid-gas systems", Trans ASME J. Fluids Engg., **118**, 614-618 (1996).

[45] Kawano, S., Hasimoto, H., Ihara, A., Shin, K., "A numerical study on motion of a sphere coated with a thin liquid film at intermediate Reynolds number", J. Fluid Engg. Trans. ASME, **119(2)**, 397-403 (1997).

[46] Kim, S., Arunachalam, P.V., "The general solution for an ellipsoid in low Reynolds number flow", J. Fluid Mech., **178**, 535-547 (1987).

[47] Kim, S., Karrila, S.J., *Microhydrodynamics: Principles and selected applications*, Butterworth-Heinemann series in chemical engineering, Stoneham, U.S.A., 1991.

[48] Kondo, T., Koishi, M., *Microcapsules* (*Sankyo*,in Japanese), 1-82 (1981).

[49] Lagerstrom, P., Kaplun, S., "Asymptotic expansions of Navier-Stokes solutions for small Reynolds number", J. Math. Mech., **6**, 585-593 (1957).

[50] Lamb, H., *Hydrodynamics*, Cambridge University Press, England, 1932.

[51] Landau, L.D., Lifshitz, E.M., *Fluid Dynamics*, Pergamon Press, 1978.

[52] Lawrence,C., Weinbaum,S., The unsteady force on a body at low Reynolds number: the axisymmetric motion of a spheroid, J. Fluid Mech., **189**, 463-489 (1988).

[53] Lecoq, N., Masmoudi, K., Anthore, R., Feuillebois, F., "Creeping motion of a sphere along the axis of a closed axisymmetric container", J. Fluid Mech., **585**, 127-152 (2007).

[54] Lee,M.C., Kendall,J.M.Jr., Bahrami,P.A., Wang,T.G., "Sensational spherical shells", Aerosp. Ann., **24**, 72-76 (1986).

[55] Lighthill, M.J., *Mathematical Biofluiddynamics*, Philadelphia: SIAM, 1975.

[56] Liu, C.F., Beskok, A., Gatsonis, Karniadakis, G.E., "Flow past a microsphere in a pipe: effects of rarefactions", Micro-Electro-Mechanical Systems(MEMS), ASME, DSC, **66**, 445-452 (1998).

[57] Lorentz, H.A., Zittingsverl. Akad. van Wet, **5**, 168-187 (1896).

[58] Lorentz, H.A., neu bearb. Abhandl theoret. phys., **1**, 23 (1907).

[59] Lovalenti, P.M., Brady,J.F., "The hydrodynamic force on a rigid particle undergoing arbitrary time-dependent motion at small Reynolds number", J. Fluid Mech., **256**, 561-605 (1993).

[60] Lovalenti, P.M., Brady,J.F., "The force on a bubble, drop or particle in arbitrary time-dependent motion at small Reynolds number", Phys. Fluids A, **5(9)**, 2104-2116 (1993).

[61] Matunobu Yaso'o, "Motion of a deformed drop in Stokes flow", J. Phy. Soc. of Japan, **21(8)**, 1596-1602 (1966).

[62] Matunobu Yaso'o, "Motion of a drop suspended in a viscous flow with arbitrary velocity profile", J. Phy. Soc. of Japan, **29(2)**, 508-513 (1970).

[63] Maul, C., Kim, S., "Image of a point force in a spherical container and its connection to the Lorentz reflection formula", J. Engg. Math., **30**, 119-130 (1996).

[64] Maxey, M.R., Riley, J.J., "Equation of motion for a small rigid sphere in a nonuniform flow", Phys. Fluids, **26(4)**, 883-889 (1983).

[65] Mazur, P., Bedeaux, D., "A generalization of Faxén theorem to nonsteady motion of a sphere through an incompressible fluid in an arbitrary flow", Physica, **76**, 235-246 (1974).

[66] McOwen, R.C., *Partial Differential Equations*, Pearson Education, U.S.A., 2003.

[67] Meleshko, V.V., Aref, H., "A blinking Rotlet model for chaotic advection", Phys. Fluids A, **8**, 3215-3217 (1996).

[68] Michaelidis, E.E., Feng, Z.G., "The equation of a small viscous sphere in an unsteady flow with interface slip", Int. J. Multiphase Flow, **21(2)**, 315-321 (1995).

[69] Moshfegh, A., Shams, M., Ahmadi, G., Ebrahimi, R., "A novel slip correction factor for spherical aerosol particles", World Academy of Science, Engineering and Technology, **46**, 108-114 (2008).

[70] Munson, B.R., Gustafson, B.K., "Sensitivity of Stokes flow to geometry", Exp. Fluids, **3**, 157-260 (1985).

[71] Naghdi, P.M., Hsu, C.S., J. Math. Mech., **10**, 233-245 (1961).

[72] O'Neill, M.E., Ranger, K.B., "On the slow motion of a fluid coated in an immiscible viscous fluid", C. R. Math. Rep. Acad. Sci. Can., **3(5)**, 261-266 (1981).

[73] Oberbeck, A., "Über stationäre Flüssigkeitsbewegungen mit Berücksichtigung der inneren Reibung", Journal für die reine und angewandte Mathematik, **81**, 62-80 (1876).

[74] Oseen, C.W., *Hydrodynamik*, Akademische Verlagsgesellschaft, Leipzig, 97-107, 1927.

[75] Padmavathi, B.S., Amaranath, T., Nigam, S.D., "Stokes flow past a sphere with mixed slip-stick boundary conditions", Fluid Dyn. Res., **11**, 229-234 (1993).

[76] Padmavathi, B.S., Amaranath, T., Palaniappan, D., "Motion inside a liquid sphere: Internal singularities", Fluid Dyn. Res., **15**, 167-176 (1995).

[77] Padmavathi, B.S., Rajasekhar, G.P., Amaranath, T., "A note on complete general solutions of Stokes equations", Quart. J. Mech. appl. Math., **50(3)**, 383-388 (1998).

[78] Palaniappan, D., Nigam, S.D, Amaranath, T., Usha, R., "A theorem for a shear-free sphere in a Stokes flow", Mech. Res. Comm., **17(6)**, 429-436 (1990).

[79] Palaniappan, D., Nigam, S.D, Amaranath, T., Usha, R., "Lamb's solution of Stokes equations: a sphere theorem", Quart. J. Mech. appl. Math., **45(1)**, 47-56 (1992).

[80] Palaniappan, D., Nigam, S.D, Amaranath, "A theorem for a fluid sphere in Stokes flow", J.Austral. Math. Soc. Ser. B, **35(3)**, 335-347 (1994).

[81] Palaniappan, D., Daripa, P., "Interior Stokes flows with stick-slip boundary conditions", Physica A: Statistical Mechanics and its Applications, **297**, 37-63 (2001).

[82] Payne, L.E., Pell, W.H., "The Stokes flow problem for a class of axially symmetric bodies", J. Fluid Mech., **7**, 529-549 (1960).

[83] Pozrikidis, C., "A singularity method for unsteady linearized flow", Phys. Fluids A, **1(9)**, 1508-1520 (1989).

[84] Pozrikidis, C., *Boundary integral and singularity methods for linearized viscous flows*, Cambridge University Press, New York, 1992.

[85] Pozrikidis, C., "A bibliographical note on the unsteady motion of a spherical drop at low Reynolds number", Phys. Fluids, **6(9)**, 3209 (1994).

[86] Prandtl, L., Verh.d.3. Intern. Ver. Heidelberg, 1904.

[87] Proudman, I., Pearson, J.R.A., "Expansions at small Reynolds numbers for the flow past a sphere and a circular cylinder", J. Fluid Mech., **2**, 237-262 (1957).

[88] Radha, R., Padmavathi, B.S., Amaranath, T., "New approximate analytical solutions for creeping flow past axisymmetric rigid bodies", Mech. Res. Comm., **37**, 256-260 (2010).

[89] Rallison, J.M., "Note on the time-dependent deformation of a viscous drop which is almost spherical", J. Fluid Mech., **98(3)**, 625-633 (1980).

[90] Rallison, J.M., "The deformation of small viscous drops and bubbles in shear flows", Ann.Rev. Fluid Mech., **16**, 45-66 (1984).

[91] Ranger, K.B., "Flow due to a point source of momentum in a viscous fluid contained in a sphere", Proc. Camb. Phil. Soc., **63**, 249-256 (1967).

[92] Ranger, K.B., "The Stokes drag for asymmetric flow past a spherical cap", ZAMP, **24**, 801-809 (1973).

[93] Ranger, K.B., "Eddies in two dimensional Stokes flow", Int. J. Engg. Sci., **18**, 181-190 (1980).

[94] Ruschak, K., J., "Coating flows", Annual Reviews of Fluid Mechanics, **17**, 65-90 (1985).

[95] Rybczynski, W. "On the translatory motion of a fluid sphere in a viscous medium", Bull. Acad. Sci. Cracow, **Ser A**, 40-46 (1911).

[96] Sano, T., "Unsteady flow past a sphere at low Reynolds number", J. Fluid Mech., **112**, 433-441 (1981).

[97] Satoyuki, K., Atsushi, S., Shohei, N., "Deformations of thin liquid spherical shells in liquid-liquid-gas systems", Phys. Fluids, **19**, 1-11 (2007).

[98] Schmitz, R., Felderhof, B.U., "Creeping flow about a sphere", Physica A, **92**, 423-437 (1978).

[99] Shail, R., "A note on a symmetric Stokes flows within a sphere", Quart. J. Mech. appl. Math., **40(2)**, 223-233 (1987).

[100] Shail, R., Onslow, S.H., "Some Stokes flows exterior to a spherical boundary", Mathematika, **35(2)**, 233-246 (1988).

[101] Sherman, F.S., *Viscous flows*, Mc Graw-Hill series in Mechanical Engineering, Mc Graw-Hill Publishing Co., 1990.

[102] Sir James Grey, *Ciliary movement*, Cambridge University press, 1928; "Undulatory Propulsion", Quart. J. Microsc. Sc., **94**, 551-578(1953); "The movement of sea urchin spermatozoa", J. Exp. Biol. **32**, 775-801 (1955).

[103] Stokes, G.G., "On the effect of the internal friction on the motions of pendulums", Trans. Camb. Philos. Soc., **9(2)**, 8-106 (1851).

[104] Stone, H.A., "Dynamics of drop deformation and break up in viscous fluids", Ann. Rev. Fluid Mech., **26**, 65-102 (1994).

[105] Stone, H.A., Bush, J.W.M., "Time-dependent drop deformation in a rotating high viscosity fluid", Quart. of Appl. Math., **54(3)**, 551-556 (1996).

[106] Sy Francisco, Lightfoot, E.N., "Transient creeping flow around fluid spheres". AIChE J., **17(1)**, 177-181 (1971).

[107] Taylor, G.I., "Analysis of the swimming of long and narrow animals", Proc. R. Soc., London A, **214**, 158-183 (1952).

[108] Taylor, T.D., Acrivos, A. "On the deformation and drag of a falling viscous drop at low Reynolds number", J. Fluid Mech., **18**, 466-476 (1964).

[109] Tophøj, L., Møller, S., Brøns, M., "Streamlines patterns and their bifurcations near a wall with Navier slip boundary condition", Phys. Fluids, **18**, 083102 (2006).

[110] Usha, R., Ph.D. Thesis, '*Flow at small Reynolds numbers*', Department of Mathematics, Indian Institute of Technology, Madras, 1980.

[111] Usha, R., Nigam, S.D., "Flow in a spherical cavity due to a Stokeslet", Fluid Dyn. Res., **11**, 75-78 (1995).

[112] Vafeas, P., Dassios, G., "Stokes flow in ellipsoidal geometry", J. Math. Phys., **47**, 0931021-38 (2006).

[113] Venkatalaxmi, A., Padmavathi, B.S., Amaranath, T., "A general solution of unsteady Stokes equations", Fluid Dyn. Res., **35**, 229-236 (2004).

[114] Venkatlaxmi, A., Padmavathi, B.S., Amaranath, T., "Unsteady Stokes equations: some complete general solutions", Proc. Indian Acad. Sci. (Math. Sci.), **114(2)**, 203-213 (2004).

[115] Wen, S.B., Lai, C.L., "Theoretical analysis of flow passing a single sphere moving in a micro-tube", Proc. R. Soc. Lond. A, **459**, 495-526 (2003).

[116] Xu, X.S., Wang, M.Z., "General complete solutions of the equations of spatial and axisymmetric Stokes flow", Quart. J. Mech. appl. Math., **44(4)**, 537-548 (1991).

[117] Yang Seung-Man, Leal, L.G., "A note on memory-integral contributions to the force on an accelerating spherical drop at low Reynolds number", Phys. Fluids A, **3(7)**, 1822-1824 (1991).